

Aus dem Centrum für Schlaganfallforschung
der Medizinischen Fakultät Charité – Universitätsmedizin Berlin

DISSERTATION

Focal brain injury in patients with aneurysmal subarachnoid
hemorrhage – A neuroradiological perspective

Fokale Hirnschädigung in Patienten mit aneurysmatischer Sub-
arachnoidalblutung – Eine neuroradiologische Perspektive

zur Erlangung des akademischen Grades
Doctor medicinae (Dr. med.)

vorgelegt der Medizinischen Fakultät
Charité – Universitätsmedizin Berlin

von

Viktor Horst

Datum der Promotion: 29. November 2024

Table of contents

List of tables	iii
List of figures	iv
List of abbreviations.....	v
Abstract	1
1 Introduction.....	4
1.1 Early brain injury.....	4
1.2 DCI.....	5
1.3 Proximal vasospasm and spreading depolarization (SD).....	5
1.4 Objective	6
2 Methods.....	7
2.1 Patient selection.....	7
2.2 Study design	8
2.3 Quantitative neuroimage analysis	10
2.4 ECoG, DSA and TCD analysis.....	11
2.5 Statistics.....	14
3 Results	16
3.1 Study population.....	16
3.2 Early brain injury.....	17
3.3 Delayed cerebral infarction.....	17
3.4 Paths from initial hemorrhage to delayed cerebral infarction.....	19
3.5 Illustrative cases.....	20
4 Discussion	24
4.1 Short summary of results	24
4.2 Interpretation of results.....	24
4.3 The current state of research	27
4.4 Strengths and limitations	28

4.5	Implications for future research	28
5	Conclusions.....	29
	Reference list.....	30
	Statutory Declaration	35
	Declaration of my own contribution to the publications.....	36
	Printing copy of publication 1	38
	Printing copy of publication 2.....	56
	Printing copy of publication 3.....	77
	Curriculum Vitae	97
	Publication list.....	98
	Acknowledgments	100

List of tables

Table 1: Variables of the manual neuroimage analysis in DISCHARGE-1 (29). (own table)	11
Table 2: Neuromonitoring and neuroimaging variables in the substudy of DISCHARGE-1 (30). (own table)	12
Table 3: Characteristics of the study populations (28-30). (Table adapted from Supplementary Table 1 in Dreier <i>et al.</i> , 2022 (29)).....	16
Table 4: Lesion volumes of the manual neuroimage analysis in DISCHARGE-1 (29). (own table)	18

List of figures

Figure 1: Illustration of the diagnostic procedures in DISCHARGE-1 (Depolarizations in ISCHemia after subARachnoid hemorrhage-1). (Figure adapted from Figure 1A in Dreier <i>et al.</i> , 2022 (29))	8
Figure 2: The continuum between intracerebral hemorrhage (ICH) and subarachnoid hematoma illustrated in a DISCHARGE-1 (Depolarizations in ISCHemia after subARachnoid hemorrhage-1) patient (29). (own figure).....	21
Figure 3: Early and delayed cerebral infarction adjacent to blood clots at the cerebral convexity in absence of severe angiographic vasospasm illustrated in the same DISCHARGE-1 (Depolarizations in ISCHemia after subARachnoid hemorrhage-1) patient (29). (own figure)	22

List of abbreviations

ACA	anterior cerebral artery
ACoA	anterior communicating artery
ADC	apparent diffusion coefficient
AUROC	area under the receiver operating characteristic curve
aSAH	aneurysmal subarachnoid hemorrhage
blood _{basal}	subarachnoid blood volume in the basal cisterns
blood _{convex}	subarachnoid blood volume on the cerebral convexity
blood _{inter}	subarachnoid blood volume in the interhemispheric fissure
blood _{Sylvian}	subarachnoid blood volume in the Sylvian fissure
COSBID	Co-Operative Studies on Brain Injury Depolarizations
CI	confidence interval
CONSCIOUS	Clazosentan to overcome neurological ischemia and infarction occurring after subarachnoid hemorrhage
CT	computed tomography
DC	direct current
DCI	delayed cerebral ischemia
DCI _{ACA}	delayed infarct volume in the territory of the anterior cerebral artery
DCI _{deep}	delayed infarct volume below the cortex, including perforator infarcts, singular white matter infarcts without cortical involvement, and anterior choroidal artery infarcts
DCI _{MCA}	delayed infarct volume in the territory of the middle cerebral artery
DCI _{PCA}	delayed infarct volume in the territory of the posterior cerebral artery
DCI _{watershed}	delayed infarct volume in the territory of the cortical watershed zones
DISCHARGE-1	Depolarizations in ISChemia after subARachnoid hemorrhage-1
DND	delayed neurological deficit
DSA	digital subtraction angiography [A1, A2, M1, M2, P1, P2 = first and second segments of anterior cerebral artery (ACA), middle cerebral artery (MCA) and posterior cerebral artery (PCA) ipsilateral to the subdural electrodes]
DSAS	digital subtraction angiography score
DWI	diffusion-weighted imaging
ECI	early cerebral infarction

ECoG	electrocorticography
eGOS	extended Glasgow Outcome Scale
FLAIR	fluid-attenuated inversion recovery
GCS	Glasgow Coma Scale
ICA	internal carotid artery
ICH	intracerebral hemorrhage
IQR	interquartile range
IVH	intraventricular hemorrhage
mbfv	transcranial Doppler-sonography (TCD)-determined mean blood flow velocity
mbfv _{ACA}	TCD-determined peak mean blood flow velocity of the anterior cerebral artery
mbfv _{MCA}	TCD-determined peak mean blood flow velocity of the middle cerebral artery
mbfv _{PCA}	TCD-determined peak mean blood flow velocity of the posterior cerebral artery
MCA	middle cerebral artery
mHSS	modified Hijdra Sum Score
MRI	magnetic resonance imaging
mRS	modified Rankin Scale
n	number
NIHSS	National Institutes of Health Stroke Scale
PCA	posterior cerebral artery
PCoA	posterior communicating artery
peak _{clusSD-delayed}	peak number of clustered spreading depolarizations of a recording day during the delayed period
peak _{clusSD-early}	peak number of clustered spreading depolarizations of a recording day during the early period
peak _{isoSD-delayed}	peak number of isoelectric spreading depolarizations of a recording day during the delayed period
peak _{isoSD-early}	peak number of isoelectric spreading depolarizations of a recording day during the early period

peak _{SD-delayed}	peak number of spreading depolarizations of any type of a recording day during the delayed period
peak _{SD-early}	peak number of spreading depolarizations of any type of a recording day during the early period
PTDDD _{delayed}	peak total spreading depolarization-induced depression duration of a recording day during the delayed period
PTDDD _{early}	peak total spreading depolarization-induced depression duration of a recording day during the early period
r	Pearson correlation coefficient
r _s	Spearman rank order correlation coefficient
RMS	Rosen-Macdonald score
ROC	receiver operating characteristic
SAH	subarachnoid hemorrhage
SD	spreading depolarization
std	standard deviation
TCD	transcranial Doppler-sonography
TDDD	total spreading depolarization-induced depression duration of a recording day
WFNS	World Federation of Neurosurgical Societies grading scale

Abstract

Focal brain injury is common in patients with aneurysmal subarachnoid hemorrhage (aSAH). Intracerebral hemorrhage (ICH), early cerebral infarction (ECI) and delayed cerebral infarction are the main etiologies. They contribute to poor functional outcome. Neuroimaging is the gold standard to demonstrate the extent of cerebral damage. However, it lacks the ability of real-time neuromonitoring. Electrocorticography (ECoG) is an innovative technique that may close this gap, as it detects spreading depolarizations (SD), the electrophysiological correlate of the initial, still reversible phase of neuronal cytotoxic gray matter edema.

Using serial magnetic resonance imaging (MRI) and ECoG, we studied focal brain injury in 205 patients enrolled in the prospective, diagnostic phase III study DISCHARGE-1 (Depolarizations in ISCHemia after subARachnoid hemorrhage-1). Volumes of ECI, ICH and delayed cerebral infarction were manually quantified on neuroimages and correlated with (i) parameters derived from ECoG recordings, (ii) parameters of proximal vasospasm derived from angiography or transcranial Doppler-sonography (TCD) and (iii) volumes of extravascular blood quantified on the initial computed tomography (CT) scan.

In a pilot study on ECI, we included 23 patients of the DISCHARGE-1 cohort with rupture of an anterior communicating artery (ACoA) aneurysm. The group with frontal ECI and/or ICH were significantly more likely to show SD on ECoG compared to those patients without early frontal brain injury. In the main study DISCHARGE-1, 162 out of 180 patients demonstrated focal brain damage. On average, ECI+ICH accounted for 46 ± 73 ml of tissue loss and delayed cerebral infarction accounted for 36 ± 80 ml. The predefined 60-min cut-off for the ECoG-parameter 'peak total spreading depolarization-induced depression duration' (PTDDD) indicated delayed ipsilateral infarction with 76% sensitivity and 59% specificity. In a secondary analysis, a new 180-min cut-off indicated delayed ipsilateral infarction with 62% sensitivity and 83% specificity. In a sub-study, we further investigated whether SD plays a causal role in the development of delayed cerebral infarction. The statistical path analysis showed that SD mediated the detrimental effect of extravascular blood resulting in delayed cerebral infarction independently of angiographic vasospasm.

This work has diagnostic and therapeutic implications. First of all, ECoG sufficiently detected focal brain injury in real-time after aSAH. The results may encourage further researchers to implement ECoG monitoring into a clinical setting. Second, the volume of

delayed cerebral infarction accounted for 42.6% of the total focal brain damage. This large amount of tissue loss emphasizes the need for effective treatments targeting delayed cerebral infarction. Future therapies should not only target angiographic vasospasm but also SD to improve patient outcome.

Zusammenfassung

Fokale Hirnschädigungen sind bei Patienten mit aneurysmatischer Subarachnoidalblutung (aSAH) häufig. Intrazerebrale Blutungen (ICH), frühe zerebrale Infarkte (ECI) und verzögerte zerebrale Infarkte sind die Hauptursachen. Sie tragen zu einem schlechten Outcome bei. Die Bildgebung ist der Goldstandard für den Nachweis von Hirnschädigungen. Allerdings ist ein Echtzeitmonitoring dadurch nicht möglich. Die Elektrokortikographie (ECoG) ist eine innovative Technik, die diese Lücke schließen könnte, da sie Spreading Depolarizations (SD) erfasst, das elektrophysiologische Korrelat der anfänglichen, noch reversiblen Phase des neuronalen zytotoxischen Ödems der grauen Substanz.

Anhand von seriellen Magnetresonanztomographien (MRI) und ECoG untersuchten wir fokale Hirnschädigungen bei 205 Patienten, die an der prospektiven, diagnostischen Phase-III-Studie DISCHARGE-1 (Depolarizations in ISCHemia after subARachnoid hemorrhage-1) teilnahmen. Die Volumina von ECI, ICH und verzögerten zerebralen Infarkten wurden manuell auf MRT- oder Computertomographie- (CT) Bildern quantifiziert und mit (i) Parametern aus ECoG Aufzeichnungen, (ii) Parametern aus Angiographie oder transkranieller Doppler-Sonographie (TCD) und (iii) extravaskulären Blutvolumina aus der initialen CT korreliert.

In einer Pilotstudie zur ECI schlossen wir 23 Patienten der DISCHARGE-1 Kohorte mit Ruptur eines Aneurysmas der Arteria communicans anterior (ACoA) ein. Die Gruppe mit frontaler ECI und/oder ICH wies im Vergleich zu den Patienten ohne frühe frontale Hirnschädigung signifikant häufiger SDs auf. In DISCHARGE-1 hatten 162 von 180 Patienten eine fokale Hirnschädigung. Im Durchschnitt entfielen 46 ± 73 ml des Gewebeverlusts auf ECI+ICH und 36 ± 80 ml auf verzögerte zerebrale Infarkte. Der vordefinierte 60-minütige Cut-off für den ECoG-Parameter "Peak total spreading depolarization-induced depression duration" (PTDDD) zeigte einen verzögerten ipsilateralen Infarkt mit 76%

Sensitivität und 59% Spezifität an. In einer sekundären Analyse zeigte ein neuer 180-minütiger Cut-off einen verzögerten ipsilateralen Infarkt mit 62% Sensitivität und 83% Spezifität an. In einer weiterführenden Studie untersuchten wir, ob SDs eine kausale Rolle bei der Entwicklung von verzögerten zerebralen Infarkten spielen. Die statistische Pfadanalyse zeigte, dass SD die schädliche Wirkung von extravaskulärem Blut, die zu einem verzögerten zerebralen Infarkt führt, unabhängig von angiographischen Gefäßspasmen vermittelt.

Diese Arbeit hat diagnostische und therapeutische Implikationen. Mittels ECoG konnten fokale Hirnschädigungen in Echtzeit nach aSAH erkannt werden. Die Ergebnisse könnten Forscher dazu ermutigen, die ECoG-Überwachung in den klinischen Alltag zu integrieren. Das Volumen des verzögerten Hirninfarkts machte 42.6% der gesamten fokalen Hirnschädigung aus. Diese Menge an Gewebeverlust unterstreicht die Notwendigkeit wirksamer Therapien, die auf den verzögerten Hirninfarkt abzielen. Zukünftige Therapien sollten nicht nur auf den angiographischen Vasospasmus, sondern auch auf SDs abzielen, um das Ergebnis der Patienten zu verbessern.

1 Introduction

Subarachnoid hemorrhage (SAH) is a severe subtype of stroke. The worldwide incidence is 8 out of 100.000 persons per year, with some regional variations (1). It affects patients at a relatively young age (median 55 years). The proportion of women is 1.6 times higher compared to men (2). Further risk factors include smoking, alcohol intake, a history of hypertension, a family history of SAH and a Japanese or Finnish ethnicity (2). SAH only accounts for 5% of all strokes but it is responsible for 27% of all years of potential life lost under the age of 65 due to stroke (3). The burden is comparable to the more common causes ischemic stroke (39%) and intracerebral hemorrhage (34%) (3). The case fatality is about 40 – 50% in population-based studies (4, 5). Rupture of an intracranial aneurysm is the cause in 85% of all patients with SAH. Non-aneurysmal perimesencephalic SAH accounts for 10% and other causes are rare (2).

1.1 Early brain injury

As Bebin and Currier pointed out, SAH is not itself a cause of death. There must be damage to the brain (6). In fact, SAH causes one of the most severe brain injuries in acute neurology. Aneurysmal SAH (aSAH) is unique insofar as injury occurs in two different phases, termed early brain injury and delayed cerebral ischemia (DCI). Early brain injury summarizes all harmful events that are directly related to the initial bleeding within the first 48 hours. When an intracranial aneurysm ruptures, blood pours into the subarachnoid space, intracranial pressure rises rapidly and generates transient global cerebral ischemia (7). As a result, early dysfunction of the blood-brain-barrier is found that contributes to the development of global cerebral edema in 20% of the patients (8, 9). The bleeding may also destruct the brain parenchyma indirectly through the formation of an occlusive hydrocephalus or through mass effects resulting in herniation. In addition to global damage to the brain, focal injury also occurs in the early period due to early cerebral infarction (ECI) and intracerebral hemorrhage (ICH). Diffusion-weighted imaging (DWI) reveals focal ECI in 51% [confidence interval (CI): 24 – 77%] of all cases (10). ICH is found in 24% of all cases (11). All in all, Broderick and colleagues stressed the importance of early brain injury in their population-based study where 22 out of 38 (61%) deaths from aSAH occurred within the first 2 days (12).

1.2 DCI

The second phase of brain injury spans from Day 3 to Day 14. At this stage, the aneurysm has been secured by surgical clip ligation or endovascular coiling and the patient has been transferred to the intensive care unit. The neurological status of the patient may deteriorate in this phase because of manifold intracranial or systemic complications. DCI is the most significant in-hospital complication that contributes to major morbidity after aSAH (13, 14). It may present clinically as a delayed neurological deficit (DND), defined as new onset of a focal neurological deficit or a decrease of consciousness by at least two points on the Glasgow Coma Scale, and/or it may present radiologically as delayed cerebral infarction on computed tomography (CT). DCI develops in one third of the patients if the diagnosis is based on clinical assessment and CT (7). Using magnetic resonance imaging (MRI), the incidence of delayed cerebral infarction is even higher. DWI demonstrated delayed cerebral infarction in 47% (CI: 35 – 59%) of the patients (10). The higher proportion of patients with delayed cerebral infarcts might be explained by the high sensitivity of DWI.

1.3 Proximal vasospasm and spreading depolarization (SD)

The pathophysiology of focal brain injury secondary to aSAH is subject of an ongoing debate (15). In 1951, Ecker and Riemenschneider provided a first theory for the occurrence of DCI. Using angiography, they demonstrated proximal vasospasm of the major cerebral arteries in patients with aSAH (16). Vasospasm usually appears on angiography from Day 3, peaks around Day 6 to 8 and subsides by Day 12 (17). In 1984, the introduction of transcranial Doppler-sonography (TCD) in patients with aSAH provided an indirect and noninvasive assessment of proximal vasospasm by measuring mean blood flow velocities (mbfv). In the 21st century, the concept of vasospasm received a major setback due to the results of the CONSCIOUS (Clazosentan to overcome neurological ischemia and infarction occurring after subarachnoid hemorrhage) trials (18-20). The endothelin receptor antagonist Clazosentan reduced vasospasm in a dose-dependent manner but had no significant effect on the incidence of delayed cerebral infarcts or functional outcome. Since then, further pathomechanisms have been discussed. One of the most promising theories dates back to discoveries made by neurophysiologist Leão in 1944 (21). It is nowadays summarized by the generic term 'spreading depolarization' (SD).

In animal experiments, ischemic injury of cerebral gray matter is practically always accompanied by the occurrence of SDs (22). SD is a wave that slowly propagates with a velocity of 2 – 9mm/min in the cortex. It is characterized by a near-complete breakdown of the transmembrane ion-gradients of neurons and astrocytes. Importantly, SD induces silencing of spontaneous electrical brain activity, called ‘spreading depression’. Using electrocorticography (ECoG), SD is observed as a negative shift of the direct current (DC) potential. The spectrum of SDs varies from transient depolarization waves with full recovery of the affected tissue, to clusters of recurrent depolarizations, to a terminal wave with a long-lasting DC shift termed negative ultraslow potential (23). In 2002, the first robust method was introduced that afforded the recording of SDs in humans with traumatic brain injury (24). Since then, SDs have also been found in 70 – 80% of patients with aSAH (25, 26). In these pilot studies, the occurrence of SDs was linked to the development of DND and delayed cerebral infarction. However, SD is not only an accompanying phenomenon of ischemic injury in the cerebral gray matter, which may be used as a diagnostic biomarker. SD is also a pathomechanism, since SD, if too long, leads to intoxication of neurons and, in addition, can trigger extreme vasoconstriction and ischemia via an impaired neurovascular response, which spreads together with SD in the cerebral cortex (= spreading ischemia) (27).

1.4 Objective

Based on this background, we hypothesized that SD is both, (i) a biomarker and (ii) a pathomechanism of developing focal brain injury in humans after aSAH. To address these two fundamental questions, we first had to characterize the focal brain injury. This was the primary objective of this work. We quantified (i) ICH, (ii) ECI and (iii) delayed cerebral infarction using serial MRI or, if not available, CT imaging. We then asked whether SD indicates the occurrence of ECI (28), the occurrence of delayed cerebral infarction (29) and whether extravascular blood products trigger SDs resulting in delayed cerebral infarction independently of proximal vasospasm (30). For this purpose, we also quantified (iv) the volume of extravascular blood on the initial CT scan.

2 Methods

2.1 Patient selection

For the first part of this work (28), patients with aSAH prospectively enrolled in the COSBID (Co-Operative Studies on Brain Injury Depolarizations) study at Campus Benjamin Franklin and Campus Virchow Klinikum, Charité University Medicine Berlin, Germany, were retrospectively screened for inclusion. First, the COSBID database was searched for patients with aSAH from an anterior communicating artery (ACoA) aneurysm, and second, for the availability of an early postoperative MRI scan within 48 hours after aneurysm treatment. Third, patients were screened for the availability of continuous ECoG recordings from the initial placement of the electrodes up to 96 hours after the bleeding onset. As of April 2016, 23 patients met the inclusion criteria. All patients were also participants of the DISCHARGE-1 (Depolarizations in ISCHemia after subARachnoid hemorrhage-1) trial.

The second part of this work contributed to the DISCHARGE-1 trial (29). This prospective, single-arm diagnostic phase III trial is embedded in COSBID as mentioned earlier. Two hundred five patients with aSAH were recruited at six participating centers from September 2009 to April 2018. Sixty-six patients were allocated at Campus Benjamin Franklin and 64 patients at Campus Virchow Klinikum of the Charité University Medicine Berlin. Twenty-six patients were allocated at the University of Bonn, 23 at the University of Frankfurt, 17 at the University of Cologne and 13 at the University of Heidelberg. One hundred eighty patients were included in the final analysis. A detailed description of the study flow, inclusion and exclusion criteria can be found in the original publication (29).

For the third part of this work (30), the DISCHARGE-1 cohort was retrospectively screened for inclusion. Patients were included if a preoperative CT scan was performed and if at least one MRI or CT scan was available in the delayed period (>132 hours up to 14 days after bleeding onset). Exclusion criteria were: (i) a missing preoperative CT (n=18), (ii) a preoperative CT with a slice thickness of <3mm or >6mm (n=3), (iii) interventional complications causing cerebral infarction (n=3), (iii) major periprocedural re-bleedings of more than 10ml (n=8), (iv) early death (n=10), (v) and malignant early brain injury (n=2). One hundred thirty-six out of 180 patients were eligible and included in the final analysis.

All studies were approved by the local ethics committee (EA4/022/09 and confirmation of the Charité ethics committee of May 3, 2018 that the research is covered by the ethics vote EA4/022/09) and conducted in accordance with the Declaration of Helsinki. Informed consent was obtained either from the patient or from a legal representative if not possible from the patient due to the clinical state.

2.2 Study design

Screening for enrollment in the DISCHARGE-1 trial began when a patient was seen in the emergency department within 72 hours after the onset of aSAH. If included in the study, the patient underwent a standardized protocol of diagnostic procedures (Figure 1).



Figure 1: Illustration of the diagnostic procedures in DISCHARGE-1 (Depolarizations in ISCHemia after subARachnoid hemorrhage-1). (Figure adapted from Figure 1A in Dreier *et al.*, 2022 (29))

In the Discharge-1 trial, clinical data (indicated in yellow), neuromonitoring data (indicated in red), and neuroimaging data (indicated in blue) were collected according to a standardized diagnostic protocol. On admission, the Rosen-Macdonald score (RMS) was collected, which includes the World Federation of Neurosurgical Societies (WFNS) grade, age, history of hypertension, blood pressure on admission, aneurysm size, aneurysm location, clot thickness on the initial CT and the presence of early angiographic vasospasm (31). After surgical or endovascular treatment of the aneurysm, the patient was transferred to the intensive care unit. The National Institutes of Health Stroke Scale (NIHSS) was documented daily and the Glasgow Coma Scale (GCS) every 6 hours. A delayed neurological deficit (DND) was defined as a new focal neurological deficit or a decrease in consciousness of at least 2 points on the GCS scale. Around day 14 and after 7 months, functional outcome was assessed using the modified Rankin Scale (mRS) and the extended Glasgow Outcome Scale (eGOS). During surgical treatment of the aneurysm, the electrode strip for electrocorticography (ECoG) was implanted via craniotomy or, in the case of endovascular treatment, via a burr hole. Recording started in the intensive care unit and was continued until day 14. Furthermore, daily transcranial Doppler-sonography (TCD) measurements of the major cerebral arteries were performed. Screening for proximal vasospasm was complemented by digital subtraction angiography (DSA) around day 7. The initial computed tomography (CT) was used to establish the diagnosis. When necessary for planning surgical therapy or endovascular coiling, DSA was subsequently performed. After the intervention, another CT scan was performed to localize the electrode strip. During the course of treatment, the patient received a CT scan if her/his clinical condition worsened or if she/he developed a DND (dashed circles). Magnetic resonance imaging (MRI) was used to demonstrate early and delayed brain damage. For this purpose, an early MRI was performed within 24-48 hours after the surgical or endovascular intervention (MRI 1). The second and third MRI were performed during the delayed period around day 7 and day 14, respectively. The fourth MRI was performed at 7 months, if the patient was still alive and able to undergo the examination.

More than 40 researchers were involved in the data collection and analysis of the DISCHARGE-1 trial and of the related sub-studies. My contribution was the quantitative analysis of the MRI and CT dataset. The methodology is described in detail in section 2.3. The analyses of the ECoG recordings, the TCD and the digital subtraction angiography (DSA) data were performed by other group members. The methodology is briefly described in section 2.4.

2.3 Quantitative neuroimage analysis

For the first part of this work (28), ECI and ICH were characterized and subsequently quantified on early post-interventional MRI (MRI 1). Because the brain region in the immediate vicinity of the source of bleeding was of primary interest, quantification was limited to the vascular territories of the anterior cerebral arteries (ACA) in the frontal lobe. ECI was defined as a hyperintense signal on DWI with corresponding signal reductions on the apparent diffusion coefficient (ADC) map. ICH was defined as a hypointense signal in the cerebral parenchyma on T2*-weighted images. Quantification was performed using Clusterize. Clusterize is a semi-automatic software that is based on a region-growing algorithm. It was validated in stroke patients (32). Clusterize allows manual correction of the segmented regions of interest after the region-growing process. In addition, the amount of extravasated blood was rated on the initial CT using the semiquantitative modified Hijdra Sum Score (mHSS) (33).

For the second part of this work (29), delayed cerebral infarction was quantified on MRI 2 and 3 in addition to ECI on MRI 1 and ICH on the initial CT (Table 1). Clusterize could not be used for this purpose because the software could not distinguish between ECI and a new delayed infarct on MRI 2 and 3. Therefore, a separate manual approach was developed since no established methods were readily available. Validation was performed by comparison with a semi-automated approach (8). Quantification was performed according to published recommendations (34). Elaborate descriptions are given in the original publication (29). In brief, ICH was assessed and quantified on the initial CT. Periprocedural rebleeding was evaluated on the initial postoperative CT. ECI was defined as in the pilot study (28). ICH and ECI were then combined to form the new variable 'volume of early focal brain injury'. Delayed cerebral infarction was defined as a new hyperintense lesion on DWI with corresponding ADC reductions on MRI 2 or 3, that was not visible on MRI 1. The lesion volumes on MRI 2 and MRI 3 were added to form the variable 'volume of delayed cerebral infarction'. Quantification was performed by manual delineation of lesions using the MRICron software (<https://www.nitrc.org/projects/mricron>). To determine the shortest distance between the lesions and the electrodes, all images were coregistered to the T1-weighted images of MRI 1. Neuroimage analysis was performed blinded to clinical and neuromonitoring data.

For the third part of this work (30), intracranial hemorrhage was segmented on the CT scan at admission into 6 predefined classes in the ipsilateral hemisphere to the ECoG

electrodes (Table 2). We chose 6 segmentation classes instead of an overall approach since we were interested in the location-specific vulnerability of the brain concerning the blood distribution. The volumes of hemorrhage were manually delineated using ITK-Snap (<http://www.itksnap.org/pmwiki/pmwiki.php>). We chose ITK-SNAP because the drawing tool allows more precise region-of-interest drawings compared to MRIcron's drawing tool. In MRIcron, a region-of-interest is created by drawing the boundary of the region of interest, whereas in ITK-SNAP, a region-of-interest is drawn pixel by pixel. Quantification of hemorrhage volumes was performed in a blinded fashion nine months after the analysis of delayed cerebral infarction. In contrast to DISCHARGE-1, ipsilateral delayed cerebral infarction was further segmented into 5 classes (Table 2). This segmentation allowed an accurate analysis between delayed cerebral infarcts and potential mediators of delayed infarcts. For example, the association between delayed middle cerebral artery (MCA) infarcts and angiographic vasospasm in the MCA could be studied.

Table 1: Variables of the manual neuroimage analysis in DISCHARGE-1 (29). (own table)

Variable	Image modality	Image sequence	Segmentation classes	Quantification software
ICH	CT on admission	CT	Ipsi-, contralateral hemisphere, infratentorial	MRIcron
ECI	MRI 1 or CT	DWI, FLAIR, (CT)	Ipsi-, contralateral hemisphere, infratentorial	MRIcron
Delayed cerebral infarction	MRI 2 and 3 or CT	DWI, FLAIR, (CT)	Ipsi-, contralateral hemisphere, infratentorial	MRIcron

CT: computed tomography, DISCHARGE-1: Depolarizations in ISCHemia after subARachnoid hemorrhage-1, DWI: diffusion-weighted imaging, ECI: early cerebral infarction, FLAIR: fluid-attenuated inversion recovery, ICH: intracerebral hemorrhage, MRI: magnetic resonance imaging.

2.4 ECoG, DSA and TCD analysis

ECoG analysis was carried out in accordance with the recommendations of the COSBID group (35). First, SDs were identified as an abrupt negative DC shift in the full band ECoG signal. SDs were differentiated if they developed in electrically active tissue or not (isoelectric SD). SDs, which were less than 1 hour apart, were denoted as clustered SDs. Second, SD-induced spreading depression was observed in the filtered ECoG signal at 0.5 – 45Hz as a reduction in the amplitudes of spontaneous electrical brain activity. The total SD-induced depression duration (TDDD) was calculated for every recording day by

summation of the depression duration of each SD within that day. Furthermore, the number of SDs of any type, the number of isoelectric SDs and the number of clustered SDs were determined for every recording day. Finally, peak values of a recording day were determined for the 4 SD-parameters: (i) the peak total SD-induced depression duration (PTDDD), (ii) the peak number of SDs of any type ($peak_{SD}$), (iii) the peak number of isoelectric SDs ($peak_{isoSD}$) and (iv) the peak number of clustered SDs ($peak_{clusSD}$). These four peak values were determined for the early period (Day 0 – 3), the delayed period (Day 4 – 14) and the entire period (Day 0 – 14).

Table 2: Neuromonitoring and neuroimaging variables in the substudy of DISCHARGE-1 (30). (own table)

Variable	Explanation	Modality	Quantification software
$blood_{convex}$	Subarachnoid blood volume on the cerebral convexity ipsilateral to the ECoG electrodes	CT on admission	ITK-SNAP
$blood_{inter}$	Subarachnoid blood volume in the interhemispheric fissure	CT on admission	ITK-SNAP
$blood_{Sylvian}$	Subarachnoid blood volume in the Sylvian fissure ipsilateral to the ECoG electrodes	CT on admission	ITK-SNAP
$blood_{basal}$	Subarachnoid blood volume in the basal cisterns ipsilateral to the ECoG electrodes	CT on admission	ITK-SNAP
ICH	Intracerebral hemorrhage in the ipsilateral hemisphere to the ECoG electrodes	CT on admission	ITK-SNAP
IVH	Intraventricular hemorrhage ipsilateral to the ECoG electrodes	CT on admission	ITK-SNAP
DCI_{ACA}	Delayed infarct volume in the cortical territory of the ACA ipsilateral to the ECoG electrodes	MRI or CT in the delayed period	MRICron
DCI_{MCA}	Delayed infarct volume in the cortical territory of the MCA ipsilateral to the ECoG electrodes	MRI or CT in the delayed period	MRICron
DCI_{PCA}	Delayed infarct volume in the cortical territory of the PCA ipsilateral to the ECoG electrodes	MRI or CT in the delayed period	MRICron
$DCI_{watershed}$	Delayed infarct volume in the territory of the cortical watershed zones	MRI or CT in the delayed period	MRICron
DCI_{deep}	Delayed infarct volume below the cortex, including perforator infarcts, singular white matter infarcts without cortical involvement, and anterior choroidal artery infarcts	MRI or CT in the delayed period	MRICron

Variable	Explanation	Modality	Quantification software
PTDDD _{de-layed}	Peak value of a recording day for the total cumulative SD-induced depression durations during the delayed period	ECoG	LabChart-8
peak _{SD-de-layed}	Peak number of SDs of any type of a recording day during the delayed period	ECoG	LabChart-8
peak _{KisoSD-de-layed}	Peak number of isoelectric SDs of a recording day during the delayed period	ECoG	LabChart-8
peak _{clusSD-delayed}	Peak number of clustered SDs of a recording day during the delayed period	ECoG	LabChart-8
mbf _{VACA}	Peak mean blood flow velocity of the ACA	TCD	None
mbf _{VMCA}	Peak mean blood flow velocity of the MCA	TCD	None
mbf _{VPCA}	Peak mean blood flow velocity of the PCA	TCD	None
DSA _{A1}	Digital subtraction angiography score of the A1-segment of the ACA (1 = no, 2 = mild, 3 = moderate, 4 = severe vasospasm)	DSA	OsiriX
DSA _{A2}	Digital subtraction angiography score of the A2-segment of the ACA	DSA	OsiriX
DSA _{M1}	Digital subtraction angiography score of the M1-segment of the MCA	DSA	OsiriX
DSA _{M2}	Digital subtraction angiography score of the M2-segment of the MCA	DSA	OsiriX
DSA _{P1}	Digital subtraction angiography score of the P1-segment of the PCA	DSA	OsiriX
DSA _{P2}	Digital subtraction angiography score of the P2-segment of the PCA	DSA	OsiriX

ACA: anterior cerebral artery, CT: computed tomography, DISCHARGE-1: Depolarizations in ISChemia after subARachnoid hemorrhage-1, DSA: digital subtraction angiography, ECoG: electrocorticography, MCA: middle cerebral artery, PCA: posterior cerebral artery, SD: spreading depolarization, MRI: magnetic resonance imaging, TCD: transcranial Doppler-sonography.

Assessment of angiographic vasospasm followed the widely-used grading score in no (<11% = 1), mild (11 – 33% = 2), moderate (34 – 66% = 3) and severe (67 – 100% = 4) vascular narrowing (36). The semi-quantitative analysis included the A1- and A2-segment of the ACA, the M1- and M2-segment of the MCA and the P1- and P2-segment of the posterior cerebral artery (PCA). If an initial DSA was available, it was used for comparison with the DSA performed around day 7. An ipsilateral DSA score (DSAS) was

then calculated for every patient by dividing the total score achieved by the number of vessels assessed.

TCD of the cerebral arteries was performed daily during neurocritical care. Peak values of the mbfv were determined from daily measurements for the ACA (mbfv_{ACA}), MCA (mbfv_{MCA}) and PCA (mbfv_{PCA}).

2.5 Statistics

Descriptive data are given in the text as median and interquartile range (1st quartile – 3th quartile) unless otherwise specified. Group-wise comparison of categorical data were carried out using Fisher's exact test for small sample sizes or using the Chi-squared test for large sample sizes. The Mann-Whitney U-test was used for group comparison of ordinal or continuous data.

We performed receiver operating characteristic (ROC) analysis with a predefined cutoff of 60 minutes to test the main hypothesis of DISCHARGE-1 (29) that the SD-parameter 'PTDDD_{delayed}' predicts delayed cerebral infarction in the ipsilateral hemisphere to the ECoG electrodes with a sensitivity of >60% and a specificity of >80%. In a secondary analysis, a new cutoff for PTDDD_{delayed} was derived. ROC analysis was also carried out for the DSAS and the ipsilateral mbfv_{MCA} and their performances were compared to PTDDD_{delayed}. Moreover, we performed association analyses to investigate the relationship between diagnostic variables (SD-variables, DSAS, mbfv_{MCA}) and the primary endpoint parameters 'early focal brain injury' and 'delayed cerebral infarction'. In a first step, we carried out logarithmic transformations so that the data approximately conformed to normality. In a second step, we used Pearson correlation for a bivariate association analysis. The same procedure was applied in the prognostic part of DISCHARGE-1 (29). Functional outcome after 7 months was set as the secondary endpoint parameter and the diagnostic variables and the volumes of focal brain damage were potential predictors.

For the third study (30), the data were not transformed. Spearman correlation was used to explore the association between blood variables, potential mediators (SD-variables, angiographic vasospasm, TCD-variables), and infarct variables. In a second step principal component analysis was carried out to reduce the dimensionality of the data. The first principal component was used for the subsequent path analysis in SPSS Amos. Amos is a structural equation modeling software.

All tests of significance were two-tailed. The level of significance was set at $p < 0.05$. Statistical analysis was performed using SPSS Version 26 and SigmaPlot Version 14.0. The statistical analyses were performed by the trial statistician of DISCHARGE-1, Prof. Peter Martus, University of Tübingen.

3 Results

3.1 Study population

All patients, who were included in this work, were participants of the DISCHARGE-1 trial. Table 1 summarizes basic demographic, clinical and admission radiographic features of the three study populations.

Table 3: Characteristics of the study populations (28-30). (Table adapted from Supplementary Table 1 in Dreier *et al.*, 2022 (29))

	Study 1 (28)	Study 2 (29)	Study 3 (30)
N of patients	23	180	136
Age, median (IQR)	57 (46 – 63)	55 (47 - 63)	56 (47 – 63)
Female	14 (60.9%)	121 (67.2%)	90 (66.2%)
WFNS, median (IQR) modified Fisher scale	3 (1 – 5)	4 (2 – 5)	4 (2 – 5)
1	0	6 (3.3%)	4 (2.9%)
2	0	5 (2.8%)	3 (1.8%)
3	5 (21.7%)	34 (18.9)	24 (17.5%)
4	18 (78.3%)	135 (75%)	105 (77.2%)
mHSS, median (IQR)	19 (15 – 27)	22 (15 – 29)	22 (16 – 29)
Aneurysm location			
ACoA	23 (100%)	62 (34.4%)	49 (36.0%)
ACA	0	8 (4.4%)	8 (5.8%)
MCA	0	67 (37.2%)	46 (33.6%)
ICA	0	11 (6.1%)	6 (4.4%)
PCoA	0	25 (13.9%)	21 (15.3%)
Posterior circulation	0	7 (3.9%)	6 (4.4%)
Clipping	14 (60.9%)	161 (89.4%)	120 (88.1%)
eGOS, median (IQR)	3 (1 – 6)	4 (1 – 7)	4 (3 – 7)

ACoA: anterior communicating artery, ACA: anterior cerebral artery, eGOS: extended Glasgow Outcome Scale, mHSS: modified Hijdra Sum Score, ICA: internal carotid artery, IQR: interquartile range, MCA: middle cerebral artery, N: number, PCoA: posterior communicating artery, WFNS: World Federation of Neurosurgical Societies grading scale.

3.2 Early brain injury

We first conducted a pilot study about early brain injury (Day 0 – 3) after aSAH (28). The study consisted of an experimental part and a clinical part. Only the results from the clinical study are reported here, as the experimental animal study was conducted by our collaborators in Cincinnati, USA. A total of 23 patients with aSAH from an ACoA aneurysm were included in the clinical study. Postoperative MRI on Day 2 (IQR 2 – 3) demonstrated ECI in the frontal territories of the ACAs in 7 (30.4%) patients. The median infarct volume was 13ml (IQR 8 – 56ml). Frontal ICH occurred in 4 (17.4%) patients. The median ICH volume was 35ml (IQR 20.5 – 39.75ml). One patient had ECI and ICH. Eleven patients (47.8%) had no early focal lesions in the frontal ACA territories. The modified Hijdra score of the interhemispheric fissure - adjacent to the frontal ACA territory - was higher in patients with early focal lesions than in patients without lesions [median score 4.0 (IQR: 3.8 – 4.0) versus 3.0 (IQR: 2.0 – 3.5), Mann-Whitney U-test, $p = 0.045$]. SDs occurred more often in patients with early focal lesions than in patients without lesions (10/12 versus 1/11, Fisher's exact test, $p < 0.001$). The median of the early SD-parameters $PTDDD_{early}$ and $peak_{SD-early}$ were also higher in the lesion group than in the no-lesion group ($PTDDD_{early}$: 109.8min versus 0min, $p < 0.001$; $peak_{SD-early}$: 12.6 versus 0, Mann-Whitney U-test, $p < 0.001$).

DISCHARGE-1 also dealt with early brain injury in patients with aSAH (29). Volumes of ECI and ICH are given in Table 4. Correlation analyses between early brain injury (ECI+ICH) in the ipsilateral hemisphere to the ECoG electrodes and the early SD-parameters confirmed the preliminary results of the pilot study. $PTDDD_{early}$ showed a strong correlation with ipsilateral ECI+ICH (Pearson correlation coefficient $r = 0.55$, $p < 0.0001$), followed by $peak_{SD-early}$ ($r = 0.48$, $p < 0.0001$), $peak_{clusSD-early}$ ($r = 0.38$, $p < 0.0001$) and $peak_{isoSD-early}$ ($r = 0.35$, $p < 0.0001$). The results remained significant after Bonferroni correction for multiple testing. Of note, the volume of ipsilateral early brain injury (ECI+ICH) was not correlated with the volume of ipsilateral delayed infarction (Spearman rank order correlation coefficient $r_s = 0.110$, $p = 0.152$).

3.3 Delayed cerebral infarction

In DISCHARGE-1 (29), the main objective was to determine the diagnostic accuracy of ECoG in comparison to known diagnostics such as DSA, TCD, and clinical scores for predicting delayed cerebral infarction. Two hundred five patients were allocated at six

participating centers. One hundred eighty patients were included in the final analysis. As 10 patients died in the early period, 170 patients were included in the analyses related to delayed cerebral infarction. The incidence and the lesion volumes of delayed cerebral infarction are given in Table 4. Manual segmentation of ECI, ICH and delayed infarction was compared with a semi-automated approach from our collaborative partner (8). The correlation was very good ($r_s = 0.811$, $p < 0.0001$). The ipsilateral DSAS could be calculated in 122/170 (71.8%) patients. The ipsilateral $mbfv_{MCA}$ was available in 157/170 (92.4%) patients.

Table 4: Lesion volumes of the manual neuroimage analysis in DISCHARGE-1 (29). (own table)

	Number of patients/ total number of patients (%)	Mean volume \pm std [ml]	Max volume in a single patient [ml]	Cumulative volume over all patients (%) [ml]
ECI				
Ipsilateral	114/180 (63.3%)	19.9 \pm 56.3	402	3589.7
Contralateral	57/180 (31.7%)	6.2 \pm 23.6	233	1121.3
Infratentorial	17/180 (9.4%)	0.8 \pm 4.5	53	136.9
Total	123/180 (68.3%)	26.9 \pm 66.8	430	4847.9 (33.4%)
ICH + subarachnoid hematoma				
Ipsilateral	82/180 (45.6%)	17.0 \pm 28.6	131	3065
Contralateral	25/180 (13.9%)	2.2 \pm 8	66	390.4
Infratentorial	3/180 (1.7%)	0.2 \pm 2.3	31	33
Total	95/180 (52.8%)	19.4 \pm 29.1	131	3488.4 (24%)
Delayed cerebral infarction				
Ipsilateral	90/170 (52.9%)	22.7 \pm 52.1	260	3861.4
Contralateral	45/170 (26.5%)	13.2 \pm 45.9	313	2241.2
Infratentorial	16/170 (9.4%)	0.5 \pm 2.6	26	80.7
Total	98/170 (57.6%)	36.4 \pm 80.1	459	6183.3 (42.6%)

DISCHARGE-1: Depolarizations in ISCHemia after subARachnoid hemorrhage-1, ECI: early cerebral infarction, ICH: intracerebral hemorrhage, std: standard deviation.

First, we performed bivariate correlation analyses to explore the association between the diagnostic variables for the delayed period and the outcome parameter 'ipsilateral volume of delayed infarction'. All four delayed SD-parameters correlated with the ipsilateral volume of delayed infarction (PTDDD_{delayed}: $r = 0.54$; peak_{SD-delayed}: $r = 0.42$; peak_{isoSD-delayed}: $r = 0.41$; peak_{clusSD-delayed}: $r = 0.37$; all four p values < 0.0001). In contrast,

the ipsilateral DSAS showed a weak correlation with delayed infarction ($r = 0.19$, $p = 0.035$). The correlation with the ipsilateral mbf_{MCA} was $r = 0.21$, $p = 0.007$.

To help clinicians to draw a line between patients who develop delayed infarction and patients who do not develop delayed infarction, we carried out ROC analyses for the SD-parameter $\text{PTDDD}_{\text{delayed}}$, the ipsilateral DSAS, and the $\text{peak}_{\text{mbfv}}$ of the ipsilateral MCA. $\text{PTDDD}_{\text{delayed}}$ showed a sensitivity of 0.76 and a specificity of 0.59 for a pre-defined cutoff value of 60 minutes. The area under the receiver operating curve (AUROC) was 0.76 (CI: 0.69 – 0.83, $p < 0.0001$) and substantially higher than the AUROC for the ipsilateral DSAS (0.64, CI: 0.54 – 0.74, $p = 0.0087$) and the ipsilateral mbf_{MCA} (0.63, CI: 0.55 – 0.72, $p = 0.0042$). In a secondary analysis, we calculated a new cut-off for $\text{PTDDD}_{\text{delayed}}$ based on a cost ratio of 1.0, i.e., equal costs for both false negatives and false positives. The new cut-off of 180min $\text{PTDDD}_{\text{delayed}}$ indicated delayed infarction with a targeted sensitivity of 0.62 and a specificity of 0.83, thus exceeding the prespecified sensitivity of 0.60 and specificity of 0.80.

Finally, we performed prognostic analyses to assess whether the diagnostic variables also predict clinical outcome at 7 months. Clinical outcome was assessed using the extended Glasgow Outcome Scale (eGOS). Of 24 predictive variables from clinical scores, neuromonitoring parameters and imaging parameters, the ipsilateral volume of early plus delayed brain injury (ICH + ECI + delayed cerebral infarction) was among the most predictive factors in univariate correlation analysis ($r = -0.55$, $p < 0.0001$).

3.4 Paths from initial hemorrhage to delayed cerebral infarction

In the substudy of DISCHARGE-1 (30), we sought to determine statistical paths from initial hemorrhage via potential pathophysiological mediators to delayed cerebral infarction. One hundred thirty-six patients were included in the final analysis. Delayed cerebral infarcts ipsilateral to the ECoG electrodes occurred in 69/136 (50.7%) patients with a total cumulative volume over all patients of 2599.7ml. Furthermore, 70.8% of the total cumulative infarct volume developed in the cortical MCA territory, 15% in the cortical ACA territory, 5.6% in the cortical PCA territory and 1.7% in the cortical watershed regions. Deep infarcts accounted for 6.9% of the total ipsilateral infarct volume. The initial CT revealed ipsilateral ICH in 39 patients (28.7%, mean volume 8.1 ± 20.5 ml), ipsilateral intraventricular

hemorrhage (IVH) in 110 patients (80.3%, mean volume 4.3 ± 10.6 ml) and large subarachnoid hematomas with space-occupying effect in 22 patients (16.2%). The mean volume of ipsilateral SAH was 18.3 ± 16.1 ml.

In a first step, we explored correlations between region-specific blood volumes, so-called mediators and region-specific infarct volumes. An elaborate depiction of the correlations is given in the original publication (30). In short, the largest correlation between blood variables and infarct volumes was found between blood on the cerebral convexity ($\text{blood}_{\text{convex}}$) and delayed infarcts in the cortical territory of the MCA (DCI_{MCA}) ($r_s = 0.32$, $p < 0.001$). All 4 SD-parameters correlated with $\text{blood}_{\text{convex}}$ and blood in the Sylvian fissure ($\text{blood}_{\text{Sylvian}}$) ($r_s = 0.21 - 0.30$, all eight p values < 0.05). The most remarkable finding between angiographic vasospasm and region-specific blood volumes was that 4 of 6 DSA-parameters significantly correlated with the ipsilateral volume of IVH ($r_s: 2.0 - 3.5$, all four p values < 0.05). Looking at TCD velocities, only the ipsilateral mbf_{MCA} was significantly correlated with DCI_{MCA} but did not remain significant after Bonferroni correction. Thus, TCD was not considered as a mediator variable and was not included in further analyses.

In a second step, we carried out principal component analysis to reduce the dimensionality of the data. Only the first component of the blood variables, the SD-parameters, the DSA-parameters and the infarct variables were included in the final path analysis. Path analysis showed that the first component of the SD-parameters mediated the detrimental effect of subarachnoid hemorrhage, leading to cortical infarction. DSA remained an extrinsic variable without a mediating effect from hemorrhage to infarction. In a last model, IVH was included. We found a path from IVH via DSA to cortical infarction. An elaborate depiction of the path models can be found in Figure 5 in the original publication (30).

3.5 Illustrative cases

Figure 2 and figure 3 illustrate the main categories of focal brain injury in patients with aSAH. For DISCHARGE-1 (29), ICH (Figure 2) was defined as any collection of blood within the cerebral parenchyma and/or any large subarachnoid clots in the basal cisterns, which also extended into brain tissue. For the substudy of DISCHARGE-1 (30), large subarachnoid blood clots and ICH were differentiated following the approach by Zande and colleagues (37).

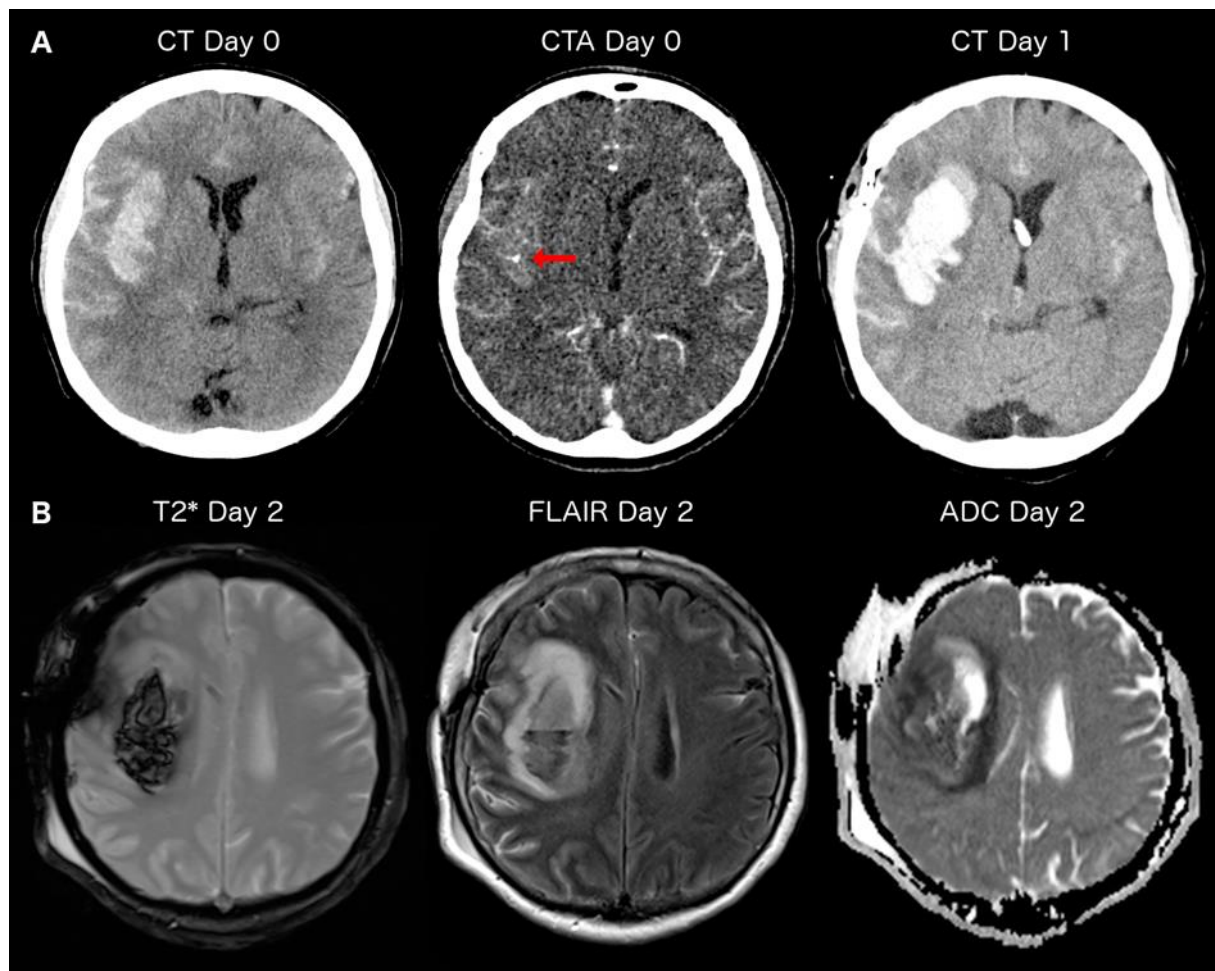


Figure 2: The continuum between intracerebral hemorrhage (ICH) and subarachnoid hematoma illustrated in a DISCHARGE-1 (Depolarizations in ISCHemia after subARachnoid hemorrhage-1) patient (29). (own figure)

Representative images of computed tomography (CT), CT angiography and magnetic resonance imaging (MRI) in axial orientation of a patient with aneurysmal subarachnoid hemorrhage (aSAH) from a right middle cerebral artery (MCA) aneurysm. **Panel A:** The female patient was admitted to the emergency department after a sudden onset of a thunderclap headache with transient loss of consciousness. The initial CT 1.5 hours after onset of symptoms demonstrated subarachnoid hemorrhage with a large right-sided hematoma (left image). CT angiography revealed a berry aneurysm with a diameter of 5mm originating from the right MCA bifurcation. Contrast-enhancing vessels were found within the large hematoma (red arrow). The hematoma was thus categorized as a Sylvian hematoma. The first postoperative CT on day 1 showed periprocedural rebleeding with expansion of the Sylvian hematoma. Since the volume of rebleeding exceeded 10ml, this case was excluded from analysis in the substudy of DISCHARGE-1 (30). **Panel B:** The first postoperative MRI was performed on Day 2. The T2* images again demonstrated the large Sylvian hematoma (hypointense signal), which also extended into the cerebral parenchyma (left image).

Fluid-attenuated inversion recovery (FLAIR) imaging revealed perihematomal hyperintensity consistent with perihematomal edema. The corresponding area was hypointense on the apparent diffusion coefficient (ADC) map. These findings were consistent with cytotoxic edema surrounding the large Sylvian hematoma. For DISCHARGE-1 (29), the volume of the Sylvian hematoma was quantified and assigned to the category ‘intracerebral hemorrhage’ since it partly extended into the cerebral parenchyma. The surrounding cytotoxic edema was not quantified following the recommendations of Vergouwen and colleagues (34).

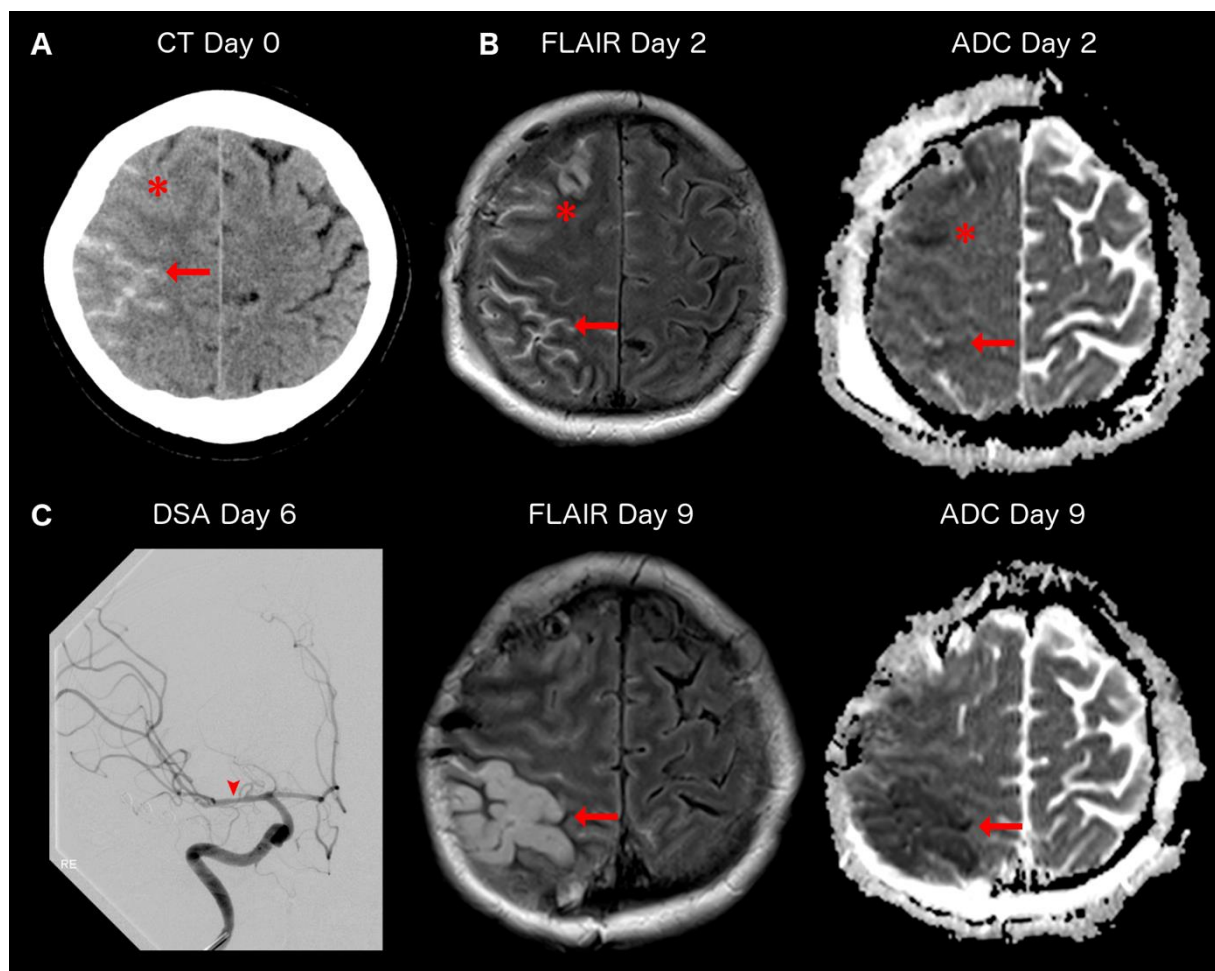


Figure 3: Early and delayed cerebral infarction adjacent to blood clots at the cerebral convexity in absence of severe angiographic vasospasm illustrated in the same DISCHARGE-1 (Depolarizations in ISChemia after subARachnoid hemorrhage-1) patient (29). (own figure)

Representative images of computed tomography (CT), magnetic resonance imaging (MRI) and digital subtraction angiography (DSA) of the same patient with aneurysmal subarachnoid hemorrhage (aSAH) as in Figure 2. **Panel A:** In addition to the large Sylvian hematoma (Figure 2), the initial CT scan on Day 0 demonstrated dense blood clots in the sulci of the right cerebral convexity. **Panel B:** The first postoperative MRI on Day 2 showed hyperintense signal abnormalities in the

same sulci at the right convexity on fluid-attenuated inversion recovery (FLAIR) consistent with subarachnoid blood (asterisk and arrow). A frontal sulcus (asterisk) appeared hyperintense on the FLAIR image and hypointense on the apparent diffusion coefficient (ADC) map. These findings are consistent with early cerebral infarction (ECI) adjacent to a sulcal blood clot. **Panel C:** The angiogram of the right internal carotid artery (ICA) and its branches on day 6 only demonstrated mild vasospasm of the right proximal segment (M1) of the middle cerebral artery (MCA) (arrowhead in the left image). However, MRI on day 9 revealed delayed cortical MCA infarction (hyperintense on FLAIR and hypointense on the ADC map) of the parietal sulci, which were filled with blood on the admission CT scan (arrows).

4 Discussion

4.1 Short summary of results

We quantified the amount of cerebral infarction and the amount of hemorrhage in patients with aSAH using neuroimaging data. Focal brain injury of the entire period (ICH + ECI + delayed cerebral infarction) showed a strong correlation with clinical outcome among 24 clinical or neuromonitoring variables. Most importantly, ECI and delayed cerebral infarction were both associated with the occurrence of SDs. The SD-parameter 'PTDDD_{delayed}' achieved a sensitivity of 76% and a specificity of 59% in our primary ROC analysis. In the secondary analysis with a new cutoff of 180min, PTDDD_{delayed} indicated delayed cerebral infarction with a targeted sensitivity of 62% and a specificity of 83%. The overall ability of PTDDD_{delayed} to discriminate between patients with delayed infarction and patients without delayed infarction was much better than it was for angiographic vasospasm or TCD (AUROC 0.76 versus 0.64 and 0.63 respectively). In addition to the promising diagnostic benefit of ECoG, ECoG also allowed us to gain insight into the pathogenesis of cerebral infarcts following aSAH. We found a statistically significant path from the amount of SAH to the occurrence of SDs in the delayed period to the development of delayed cortical infarcts. Noteworthy, blood_{convex} was included in the path. To the best of our knowledge, this has never been described in humans before. Another path was found from IVH to angiographic vasospasm to delayed cortical infarction.

4.2 Interpretation of results

It was previously proposed that cerebral infarction and functional outcome should be the main outcome measures in clinical aSAH studies (34). Our results confirm this notion as we found a strong association between functional outcome and focal brain injury. Functional outcome is certainly the most important parameter for the well-being of the patient as well as for the verification of effective therapies. However, it is an overall parameter that does not allow conclusions to be drawn about the underlying cause or pathomechanism. Thus, our primary analyses were carried out with lesion incidences or lesion volumes derived from neuroimaging. Since MRI is more sensitive in detecting cerebral infarction than CT (38), the incidence of ECI (68.7%) and delayed cerebral infarction (57.6%) was high in our cohort. However, the incidences are comparable to other MRI-based studies (10). When considered separately, as in the substudy of DISCHARGE-1

(30), the incidence of ICH (28.7%) was similar to other reports (11, 39). Angiographic vasospasm was not predictive for functional outcome. This is in accordance with the result of a meta-analysis, where 14 pharmaceutical studies randomizing 4,235 patients were included (40). Despite a significant reduction in angiographic vasospasm no effect on functional outcome was found. In the past, many pharmaceutical trials were designed to prevent angiographic vasospasm. Although a certain pathophysiological role of angiographic vasospasm in the development of delayed cerebral infarction is undisputed, our results are consistent with a body of literature which questions that angiographic vasospasm is the predominant etiology of delayed infarction and an appropriate outcome measure in clinical trials (41).

SD is a phenomenon that only occurs under pathological conditions in the human brain (42). Our results support this hypothesis as SDs were associated with cerebral infarction in the early and delayed period after aSAH. In fact, SD and the initiation of cerebral infarction are inevitably linked through the formation of the so-called neuronal 'cytotoxic edema'. Cytotoxic edema is characterized by a net influx of water and ions from the extracellular space into the intracellular space leading to beading of neuronal dendrites (43). The same process is evident by high signal intensity on diffusion MRI (44, 45) and is also recorded as a negative DC shift (SD) on ECoG (46). Why did we not observe a perfect match between SD and cerebral infarction then? First, SD-induced cytotoxic edema is reversible up to a certain point, so infarction does not occur (47, 48). We believe DISCHARGE-1 might have failed to meet the primary endpoint for this reason. The sensitivity was 76% for the predefined cut-off of 60min PTDDD_{delayed} but the specificity was 59%, which was below 80% of our primary hypothesis. In the secondary analysis with a new cut-off of 180min PTDDD_{delayed}, sensitivity was 62% and specificity was 83% and thus above the values of our primary hypothesis. Consequently, the longer the cut-off for PTDDD, the more specifically it indicates cerebral infarction. With increasing PTDDD, the probability decreases that SD-induced cytotoxic edema is reversible. Second, the 6 ECoG electrodes only covered a distance of 5cm of the cortex. Although SDs spread over long distances, we certainly did not record all SDs in the ipsilateral hemisphere due to the small recording area. Third, diffusion MRI detects cytotoxic edema with highest sensitivity (49), but continuous MRI is not feasible in a clinical setting. We performed 2 to 3 imaging sessions in the entire ECoG recording period that allowed us to detect irreversible cytotoxic edema, i.e., cerebral infarction, but not reversible edema. This may also have re-

duced the diagnostic accuracy of ECoG. Nonetheless, a major advantage was the continuity of ECoG recording compared to daily or even weekly measurements of other diagnostic modalities. It allowed stratification of patients at risk for the development of cerebral infarction and patients at low risk for cerebral infarction. Furthermore, diagnostic accuracy of ECoG was better than the diagnostic performances of DSA and TCD (AUROC 0.76 versus 0.64 and 0.63 respectively). These results are consistent with meta-analyses in which the diagnostic performance of DSA and TCD is also low to moderate (50, 51).

In the autopsy study of Stoltenburg-Didinger and Schwarz, the authors found cortical infarcts predominantly in areas covered with subarachnoid blood (52). The same pattern was recently found in a case with traumatic SAH (53). These findings suggest that the exposure of blood alone is sufficient to trigger adjacent cortical infarction. Our results show this to be true for both ECI and delayed cerebral infarcts. Frontal ECI in the ACA territory was significantly correlated with local blood collection, i.e. the modified Hijdra score of the interhemispheric fissure, but not with the modified Hijdra Sum Score. Thus, the presence of local blood seems to be more important than the overall distribution of blood for ECI. We found a similar situation for delayed cerebral infarction. The largest correlation was between blood in the sulci of the cerebral convexity ($\text{blood}_{\text{convex}}$) and underlying infarcts in the MCA territory (DCI_{MCA}). This, however, raises the question of why most rating scales ignore the presence of blood on the cerebral convexity. First, CT scanners that were used in the studies of the 80s and 90s had a lower spatial resolution and thus, were not able to demonstrate thin blood in the sulci on the cerebral convexity accurately. Second, early studies often investigated the association between angiographic vasospasm and SAH and thus, focused on cisternal blood adjacent to the major cerebral arteries (54). In this work, we cannot explain the exact pathomechanism, which details how extravasated blood induces cerebral infarction, but we found SD to be a statistical mediator between blood and delayed cortical infarction. Whether factors released from the blood clot such as potassium and hemoglobin directly induce SDs or whether factors released from the blood clot first trigger microvascular constriction, which in turn lowers the threshold for SD, remains enigmatic.

The association between IVH and delayed cerebral infarcts is well described (55). Hijdra and colleagues were the first, who found IVH to be an additional risk factor for the development of DCI (56). Since the original Fisher scale had a focus exclusively on cisternal SAH, the scale was revised in the 2000s due to growing evidence that IVH also contributes to the development of DCI (9, 57). We quantified the volume of IVH instead

of using the modified Fisher Scale or the mHSS since volume measurements achieve better accuracy for predicting DCI (58). Only two studies also quantified the volume of IVH separately rather than using qualitative or semi-quantitative grading scales. Ko and colleagues showed that the median volume of IVH was higher in patients with DCI than in patients without DCI (59). The result was confirmed by the second study although the odds ratio was not significant in the logistic regression model for IVH (1.02; CI: 1.00 – 1.04) (60). The authors suggested that it might be due to a lack of power although 282 patients were included. Hijdra and colleagues postulated that the detrimental effect of IVH is explained by consecutive hydrocephalus leading to microcirculatory impairment. We observed a pathophysiological sequence from IVH via angiographic vasospasm to delayed cortical infarction. This has rarely been investigated systematically since most studies only performed late angiography when vasospasm was suspected because of clinical deterioration. Inagawa and colleagues reported an association between IVH and severe vasospasm among 370 patients with angiography between day 7 and 9 (61). However, the relation was not significant in multivariate analysis. Of note, angiographic vasospasm occurs in isolated IVH of patients with ruptured arteriovenous malformation (62). We believe that IVH similar to cisternal clots might serve as a reservoir for the delayed release of spasmogens. TCD was not predictive in our model. It brings into question the clinical importance of daily TCD measurements. Further investigations are warranted.

4.3 The current state of research

This translational work was designed to close a gap between experimental stroke research and clinical application. Experimental neuroscientists have been dealing with SD for decades, while translation into clinical thinking has been rudimentary. Since 1998, it is known from animal experiments that hemoglobin in conjunction with potassium triggers SD and SD-induced cortical spreading ischemia, when released into the subarachnoid space due to lysis of erythrocytes (27). The present work in aSAH patients supports this concept by demonstrating a mediating role of SDs between subarachnoid blood and delayed cerebral infarction. It may pave the way for the development of effective therapies targeting SDs and spreading ischemia.

4.4 Strengths and limitations

This work has strengths and limitations. Strengths of our approach were serial imaging to detect early brain injury and delayed cerebral infarction, quantification of focal brain injury instead of qualitative evaluation, and an exhaustive use of MRI instead of CT. DISCHARGE-1 (29) and its related substudy (30) are among the largest MRI studies quantifying focal brain injury after aSAH (36, 63). A limitation is our manual quantification method, which is cumbersome and subjective. Automatic image recognition based on neural networks is increasingly used in neuroradiology (64). However, the implementation for severely damaged brains is not yet feasible. For example, even preprocessing steps such as brain extraction often fail in patients with aSAH (65). Nevertheless, our collaborators in Be'er Sheva, Israel, managed to develop a semi-automated method (8). When compared, the semi-automated approach is more objective, while our manual method has the advantage of distinguishing different pathologies, e.g. vasogenic edema from cytotoxic edema and ECI from delayed cerebral infarction. All in all, correlation analysis between both methods showed a very good agreement.

4.5 Implications for future research

Three aspects emerge from this work as worthy of future research. First, cerebral infarction should be used as a primary outcome parameter in further clinical trials aiming to prevent DCI as it is the strongest predictor for functional outcome. Second, ECoG has been found to be the more sensitive and specific diagnostic method to predict delayed cerebral infarction compared with DSA and TCD. Whether the translation of ECoG into the clinic will be successful has to be verified by feasibility studies. Third, it was found that SDs arise independently of angiographic vasospasm after aSAH and independently contribute to delayed infarction. Future pharmacological trials should target both, SDs and angiographic vasospasm, to improve patient outcome.

5 Conclusions

This work contributed to the DISCHARGE-1 trial (29) by quantifying the primary outcome parameter. A pilot study (28) and a substudy (30) confirmed the essential pathophysiological role of SD in the pathogenesis of focal brain injury in patients with aSAH. It is now time to acknowledge the multifactorial genesis of focal brain injury after aSAH and to translate this new concept into clinical practice for the benefit of the patients (15).

Reference list

1. Etminan N, Chang HS, Hackenberg K, de Rooij NK, Vergouwen MDI, Rinkel GJE, Algra A. Worldwide Incidence of Aneurysmal Subarachnoid Hemorrhage According to Region, Time Period, Blood Pressure, and Smoking Prevalence in the Population A Systematic Review and Meta-analysis. *Jama Neurol.* 2019;76(5):588-97.
2. Macdonald RL, Schweizer TA. Spontaneous subarachnoid haemorrhage. *Lancet.* 2017;389(10069):655-66.
3. Johnston SC, Selvin S, Gress DR. The burden, trends, and demographics of mortality from subarachnoid hemorrhage. *Neurology.* 1998;50(5):1413-8.
4. van Gijn J, Kerr RS, Rinkel GJ. Subarachnoid haemorrhage. *Lancet.* 2007;369(9558):306-18.
5. Nieuwkamp DJ, Setz LE, Algra A, Linn FH, de Rooij NK, Rinkel GJ. Changes in case fatality of aneurysmal subarachnoid haemorrhage over time, according to age, sex, and region: a meta-analysis. *Lancet Neurol.* 2009;8(7):635-42.
6. BEBIN J, CURRIER RD. Cause of Death in Ruptured Intracranial Aneurysms. *AMA Archives of Internal Medicine.* 1957;99(5):771-90.
7. Macdonald RL. Delayed neurological deterioration after subarachnoid haemorrhage. *Nat Rev Neurol.* 2014;10(1):44-58.
8. Lublinsky S, Major S, Kola V, Horst V, Santos E, Platz J, Sakowitz O, Scheel M, Dohmen C, Graf R, Vatter H, Wolf S, Vajkoczy P, Shelef I, Woitzik J, Martus P, Dreier JP, Friedman A. Early blood-brain barrier dysfunction predicts neurological outcome following aneurysmal subarachnoid hemorrhage. *EBioMedicine.* 2019;43:460-72.
9. Claassen J, Bernardini GL, Kreiter K, Bates J, Du YE, Copeland D, Connolly ES, Mayer SA. Effect of cisternal and ventricular blood on risk of delayed cerebral ischemia after subarachnoid hemorrhage: the Fisher scale revisited. *Stroke.* 2001;32(9):2012-20.
10. van der Kleij LA, De Vis JB, Olivot JM, Calviere L, Cognard C, Zuithoff NP, Rinkel GJ, Hendrikse J, Vergouwen MD. Magnetic Resonance Imaging and Cerebral Ischemia After Aneurysmal Subarachnoid Hemorrhage: A Systematic Review and Meta-Analysis. *Stroke.* 2017;48(1):239-45.
11. Platz J, Guresir E, Wagner M, Seifert V, Konczalla J. Increased risk of delayed cerebral ischemia in subarachnoid hemorrhage patients with additional intracerebral hematoma. *J Neurosurg.* 2017;126(2):504-10.
12. Broderick JP, Brott TG, Duldner JE, Tomsick T, Leach A. Initial and recurrent bleeding are the major causes of death following subarachnoid hemorrhage. *Stroke.* 1994;25(7):1342-7.
13. Frontera JA, Fernandez A, Schmidt JM, Claassen J, Wartenberg KE, Badjatia N, Connolly ES, Mayer SA. Defining Vasospasm After Subarachnoid Hemorrhage What Is the Most Clinically Relevant Definition? *Stroke.* 2009;40(6):1963-8.
14. Rosengart AJ, Schultheiss KE, Tolentino J, Macdonald RL. Prognostic factors for outcome in patients with aneurysmal subarachnoid hemorrhage. *Stroke.* 2007;38(8):2315-21.
15. Pluta RM, Hansen-Schwartz J, Dreier J, Vajkoczy P, Macdonald RL, Nishizawa S, Kasuya H, Wellman G, Keller E, Zauner A, Dorsch N, Clark J, Ono S, Kiris T, Leroux P, Zhang JH. Cerebral vasospasm following subarachnoid hemorrhage: time for a new world of thought. *Neurol Res.* 2009;31(2):151-8.
16. Ecker A, Riemenschneider PA. Arteriographic demonstration of spasm of the intracranial arteries, with special reference to saccular arterial aneurysms. *J Neurosurg.* 1951;8(6):660-7.

17. Weir B, Grace M, Hansen J, Rothberg C. Time course of vasospasm in man. *J Neurosurg.* 1978;48(2):173-8.
18. Macdonald RL, Higashida RT, Keller E, Mayer SA, Molyneux A, Raabe A, Vajkoczy P, Wanke I, Bach D, Frey A, Marr A, Roux S, Kassell N. Clazosentan, an endothelin receptor antagonist, in patients with aneurysmal subarachnoid haemorrhage undergoing surgical clipping: a randomised, double-blind, placebo-controlled phase 3 trial (CONSCIOUS-2). *Lancet Neurol.* 2011;10(7):618-25.
19. Macdonald RL, Higashida RT, Keller E, Mayer SA, Molyneux A, Raabe A, Vajkoczy P, Wanke I, Bach D, Frey A, Nowbakht P, Roux S, Kassell N. Randomized trial of clazosentan in patients with aneurysmal subarachnoid hemorrhage undergoing endovascular coiling. *Stroke.* 2012;43(6):1463-9.
20. Macdonald RL, Kassell NF, Mayer S, Ruefenacht D, Schmiedek P, Weidauer S, Frey A, Roux S, Pasqualin A, Investigators C-. Clazosentan to overcome neurological ischemia and infarction occurring after subarachnoid hemorrhage (CONSCIOUS-1): randomized, double-blind, placebo-controlled phase 2 dose-finding trial. *Stroke.* 2008;39(11):3015-21.
21. Leao AA. SPREADING DEPRESSION OF ACTIVITY IN THE CEREBRAL CORTEX. *Journal of Neurophysiology.* 1944;7(6):359-90.
22. Dijkhuizen RM, Beekwilder JP, van der Worp HB, van der Sprenkel JWB, Tulleken KAF, Nicolay K. Correlation between tissue depolarizations and damage in focal ischemic rat brain. *Brain Research.* 1999;840(1-2):194-205.
23. Dreier JP, Reiffurth C. The Stroke-Migraine Depolarization Continuum. *Neuron.* 2015;86(4):902-22.
24. Strong AJ, Fabricius M, Boutelle MG, Hibbins SJ, Hopwood SE, Jones R, Parkin MC, Lauritzen M. Spreading and synchronous depressions of cortical activity in acutely injured human brain. *Stroke.* 2002;33(12):2738-43.
25. Dreier JP, Woitzik J, Fabricius M, Bhatia R, Major S, Drenckhahn C, Lehmann TN, Sarrafzadeh A, Willumsen L, Hartings JA, Sakowitz OW, Seemann JH, Thieme A, Lauritzen M, Strong AJ. Delayed ischaemic neurological deficits after subarachnoid haemorrhage are associated with clusters of spreading depolarizations. *Brain.* 2006;129(Pt 12):3224-37.
26. Dreier JP, Major S, Manning A, Woitzik J, Drenckhahn C, Steinbrink J, Tolias C, Oliveira-Ferreira AI, Fabricius M, Hartings JA, Vajkoczy P, Lauritzen M, Dirnagl U, Bohner G, Strong AJ, Grp CS. Cortical spreading ischaemia is a novel process involved in ischaemic damage in patients with aneurysmal subarachnoid haemorrhage. *Brain.* 2009;132:1866-81.
27. Dreier JP, Körner K, Ebert N, Görner A, Rubin I, Back T, Lindauer U, Wolf T, Villringer A, Einhupl KM, Lauritzen M, Dirnagl U. Nitric oxide scavenging by hemoglobin or nitric oxide synthase inhibition by N-nitro-L-arginine induces cortical spreading ischemia when K⁺ is increased in the subarachnoid space. *J Cereb Blood Flow Metab.* 1998;18(9):978-90.
28. Hartings JA, York J, Carroll CP, Hinzman JM, Mahoney E, Krueger B, Winkler MKL, Major S, Horst V, Jahnke P, Woitzik J, Kola V, Du Y, Hagen M, Jiang J, Dreier JP. Subarachnoid blood acutely induces spreading depolarizations and early cortical infarction. *Brain.* 2017;140(10):2673-90.
29. Dreier JP, Winkler MKL, Major S, Horst V, Lublinsky S, Kola V, Lemale CL, Kang EJ, Maslarova A, Salur I, Luckl J, Platz J, Jorks D, Oliveira-Ferreira AI, Schoknecht K, Reiffurth C, Milakara D, Wiesenthal D, Hecht N, Dengler NF, Liotta A, Wolf S, Kowoll CM, Schulte AP, Santos E, Guresir E, Unterberg AW, Sarrafzadeh A, Sakowitz OW, Vatter H, Reiner M, Brinker G, Dohmen C, Shelef I, Bohner G, Scheel M, Vajkoczy P, Hartings JA,

- Friedman A, Martus P, Woitzik J. Spreading depolarizations in ischaemia after subarachnoid haemorrhage, a diagnostic phase III study. *Brain*. 2022;145(4):1264-84.
30. Horst V, Kola V, Lemale CL, Major S, Winkler MKL, Hecht N, Santos E, Platz J, Sakowitz OW, Vatter H, Dohmen C, Scheel M, Vajkoczy P, Hartings JA, Woitzik J, Martus P, Dreier JP. Spreading depolarization and angiographic spasm are separate mediators of delayed infarcts. *Brain Communications*. 2023;5(2).
31. Rosen DS, Macdonald RL. Grading of subarachnoid hemorrhage: modification of the world World Federation of Neurosurgical Societies scale on the basis of data for a large series of patients. *Neurosurgery*. 2004;54(3):566-75; discussion 75-6.
32. de Haan B, Clas P, Juenger H, Wilke M, Karnath HO. Fast semi-automated lesion demarcation in stroke. *Neuroimage Clin*. 2015;9:69-74.
33. Bretz JS, Von Dincklage F, Woitzik J, Winkler MK, Major S, Dreier JP, Bohner G, Scheel M. The Hijdra scale has significant prognostic value for the functional outcome of Fisher grade 3 patients with subarachnoid hemorrhage. *Clin Neuroradiol*. 2016.
34. Vergouwen MDI, Vermeulen M, van Gijn J, Rinkel GJE, Wijndicks EF, Muizelaar JP, Mendelow AD, Juvela S, Yonas H, Terbrugge KG, Macdonald RL, Diringner MN, Broderick JP, Dreier JP, Roos YBWEM. Definition of Delayed Cerebral Ischemia After Aneurysmal Subarachnoid Hemorrhage as an Outcome Event in Clinical Trials and Observational Studies Proposal of a Multidisciplinary Research Group. *Stroke*. 2010;41(10):2391-5.
35. Dreier JP, Fabricius M, Ayata C, Sakowitz OW, William Shuttleworth C, Dohmen C, Graf R, Vajkoczy P, Helbok R, Suzuki M, Schiefecker AJ, Major S, Winkler MK, Kang EJ, Milakara D, Oliveira-Ferreira AI, Reiffurth C, Revankar GS, Sugimoto K, Dengler NF, Hecht N, Foreman B, Feyen B, Kondziella D, Friberg CK, Piilgaard H, Rosenthal ES, Westover MB, Maslarova A, Santos E, Hertle D, Sanchez-Porras R, Jewell SL, Balanca B, Platz J, Hinzman JM, Luckl J, Schoknecht K, Scholl M, Drenckhahn C, Feuerstein D, Eriksen N, Horst V, Bretz JS, Jahnke P, Scheel M, Bohner G, Rostrup E, Pakkenberg B, Heinemann U, Claassen J, Carlson AP, Kowoll CM, Lublinsky S, Chassidim Y, Shelef I, Friedman A, Brinker G, Reiner M, Kirov SA, Andrew RD, Farkas E, Guresir E, Vatter H, Chung LS, Brennan KC, Lieutaud T, Marinesco S, Maas AI, Sahuquillo J, Dahlem MA, Richter F, Herreras O, Boutelle MG, Okonkwo DO, Bullock MR, Witte OW, Martus P, van den Maagdenberg AM, Ferrari MD, Dijkhuizen RM, Shutter LA, Andaluz N, Schulte AP, MacVicar B, Watanabe T, Woitzik J, Lauritzen M, Strong AJ, Hartings JA. Recording, analysis, and interpretation of spreading depolarizations in neurointensive care: Review and recommendations of the COSBID research group. *J Cereb Blood Flow Metab*. 2017;37(5):1595-625.
36. Weidauer S, Lanfermann H, Raabe A, Zanella F, Seifert V, Beck J. Impairment of cerebral perfusion and infarct patterns attributable to vasospasm after aneurysmal subarachnoid hemorrhage: a prospective MRI and DSA study. *Stroke*. 2007;38(6):1831-6.
37. van der Zande JJ, Hendrikse J, Rinkel GJE. CT Angiography for Differentiation between Intracerebral and Intra-Sylvian Hematoma in Patients with Ruptured Middle Cerebral Artery Aneurysms. *American Journal of Neuroradiology*. 2011;32(2):271-5.
38. Korbakis G, Prabhakaran S, John S, Garg R, Connors JJ, Bleck TP, Lee VH. MRI Detection of Cerebral Infarction in Subarachnoid Hemorrhage. *Neurocrit Care*. 2016;24(3):428-35.
39. Guresir E, Beck J, Vatter H, Setzer M, Gerlach R, Seifert V, Raabe A. Subarachnoid hemorrhage and intracerebral hematoma: incidence, prognostic factors, and outcome. *Neurosurgery*. 2008;63(6):1088-93; discussion 93-4.
40. Etminan N, Vergouwen MD, Ilodigwe D, Macdonald RL. Effect of pharmaceutical treatment on vasospasm, delayed cerebral ischemia, and clinical outcome in patients with

- aneurysmal subarachnoid hemorrhage: a systematic review and meta-analysis. *J Cereb Blood Flow Metab.* 2011;31(6):1443-51.
41. Vergouwen MD, Etminan N, Ildigwe D, Macdonald RL. Lower incidence of cerebral infarction correlates with improved functional outcome after aneurysmal subarachnoid hemorrhage. *J Cereb Blood Flow Metab.* 2011;31(7):1545-53.
 42. Dreier JP, Lemale CL, Kola V, Friedman A, Schoknecht K. Spreading depolarization is not an epiphenomenon but the principal mechanism of the cytotoxic edema in various gray matter structures of the brain during stroke. *Neuropharmacology.* 2017.
 43. Risher WC, Ard D, Yuan J, Kirov SA. Recurrent spontaneous spreading depolarizations facilitate acute dendritic injury in the ischemic penumbra. *J Neurosci.* 2010;30(29):9859-68.
 44. Budde MD, Frank JA. Neurite beading is sufficient to decrease the apparent diffusion coefficient after ischemic stroke. *Proc Natl Acad Sci U S A.* 2010;107(32):14472-7.
 45. Hartings JA, Carroll CP, Lee G. Spreading Diffusion-Restriction Events in the Gyrencephalic Brain After Subarachnoid Hemorrhage Revealed by Continuous Magnetic Resonance Imaging. *Neurocrit Care.* 2022;37(Suppl 1):60-6.
 46. Van Harreveld A, Malhotra SK. Extracellular space in the cerebral cortex of the mouse. *J Anat.* 1967;101(Pt 2):197-207.
 47. Nedergaard M, Hansen AJ. Spreading Depression Is Not Associated with Neuronal Injury in the Normal Brain. *Brain Research.* 1988;449(1-2):395-8.
 48. Lemale CL, Luckl J, Horst V, Reiffurth C, Major S, Hecht N, Woitzik J, Dreier JP. Migraine Aura, Transient Ischemic Attacks, Stroke, and Dying of the Brain Share the Same Key Pathophysiological Process in Neurons Driven by Gibbs-Donnan Forces, Namely Spreading Depolarization. *Front Cell Neurosci.* 2022;16:837650.
 49. Warach S, Gaa J, Siewert B, Wielopolski P, Edelman RR. Acute human stroke studied by whole brain echo planar diffusion-weighted magnetic resonance imaging. *Ann Neurol.* 1995;37(2):231-41.
 50. Kumar G, Shahripour RB, Harrigan MR. Vasospasm on transcranial Doppler is predictive of delayed cerebral ischemia in aneurysmal subarachnoid hemorrhage: a systematic review and meta-analysis. *J Neurosurg.* 2016;124(5):1257-64.
 51. Kumar G, Dumitrascu OM, Chiang CC, O'Carroll CB, Alexandrov AV. Prediction of Delayed Cerebral Ischemia with Cerebral Angiography: A Meta-Analysis. *Neurocrit Care.* 2019;30(1):62-71.
 52. Stoltenburg-Didinger G, Schwarz K. Brain lesions secondary to subarachnoid hemorrhage due to ruptured aneurysms. In: Cervós-Navarro J, Ferszt R, editors. *Stroke and microcirculation.* New York: Raven Press; 1987. p. 471– 80.
 53. Schinke C, Horst V, Schlemm L, Wawra M, Scheel M, Hartings JA, Dreier JP. A case report of delayed cortical infarction adjacent to sulcal clots after traumatic subarachnoid hemorrhage in the absence of proximal vasospasm. *BMC Neurol.* 2018;18(1):210.
 54. Fisher CM, Kistler JP, Davis JM. Relation of cerebral vasospasm to subarachnoid hemorrhage visualized by computerized tomographic scanning. *Neurosurgery.* 1980;6(1):1-9.
 55. Ferguson S, Macdonald RL. Predictors of cerebral infarction in patients with aneurysmal subarachnoid hemorrhage. *Neurosurgery.* 2007;60(4):658-67; discussion 67.

56. Hijdra A, van Gijn J, Nagelkerke NJ, Vermeulen M, van Crevel H. Prediction of delayed cerebral ischemia, rebleeding, and outcome after aneurysmal subarachnoid hemorrhage. *Stroke*. 1988;19(10):1250-6.
57. Frontera JA, Claassen J, Schmidt JM, Wartenberg KE, Temes R, Connolly ES, Jr., MacDonald RL, Mayer SA. Prediction of symptomatic vasospasm after subarachnoid hemorrhage: the modified fisher scale. *Neurosurgery*. 2006;59(1):21-7; discussion -7.
58. van der Steen WE, Marquering HA, Boers AMM, Ramos LA, van den Berg R, Vergouwen MDI, Majoie C, Coert BA, Vandertop WP, Verbaan D, Roos Y. Predicting Delayed Cerebral Ischemia with Quantified Aneurysmal Subarachnoid Blood Volume. *World Neurosurg*. 2019;130:e613-e9.
59. Ko SB, Choi HA, Carpenter AM, Helbok R, Schmidt JM, Badjatia N, Claassen J, Connolly ES, Mayer SA, Lee K. Quantitative analysis of hemorrhage volume for predicting delayed cerebral ischemia after subarachnoid hemorrhage. *Stroke*. 2011;42(3):669-74.
60. van der Steen WE, Zijlstra IA, Verbaan D, Boers AMM, Gathier CS, van den Berg R, Rinkel GJE, Coert BA, Roos Y, Majoie C, Marquering HA. Association of Quantified Location-Specific Blood Volumes with Delayed Cerebral Ischemia after Aneurysmal Subarachnoid Hemorrhage. *AJNR Am J Neuroradiol*. 2018;39(6):1059-64.
61. Inagawa T, Yahara K, Ohbayashi N. Risk factors associated with cerebral vasospasm following aneurysmal subarachnoid hemorrhage. *Neurologia medico-chirurgica*. 2014;54(6):465-73.
62. Amuluru K, Al-Mufti F, Romero CE, Gandhi CD. Isolated Intraventricular Hemorrhage Associated with Cerebral Vasospasm and Delayed Cerebral Ischemia following Arteriovenous Malformation Rupture. *Interv Neurol*. 2018;7(6):479-89.
63. Shimoda M, Takeuchi M, Tominaga J, Oda S, Kumasaka A, Tsugane R. Asymptomatic versus symptomatic infarcts from vasospasm in patients with subarachnoid hemorrhage: serial magnetic resonance imaging. *Neurosurgery*. 2001;49(6):1341-8; discussion 8-50.
64. Zaharchuk G, Gong E, Wintermark M, Rubin D, Langlotz CP. Deep Learning in Neuroradiology. *AJNR Am J Neuroradiol*. 2018;39(10):1776-84.
65. Milakara D, Grozea C, Dahlem M, Major S, Winkler MKL, Luckl J, Scheel M, Kola V, Schoknecht K, Lublinsky S, Friedman A, Martus P, Hartings JA, Woitzik J, Dreier JP. Simulation of spreading depolarization trajectories in cerebral cortex: Correlation of velocity and susceptibility in patients with aneurysmal subarachnoid hemorrhage. *Neuroimage Clin*. 2017;16:524-38.

Statutory Declaration

“I, Viktor Horst, by personally signing this document in lieu of an oath, hereby affirm that I prepared the submitted dissertation on the topic “Focal brain injury in patients with aneurysmal subarachnoid hemorrhage – A neuroradiological perspective (Fokale Hirnschädigung in Patienten mit aneurysmatischer Subarachnoidalblutung – Eine neuro-radiologischer Perspektive)”, independently and without the support of third parties, and that I used no other sources and aids than those stated.

All parts which are based on the publications or presentations of other authors, either in letter or in spirit, are specified as such in accordance with the citing guidelines. The sections on methodology (in particular regarding practical work, laboratory regulations, statistical processing) and results (in particular regarding figures, charts and tables) are exclusively my responsibility.

Furthermore, I declare that I have correctly marked all of the data, the analyses, and the conclusions generated from data obtained in collaboration with other persons, and that I have correctly marked my own contribution and the contributions of other persons (cf. declaration of contribution). I have correctly marked all texts or parts of texts that were generated in collaboration with other persons.

My contributions to any publications to this dissertation correspond to those stated in the below joint declaration made together with the supervisor. All publications created within the scope of the dissertation comply with the guidelines of the ICMJE (International Committee of Medical Journal Editors; <http://www.icmje.org>) on authorship. In addition, I declare that I shall comply with the regulations of Charité – Universitätsmedizin Berlin on ensuring good scientific practice.

I declare that I have not yet submitted this dissertation in identical or similar form to another Faculty.

The significance of this statutory declaration and the consequences of a false statutory declaration under criminal law (Sections 156, 161 of the German Criminal Code) are known to me.”

Date

Signature

Declaration of my own contribution to the publications

Viktor Horst contributed the following to the below listed publications:

Publication 1: Hartings JA, York J, Carroll CP, Hinzman JM, Mahoney E, Krueger B, Winkler MKL, Major S, **Horst V**, Jahnke P, Woitzik J, Kola V, Du Y, Hagen M, Jiang J, Dreier JP, Subarachnoid blood acutely induces spreading depolarizations and early cortical infarction, *Brain*, 2017

Contribution in percent: 15; Contribution in detail: Participation in the clinical part of the publication. Screened for inclusion using the COSBID database. Performed the MR image analysis of the 23 included patients. Characterized early focal brain injuries into hemorrhagic or ischemic in the frontal lobes using the T1, T2*, FLAIR and diffusion sequence. Quantified the lesions using the software Clusterize. Designed Table 1 and Figure 7C in the results section. Co-drafted the manuscript in the section on methodology. Made critical review of the manuscript.

Publication 2: Dreier JP, Winkler MKL, Major S, **Horst V**, Lublinsky S, Kola V, Lemale CL, Kang EJ, Maslarova A, Salur I, Luckl J, Platz J, Jorks D, Oliveira-Ferreira AI, Schoknecht K, Reiffurth C, Milakara D, Wiesenthal D, Hecht N, Dengler NF, Liotta A, Wolf S, Kowoll CM, Schulte AP, Santos E, Guresir E, Unterberg AW, Sarrafzadeh A, Sakowitz OW, Vatter H, Reiner M, Brinker G, Dohmen C, Shelef I, Bohner G, Scheel M, Vajkoczy P, Hartings JA, Friedman A, Martus P, Woitzik J, Spreading depolarizations in ischaemia after subarachnoid haemorrhage, a diagnostic phase III study, *Brain*, 2022

Contribution in percent: 15; Contribution in detail: Pseudonymized imaging data. Transferred imaging data from the clinical PACS server to the XNAT server. Found imaging evidence of hypoxic-ischemic encephalopathy in 4 patients and took part in the discussion on their exclusion from analysis. Characterized and manually quantified intracerebral hemorrhage, early cerebral infarction and delayed cerebral infarction on serial neuroimages in 200 patients using MRICron. Designed Figure 1D, 4A and 6Bii. Co-drafted the manuscript in the section on methodology. Made critical review of the manuscript.

Publication 3: **Horst V**, Kola V, Lemale CL, Major S, Winkler MKL, Hecht N, Santos E, Platz J, Sakowitz OW, Vatter H, Dohmen C, Scheel M, Vajkoczy P, Hartings JA, Woitzik

J, Martus P, Dreier JP, Spreading depolarization and angiographic spasm are separate mediators of delayed infarcts, Brain Communications, 2023

Contribution in percent: 70; Contribution in detail: Designed the study. Characterized and quantified delayed cerebral infarcts on neuroimages in 136 patients using MRI-cron. Quantified intracranial hemorrhage volumes using ITK-SNAP. Participated in the statistical analysis in collaboration with Prof. Peter Martus (trial statistician), especially in descriptive statistics and correlation analyses. Designed Figure 1 – 3 and all Tables. Co-drafted the manuscript. Accompanied the process of the peer review and partly revised the manuscript according to the specifications of the reviewers.

Signature, date and stamp of first supervising university professor / lecturer

Signature of doctoral candidate

Printing copy of publication 1

Hartings JA, York J, Carroll CP, Hinzman JM, Mahoney E, Krueger B, Winkler MKL, Major S, Horst V, Jahnke P, Woitzik J, Kola V, Du Y, Hagen M, Jiang J, Dreier JP. Subarachnoid blood acutely induces spreading depolarizations and early cortical infarction. *Brain*. 2017;140(10):2673-90.

<https://doi.org/10.1093/brain/awx214>

Printing copy of publication 2

Dreier JP, Winkler MKL, Major S, Horst V, Lublinsky S, Kola V, Lemale CL, Kang EJ, Maslarova A, Salur I, Luckl J, Platz J, Jorks D, Oliveira-Ferreira AI, Schoknecht K, Reiffurth C, Milakara D, Wiesenthal D, Hecht N, Dengler NF, Liotta A, Wolf S, Kowoll CM, Schulte AP, Santos E, Guresir E, Unterberg AW, Sarrafzadeh A, Sakowitz OW, Vatter H, Reiner M, Brinker G, Dohmen C, Shelef I, Bohner G, Scheel M, Vajkoczy P, Hartings JA, Friedman A, Martus P, Woitzik J. Spreading depolarizations in ischaemia after subarachnoid haemorrhage, a diagnostic phase III study. *Brain*. 2022;145(4):1264-84.

<https://doi.org/10.1093/brain/awab457>

BRAIN COMMUNICATIONS

Spreading depolarization and angiographic spasm are separate mediators of delayed infarcts

Viktor Horst,¹ Vasilis Kola,¹ Coline L. Lemale,^{1,2} Sebastian Major,^{1,2,3} Maren K. L. Winkler,^{1,4} Nils Hecht,^{1,5} Edgar Santos,⁶ Johannes Platz,⁷ Oliver W. Sakowitz,⁶ Hartmut Vatter,⁸ Christian Dohmen,⁹ Michael Scheel,¹⁰ Peter Vajkoczy,^{1,5} Jed A. Hartings,¹¹ Johannes Woitzik,^{1,12} Peter Martus,¹³ and  Jens P. Dreier^{1,2,3,14,15}

In DISCHARGE-1, a recent Phase III diagnostic trial in aneurysmal subarachnoid haemorrhage patients, spreading depolarization variables were found to be an independent real-time biomarker of delayed cerebral ischaemia. We here investigated based on prospectively collected data from DISCHARGE-1 whether delayed infarcts in the anterior, middle, or posterior cerebral artery territories correlate with (i) extravascular blood volumes; (ii) predefined spreading depolarization variables, or proximal vasospasm assessed by either (iii) digital subtraction angiography or (iv) transcranial Doppler-sonography; and whether spreading depolarizations and/or vasospasm are mediators between extravascular blood and delayed infarcts. Relationships between variable groups were analysed using Spearman correlations in 136 patients. Thereafter, principal component analyses were performed for each variable group. Obtained components were included in path models with *a priori* defined structure. In the first path model, we only included spreading depolarization variables, as our primary interest was to investigate spreading depolarizations. Standardised path coefficients were 0.22 for the path from extravascular blood_{component} to depolarization_{component} ($P=0.010$); and 0.44 for the path from depolarization_{component} to the first principal component of delayed infarct volume ($P<0.001$); but only 0.07 for the direct path from blood_{component} to delayed infarct_{component} ($P=0.36$). Thus, the role of spreading depolarizations as a mediator between blood and delayed infarcts was confirmed. In the principal component analysis of extravascular blood volume, intraventricular haemorrhage was not represented in the first component. Therefore, based on the correlation analyses, we also constructed another path model with blood_{component} without intraventricular haemorrhage as first and intraventricular haemorrhage as second extrinsic variable. We found two paths, one from (subarachnoid) blood_{component} to delayed infarct_{component} with depolarization_{component} as mediator (path coefficients from blood_{component} to depolarization_{component} = 0.23, $P=0.03$; path coefficients from depolarization_{component} to delayed infarct_{component} = 0.29, $P=0.002$), and one from intraventricular haemorrhage to delayed infarct_{component} with angiographic vasospasm_{component} as mediator variable (path coefficients from intraventricular haemorrhage to vasospasm_{component} = 0.24, $P=0.03$; path coefficients from vasospasm_{component} to delayed infarct_{component} = 0.35, $P<0.001$). Human autopsy studies shaped the hypothesis that blood clots on the cortex surface suffice to cause delayed infarcts beneath the clots. Experimentally, clot-released factors induce cortical spreading depolarizations that trigger (i) neuronal cytotoxic oedema and (ii) spreading ischaemia. The statistical mediator role of spreading depolarization variables between subarachnoid blood volume and delayed infarct volume supports this pathogenetic concept. We did not find that angiographic vasospasm triggers spreading depolarizations, but angiographic vasospasm contributed to delayed infarct volume. This could possibly result from enhancement of spreading depolarization-induced spreading ischaemia by reduced upstream blood supply.

- 1 Centre for Stroke Research Berlin, Charité—Universitätsmedizin Berlin, Corporate Member of Freie Universität Berlin, Humboldt-Universität zu Berlin, and Berlin Institute of Health, Berlin, Germany
- 2 Department of Experimental Neurology, Charité—Universitätsmedizin Berlin, Corporate Member of Freie Universität Berlin, Humboldt-Universität zu Berlin, and Berlin Institute of Health, Berlin, Germany
- 3 Department of Neurology, Charité—Universitätsmedizin Berlin, Corporate Member of Freie Universität Berlin, Humboldt-Universität zu Berlin, and Berlin Institute of Health, Berlin, Germany
- 4 Robert Koch Institute, Berlin, Germany
- 5 Department of Neurosurgery, Charité—Universitätsmedizin Berlin, Corporate Member of Freie Universität Berlin, Humboldt-Universität zu Berlin, and Berlin Institute of Health, Berlin, Germany
- 6 Department of Neurosurgery, Heidelberg University Hospital, Ruprecht-Karls-University Heidelberg, Heidelberg, Germany
- 7 Department of Neurosurgery, Herz-Neuro-Zentrum Bodensee, Kreuzlingen, Switzerland
- 8 Department of Neurosurgery, University Hospital and Friedrich-Wilhelms-University Bonn, Bonn, Germany
- 9 Department for Neurology and Neurological Intensive Care Medicine, LVR-Klinik Bonn, Bonn, Germany
- 10 Department of Neuroradiology, Charité—Universitätsmedizin Berlin, Corporate Member of Freie Universität Berlin, Humboldt-Universität zu Berlin, and Berlin Institute of Health, Berlin, Germany
- 11 Department of Neurosurgery, University of Cincinnati College of Medicine, Cincinnati, OH, USA
- 12 Department of Neurosurgery, Evangelisches Krankenhaus Oldenburg, University of Oldenburg, Oldenburg, Germany
- 13 Institute for Clinical Epidemiology and Applied Biometry, University of Tübingen, Tübingen, Germany
- 14 Bernstein Centre for Computational Neuroscience Berlin, Berlin, Germany
- 15 Einstein Centre for Neurosciences Berlin, Berlin, Germany

Correspondence to: Jens P. Dreier

Centre for Stroke Research, Campus Charité Mitte

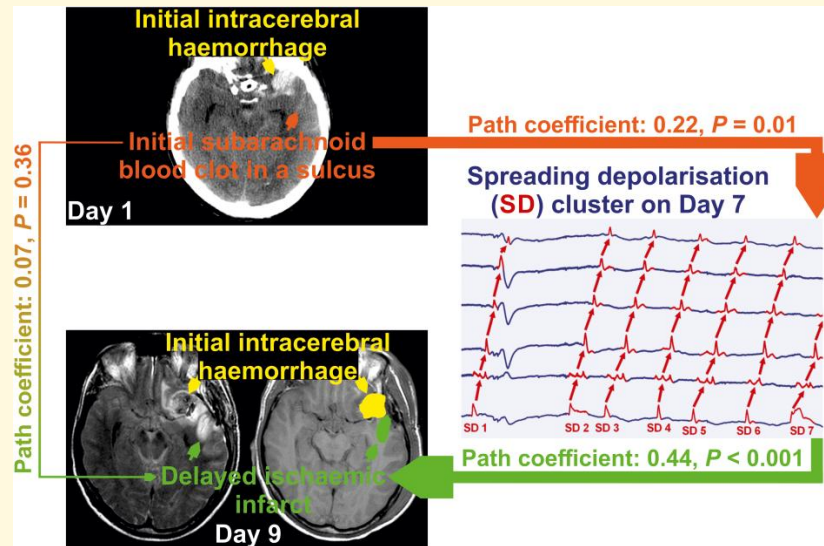
Charité—Universitätsmedizin Berlin, Charitéplatz 1, 10117 Berlin, Germany

E-mail: jens.dreier@charite.de

Keywords: cytotoxic oedema; spreading depolarization; spreading ischaemia; subarachnoid haemorrhage; vasospasm

Abbreviations: ACA = anterior cerebral artery; aCSF = artificial cerebrospinal fluid; aSAH = aneurysmal subarachnoid haemorrhage; blood_{basal} = subarachnoid blood volume in the basal cisterns; blood_{component} = first principal component of the blood volume variables; blood_{convex} = subarachnoid blood volume on the cerebral convexity; blood_{inter} = subarachnoid blood volume in the interhemispheric fissure; blood_{Sylvian} = subarachnoid blood volume in the Sylvian fissure; CBF = cerebral blood flow; COSBID = Co-Operative Studies on Brain Injury Depolarisations; CTA = computed tomography angiography; DC potential = direct current (steady) potential; DCI = delayed cerebral ischaemia; DCI_{ACA} = delayed infarct volume in the territory of the anterior cerebral artery; DCI_{deep} = delayed infarct volume below the cortex, including perforator infarcts, singular white matter infarcts without cortical involvement and anterior choroidal artery infarcts; DCI_{MCA} = delayed infarct volume in the territory of the middle cerebral artery; DCI_{PCA} = delayed infarct volume in the territory of the posterior cerebral artery; DCI_{watershed} = delayed infarct volume in the territory of the cortical watershed zones; DISCHARGE-1 = Depolarisations in ISCHAemia after subARachnoid haemorrhage-1; DSA = digital subtraction angiography [A1, A2, M1, M2, P1, P2 = first and second segments of anterior cerebral artery (ACA), middle cerebral artery (MCA) and posterior cerebral artery (PCA) ipsilateral to the subdural electrodes]; DSA_{component} = first principal component of the digital subtraction angiography variables to quantify the degree of vasospasm; ECI = early cerebral ischaemia; ECI_{ACA} = early infarct volume in the territory of the anterior cerebral artery; ECI_{deep} = early infarct volume below the cortex including perforator infarcts, singular white matter infarcts without cortical involvement and anterior choroidal artery infarcts; ECI_{MCA} = early infarct volume in the territory of the middle cerebral artery; ECI_{PCA} = early infarct volume in the territory of the posterior cerebral artery; ECI_{watershed} = early infarct volume in the territory of the cortical watershed zones; ECoG = electrocorticography; eGOS = extended Glasgow Outcome Scale; FLAIR = fluid-attenuated inversion recovery; ICH = intracerebral haemorrhage; Image_{early} = post-interventional MRI or CT performed no later than Day 5; Image_{late} = follow-up MRI or CT performed after the end of neuromonitoring around Day 14; IQR = interquartile range; IVH = intraventricular haemorrhage; [K⁺]_{aCSF} = potassium concentration in the artificial cerebrospinal fluid; mbfv = transcranial Doppler-sonography (TCD)-determined mean blood flow velocity; mbfv_{ACA} = TCD-determined peak mean blood flow velocity of the anterior cerebral artery; mbfv_{component} = first principal component of the TCD-determined peak mean blood flow velocity variables; mbfv_{MCA} = TCD-determined peak mean blood flow velocity of the middle cerebral artery; mbfv_{PCA} = TCD-determined peak mean blood flow velocity of the posterior cerebral artery; MCA = middle cerebral artery; NO = nitric oxide; NOS = nitric oxide synthase; NUP = negative ultraslow potential; pc = path coefficients; PCA = posterior cerebral artery; peak_{clusSD-delayed} = peak number of clustered spreading depolarizations (SD) of a recording day during the delayed period between the early post-intervention neuroimage and the late neuroimage after completion of neuromonitoring (clustered SD = SD that occurred less than 1 h apart from the previous SD); peak_{isoSD-delayed} = peak number of isoelectric SDs of a recording day during the delayed period (isoelectric SD = SD in electrically inactive tissue); peak_{SD-delayed} = peak number of SDs of any type of a recording day during the delayed period; PTDDD_{delayed} = peak value of a recording day for the total (cumulative) SD-induced depression durations during the delayed period; rCBF = regional cerebral blood flow; SD = spreading depolarization; TCD = transcranial Doppler-sonography; TDDD = total (cumulative) spreading depolarization-induced depression duration of a recording day

Graphical Abstract



Introduction

Subarachnoid haemorrhage (SAH) is the second most common type of haemorrhagic stroke.^{1,2} In 85%, SAH is caused by the rupture of an aneurysm. Although SAH accounts for only ~3% of all strokes and ~5% of deaths from stroke, the relative youth of the affected individuals means that it is responsible for a quarter of all stroke-related years of potential life lost before age 65.³ In Depolarisations in ISCHAemia after subARachnoid haemorrhage-1 (DISCHARGE-1), a recent prospective, observational, multicentre, cohort, Phase III diagnostic trial of 180 patients with severe aneurysmal SAH (aSAH), the strongest predictor of long-term outcome was total focal brain damage detected by neuroimaging two weeks after the initial haemorrhage.⁴ Most prominent aetiologies of focal brain damage associated with aSAH are intracerebral haemorrhage (ICH), and infarction due to either early (ECI), or delayed cerebral ischaemia (DCI). DISCHARGE-1 found that the average patient admitted to the neurocritical care unit after aneurysm treatment had already lost 46 ± 73 ml (mean \pm standard deviation) of brain tissue due to ICH and ECI and lost an additional 36 ± 80 ml (44% of the total focal brain damage) over the next two weeks because of delayed ischaemic infarcts. This tissue could be saved if we knew effective treatments, because DCI is a potentially modifiable aetiology of focal brain damage during neurocritical care, as it allows treatment with a neuroprotective intervention before the potential insult or soon after. The risk of DCI is particularly high after severe aSAH. Thus, delayed infarct volume in DISCHARGE-1 was significantly higher in deeply comatose patients than in patients who were at least transiently clinically assessable

(48 ± 92 ml versus 23 ± 74 ml, $P < 0.001$).⁴ Severe cases require mechanical ventilation and sedation more often, which limits neurological assessment. Therefore, in the high-risk population, it is particularly difficult to identify and treat those patients who suffer from the complication. However, neurosurgical procedures are indicated early after aSAH, allowing implantation of invasive probes. This enables recording of the entire period of ischaemic stroke development, early treatment stratification according to changes in diagnostic summary measures recorded by neuromonitoring devices in real time and then re-assessment of these measures after neuroprotective interventions.⁵ In awake patients, neurologic examination might be the strongest DCI predictor.⁶ However, particularly in comatose or sleeping patients, the results of DISCHARGE-1 suggest that spreading depolarization (SD) variables are currently the most promising DCI predictor.⁴

SD is a phenomenon of the brain grey matter. Using subdural electrocorticography (ECoG), it is observed as a large negative direct current (DC) shift which spreads between adjacent recording sites (frequency band: < 0.05 Hz). SD is characterised by abrupt, near-complete breakdown of the transmembrane neuronal ion gradients with entropy increase, release of 90% of Gibbs free energy normally contained in the ion gradients, neuronal water uptake, soma swelling, dendritic beading, and MRI diffusion restriction.⁷⁻⁹ Collectively, SD is the prime process that initiates and maintains neuronal cytotoxic oedema in grey matter.^{9,10} This means that SD initiates toxic changes that eventually lead to neuronal death, but is not a marker of death *per se*, as it is reversible—up to a point—with restoration of the physiological state of low entropy by Na^+/K^+ -ATPase

(NaKA) activation.¹¹ The most important NaKA activators in this context are the extreme increases in cytoplasmic Na⁺ and extracellular K⁺ concentration, which are nowhere near as high in any other grey matter pathological phenomenon as in SD.¹¹⁻¹⁵ However, if NaKAs cannot be sufficiently activated, e.g. due to enzyme inhibition or as a result of ATP deficiency, the neurons die, which is indicated by the transition to a negative ultraslow potential (NUP) in ECoG and a persistent diffusion restriction in MRI.^{8,16-18}

Importantly, SDs induce tone alterations in resistance vessels, causing either predominant hyperperfusion followed by a mild oligoemia (physiological haemodynamic response) in healthy tissue^{19,20}; or severe and prolonged initial hypoperfusion (inverse haemodynamic response = spreading ischaemia) where the neurovascular unit is severely disturbed.^{5,21,22} SD in naive tissue associated with a normal haemodynamic response does not cause neuronal damage.²³ However, SD-induced spreading ischaemia can lead to infarction even in brain tissue that was not yet ischaemic at the onset of SD.²⁴ This is because spreading ischaemia-induced ATP deficiency keeps the neurons in the SD/cytotoxic oedema state, the SD/cytotoxic oedema state maintains vasoconstriction and the vasoconstriction restricts the substrate supply for ATP production.⁵ If this vicious circle is not interrupted, it eventually leads to ischaemic necrosis.^{5,21} Spreading ischaemia is thus distinguished from primary ischaemia, such as occurs in the setting of embolic or thrombotic occlusion of a major cerebral artery or cardiocirculatory arrest. Whereas in the case of spreading ischaemia, SD occurs first and is followed by ischaemia with a latency of several seconds, and both SD and ischaemia propagate in the tissue,^{5,21} in the case of severe primary ischaemia, ischaemia occurs first, followed by SD with a substantial latency of ~1–5 minutes, and only SD, but not ischaemia, propagates in the tissue.¹⁶ Nevertheless, the process of spreading ischaemia can also build up on incomplete primary ischaemia.²⁵⁻²⁹ If primary ischaemia of the cortex does not lead to at least one SD, infarction does not occur.^{16,30-32} If primary ischaemia leads to SD but timely reperfusion occurs, no lesion develops either.^{16,33}

The main principles of the SD process known from animal experiments could be verified in experiments with human brain slices.³⁴⁻⁴⁰ The entire SD continuum from short duration, to intermediate duration, to terminal waves has now been demonstrated in aSAH patients.^{4,41,42} After aSAH, SDs have been recorded in association with (i) migraine aura⁴³; (ii) transitory ischaemic attacks⁴; (iii) status epilepticus^{36,44,45}; (iv) vasogenic oedema development without infarction⁴; (v) ICH⁴⁶; (vi) early ischaemic infarcts^{4,47,48}; (vii) delayed ischaemic infarcts^{4,22,49}; (viii) brain death development^{4,50,51} and (ix) dying from cardiocirculatory arrest.^{4,52} The broad range of conditions under which SD has been detected in patients using ECoG closely matches the wide range of conditions under which cytotoxic oedema is detected using neuroimaging. Importantly, however, this does not mean that every SD has a correlate on clinical MRI, as SD/neuronal cytotoxic oedema is usually initially reversible

and once regressed is no longer detectable on neuroimaging.^{53,54} In addition, SD-induced spreading ischaemia and transition from clustered SDs to NUP were demonstrated in a small population of aSAH patients in whom optoelectrodes for laser-Doppler flowmetry and ECoG were located directly over newly developing delayed infarcts proven by longitudinal neuroimaging.^{4,16,17}

SD is associated with different changes in spontaneous brain activity in the alternating current (AC) band of the ECoG (>0.5 Hz). These are non-spreading activity depression, spreading activity depression and epileptiform activity.^{11,36,52} The same SD wave may be associated with different activity changes and different haemodynamic responses in adjacent brain regions. In DISCHARGE-1, for each recording day of each patient, we determined (i) the total (cumulative) SD-induced depression duration (TDDD) and (ii) the number of SDs as the most important ECoG variables. While the *a priori* defined 60-min cut-off of TDDD indicated a reversible delayed neurological deficit, only a 180-min cut-off indicated new infarction with >0.60 sensitivity and >0.80 specificity.⁴ On this basis, it was recommended that rescue treatment be initiated at the 60-min cut-off rather than at the 180-min cut-off if progression of injury to infarction is to be prevented. Overall, SD variables were included in each multiple regression model for early, delayed and total brain damage, 7-month outcome, and death, suggesting that they are an independent biomarker of progressive brain injury.⁴

Traditional pathology literature describes delayed infarcts after aSAH as focal anaemic necroses, suggesting arterial/arteriolar spasm as underlying aetiology and ruling out mechanisms such as thrombotic occlusion, endothelial swelling, or venous compression.⁵⁵ SD-induced vasoconstriction, the cause of spreading ischaemia, is in fact the most extreme form of vasospasm in the brain currently known.^{5,21,22,24} In addition, two slowly evolving forms of vasospasm emerge after aSAH: angiographic (proximal) vasospasm and chronic constriction of distal arteries/arterioles.⁵⁶⁻⁵⁸ In the autopsy studies, the predominant lesion pattern consisted of widespread infarcts in the cerebral cortex.^{55,59-63} Seventy to 80% of patients showed such cortical infarcts in the large autopsy series.^{55,59} In particular, Stoltenburg-Didinger and Schwarz⁵⁵ noted that these lesions typically develop beneath subarachnoid clots. In animal experiments, haemolysis products in the subarachnoid space without the simultaneous presence of proximal vasospasm are sufficient to cause SD, SD-induced spreading ischaemia and cortical infarction.^{13,21,24,42,64,65} However, upstream restriction of regional cerebral blood flow (rCBF), if severe enough, can also trigger SDs⁶⁶⁻⁶⁹ and shift the normal, predominantly hyperaemic response to SD towards an inverse ischaemic response.^{25-27,70,71} Accordingly, there are two alternative hypotheses for the development of delayed SDs after aSAH: (i) blood degradation products around the basal conductive arteries trigger angiographic vasospasm, which acts as a mediator of SDs through a mismatch between supply and demand; or (ii) blood degradation products located

on the cortex trigger SDs directly in the underlying cortex through other mechanisms, including neuronal, astrocytic and microvascular disruption and/or local inflammation. To test these two hypotheses, we here investigated based on prospectively collected data from DISCHARGE-1 whether delayed infarcts in the anterior (ACA), middle (MCA) or posterior cerebral artery (PCA) territories ipsilateral to the subdural electrodes correlate with (i) extravascular blood volumes in different compartments; (ii) predefined SD variables, or proximal vasospasm assessed by either (iii) digital subtraction angiography (DSA) or (iv) transcranial Doppler-sonography (TCD); and whether proximal vasospasm and/or SD variables are mediators between extravascular blood volumes and delayed infarcts.

Materials and methods

Study design and protocol

This study was designed and performed as a substudy of the Depolarisations in ISCHAemia after subARachnoid haemorrhage-1 (DISCHARGE-1) trial.⁴ As reported previously, patients with aSAH were screened for study inclusion and were consecutively enrolled in DISCHARGE-1 at six university-hospitals (Campus Benjamin Franklin and Campus Virchow Klinikum, Charité—Universitätsmedizin Berlin; University of Bonn; Goethe-University Frankfurt; University of Cologne and University Hospital Heidelberg) between September 2009 and April 2018.⁴ The protocol was approved by the local ethics committees. Either informed consent or surrogate informed consent was obtained. Research was conducted in accordance with the Declaration of Helsinki. Results were reported following the STROBE guidelines (<https://www.strobe-statement.org>). DISCHARGE-1 was preregistered (<http://www.isrctn.com/ISRCTN05667702>). If the patient was eligible, a subdural electrode strip (Wyler, Ad-Tech Medical, Racine, WI, USA) for SD monitoring was placed over vital cortex.

In DISCHARGE-1, 180 of 205 (87.8%) patients could be analysed. For the present substudy, 44 additional patients were excluded because (i) the preoperative CT was missing ($n = 18$); (ii) the CT slice thickness was <3 mm or >6 mm ($n = 3$); (iii) the patient died early before the occurrence of delayed infarction could be assessed ($n = 10$); (iv) the patient experienced a periprocedural postoperative haemorrhage with a volume >10 ml ($n = 8$); (v) the first postoperative neuroimage showed malignant early brain injury ($n = 2$) or (vi) an interventional complication occurred such as infarction due to clip stenosis ($n = 3$). Placement of the electrode strip was performed either directly after surgical treatment of the aneurysm via craniotomy ($n = 120$) or, in coiled patients, after burr hole trepanation simultaneously with the placement of a ventricular drain or oxygen sensor ($n = 16$). All evaluators were blinded to other measures.

The study design of DISCHARGE-1 has been previously described in great detail.⁴ Figure 1A shows the study flow.

In brief, neuroimaging included the pre-interventional CT to establish the diagnosis of aSAH and the post-interventional CT to locate the subdural ECoG electrodes. For the present substudy, early ischaemic cerebral infarcts were assessed using either a post-interventional MRI ($n = 118$) or CT ($n = 18$) performed no later than Day 5. The median day of this neuroimage, referred to as Image_{early}, was Day 2 [interquartile range (IQR): 1–3]. Delayed ischaemic infarcts were assessed using a follow-up Image_{late} (MRI: $n = 120$, CT: $n = 16$) on Day 14 (IQR: 13–15) in comparison to Image_{early}. Recording, analysis and interpretation of SDs followed the published recommendations of the Co-Operative Studies on Brain Injury Depolarisations (COSBID) group.⁷² Importantly, in every patient, the first 24-h period after the initial haemorrhage was always denoted as ‘Day 0’, the second 24-h period as ‘Day 1’ and so on. Using LabChart-8 software (ADInstruments, Bella Vista, New South Wales, Australia), M.K.L.W. and C.L.L. determined the following for each recording day of each patient: (i) total (cumulative) SD-induced depression duration (TDDD); (ii) number of SDs; (iii) number of SDs in electrically inactive tissue (isoelectric SDs)^{72,73} and (iv) number of clustered SDs, i.e. SDs that occurred less than 1 h apart from the previous SD. For the present substudy, we used peak values of a recording day for each SD-variable resulting in (i) PTDDD_{delayed}; (ii) peak number of SDs of any type (peak_{SD-delayed}); (iii) peak number of isoelectric SDs (peak_{isoSD-delayed}) and (iv) peak number of clustered SDs (peak_{clusSD-delayed}) for the delayed period between Image_{early} and Image_{late} after the end of neuromonitoring. TCD to determine mean blood flow velocities (mbfv) of the ACA (788 measurements), MCA (1060 measurements) and PCA (606 measurements) ipsilateral to the subdural electrodes was performed daily ($n = 128$). On this basis, peak values were determined for each of the three arteries and each patient. V.K. determined vascular narrowing using a qualitative grading score (no vascular narrowing = 1, vascular narrowing by 11–33% = 2, vascular narrowing by 34–66% = 3, vascular narrowing $>67\%$ = 4) for all DSAs performed between Days 5 and 17 [median Day 7 (IQR: 7–8), $n = 106$].⁴ The assessment included the first and second segments of MCA, ACA and PCA ipsilateral to the subdural electrodes (see also DSA grading score in the [Supplementary Material](#) and [Supplementary Fig. 1](#)).

Delayed cerebral infarcts

We adopted parenchymal lesion volumes derived from manual segmentation in DISCHARGE-1.⁴ For the present substudy, we only used delayed ischaemic infarct volumes in the cerebral hemisphere ipsilateral to the subdural electrodes. Following Weidauer *et al.*,⁷⁴ the volumes of ipsilateral delayed infarction were further segmented into five categories: cortical ACA infarction, cortical MCA infarction, cortical PCA infarction, cortical watershed infarction and deep infarction. The latter included perforator infarcts, singular white matter infarcts without cortical involvement

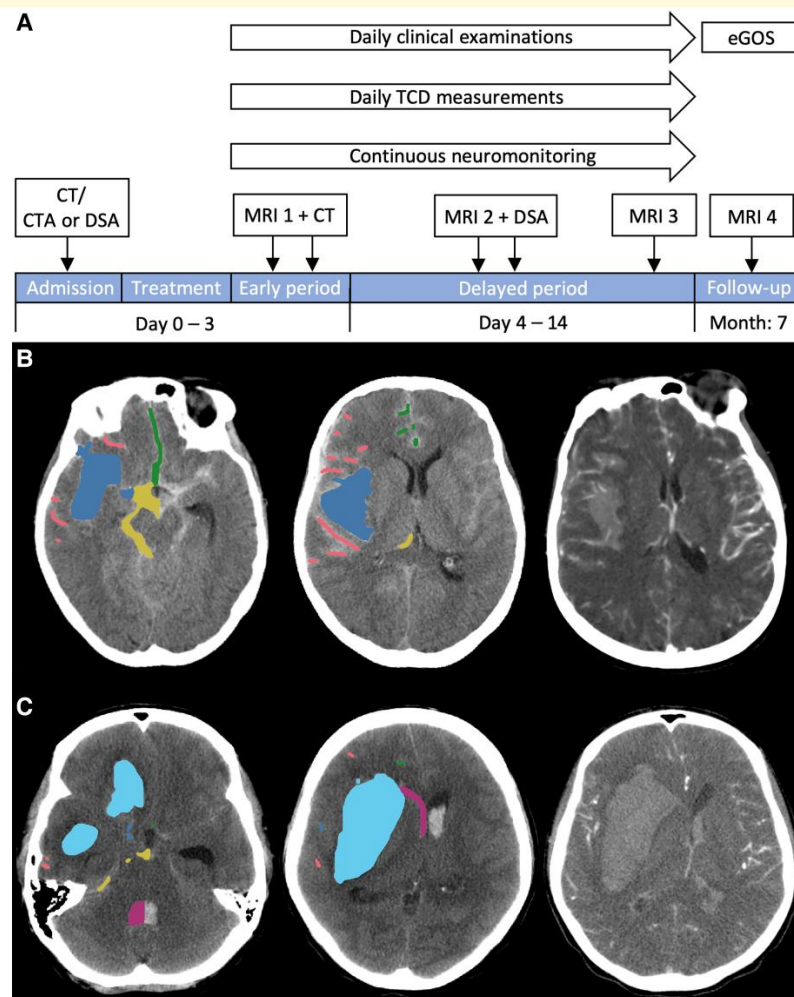


Figure 1 Diagnostic flow of the DISCHARGE-I study and quantification method for ipsilateral haemorrhage on the initial CT scan according to six predefined compartments. **(A)** CT and CTA were performed on admission. If necessary, CTA was complemented by DSA. The first MRI (MRI 1) was acquired 24–48 h after surgical or endovascular treatment of the aneurysm. In addition, a postoperative CT was performed to locate the subdural electrodes. In the delayed period, MRI 2 was performed around Day 7 and MRI 3 around Day 14. Note that delayed infarct volumes were quantified for both sessions separately and then added up for further analysis. A second DSA was performed around Day 7 to assess angiographic vasospasm. After treatment of the aneurysm, the patient was transferred to the neurocritical care unit, where continuous neuromonitoring, daily TCD and clinical examinations started and continued until Day 14. After 7 months, a follow-up MRI 4 was performed. Furthermore, functional outcome was documented using the extended Glasgow Outcome Scale (eGOS). **(B)** Representative CT and CTA images of a patient with aSAH from a right MCA aneurysm. Note that haemorrhage was only quantified in the hemisphere ipsilateral to the subdural electrodes. CTA (right image) demonstrated contrast-enhancing vessels inside a large right-sided haematoma. Therefore, the volume of this haematoma was quantified according to the category of subarachnoid blood in the Sylvian fissure ($\text{blood}_{\text{Sylvian}}$) (blue label in left and middle image). $\text{Blood}_{\text{convex}}$ comprised blood in the sulci at the cerebral convexity including the rami of the Sylvian fissure (red label). $\text{Blood}_{\text{inter}}$ was composed of blood in the anterior and posterior interhemispheric fissure as well as adjacent sulci (green label). Interhemispheric blood that crossed the midline was classified as contralateral and was not considered. $\text{Blood}_{\text{basal}}$ included blood in the following cisterns: prepontine, interpeduncular, suprasellar, ipsilateral ambient, quadrigeminal and the interpositum cistern (yellow label). Subdural blood, seen as narrow hyperdense fringe overlying the left frontal cortex, was not quantified. **(C)** Representative CT and CTA images of another patient with aSAH from a right MCA aneurysm. CTA (right image) demonstrated contrast-enhancing vessels of the M2 segment of the MCA outside a large right-sided haematoma. Therefore, this haematoma volume was quantified within the ICH category (cyan label in left and middle image). Blood in the ventricular system is shown in purple. Most notably, a large clot was found in the fourth ventricle. This was only quantified until the midline (purple label). $\text{Blood}_{\text{basal}}$ (yellow label), $\text{blood}_{\text{inter}}$ (green label) and $\text{blood}_{\text{convex}}$ (red label) were small in this patient.

Table 1 Radiographic characteristics of the ipsilateral hemisphere

	Number of patients/total number of patients (%)	Mean volume \pm standard deviation (ml) ^a	Minimum–maximum in single patients (ml)	Cumulative volume over all 136 patients (ml) (% of total cumulative volume)	
blood _{convex}	118/136 (86.8%)	2.7 \pm 3.0	0–16.3	371.8 (8.9%)	
blood _{inter}	131/136 (96.3%)	3.5 \pm 4.3	0–28.8	471.0 (11.3%)	
blood _{Sylvian}	133/136 (97.8%)	8.1 \pm 13.1	0–78.2	1099.7 (26.4%)	
blood _{basal}	132/136 (97.1%)	4.0 \pm 3.5	0–22.4	545.4 (13.1%)	
ICH	39/136 (28.7%)	8.1 \pm 20.5	0–101.4	1103.6 (26.4%)	
IVH	109/136 (80.1%)	4.3 \pm 10.6	0–70.1	581.3 (13.9%)	
ECl _{ACA}	37/136 (27.2%)	2.7 \pm 11.4	0–105.0	370.5 (32.0%)	
ECl _{MCA}	33/136 (24.3%)	3.5 \pm 17.1	0–186.0	472.6 (40.9%)	
ECl _{PCA}	8/136 (5.9%)	0.6 \pm 4.3	0–46.7	87.9 (7.6%)	
ECl _{watershed}	12/136 (8.8%)	0.5 \pm 3.1	0–34.6	63.1 (5.5%)	
ECl _{deep}	45/136 (33.1%)	1.2 \pm 3.2	0–23.0	162.2 (14.0%)	
DCI _{ACA}	18/136 (13.2%)	2.9 \pm 11.5	0–76.6	391.2 (15.0%)	
DCI _{MCA}	49/136 (36.0%)	13.5 \pm 33.9	0–188.0	1839.4 (70.8%)	
DCI _{PCA}	9/136 (6.6%)	1.1 \pm 6.0	0–50.0	145.3 (5.6%)	
DCI _{watershed}	7/136 (5.1%)	0.3 \pm 1.8	0–16.2	43.2 (1.7%)	
DCI _{deep}	30/136 (22.1%)	1.3 \pm 5.4	0–50.0	180.6 (6.9%)	
	No vasospasm^b		Mild^c	Moderate^d	Severe^e
DSA _{A1}	38/103		38/103	16/103	11/103
DSA _{A2}	47/104		33/104	18/104	6/104
DSA _{M1}	54/105		29/105	17/105	5/105
DSA _{M2}	47/105		43/105	12/105	3/105
DSA _{P1}	70/91		17/91	3/91	1/91
DSA _{P2}	77/90		11/90	2/90	0/90
	Variable		Spearman coefficient	P-value	Number of patients
Sum of DCI _{ACA} + MCA + PCA	Sum of blood _{convex} + inter + Sylvian + basal		0.21	0.015	136
	Sum of blood _{convex} + inter + Sylvian + basal + IVH		0.17	0.046	136
	Average mbfv _{ACA/MCA/PCA}		0.25	0.004	128
	DSA _{A1–P2} score		0.26	0.008	106
	PTDDD _{delayed}		0.55	<0.001	136
	peak _{SD} -delayed		0.46	<0.001	136
	peak _{isoSD} -delayed		0.47	<0.001	136
	peak _{clusSD} -delayed		0.43	<0.001	136

Statistically significant values are marked in bold.

All given data only refer to the hemisphere ipsilateral to the subdural electrodes.

Average mbfv_{ACA/MCA/PCA} = average of the peak mean blood flow velocities of anterior cerebral artery (ACA), middle cerebral artery (MCA) and posterior cerebral artery (PCA); blood_{basal} = subarachnoid blood volume in the basal cisterns; blood_{convex} = subarachnoid blood volume on the cerebral convexity; blood_{inter} = subarachnoid blood volume in the interhemispheric fissure; blood_{Sylvian} = subarachnoid blood volume in the Sylvian fissure; DCI_{ACA} = delayed infarct volume in the territory of the ACA; DCI_{deep} = delayed infarct volume below the cortex including perforator infarcts, singular white matter infarcts without cortical involvement and anterior choroidal artery infarcts; DCI_{MCA} = delayed infarct volume in the territory of the MCA; DCI_{PCA} = delayed infarct volume in the territory of the PCA; DCI_{watershed} = delayed infarct volume in the territory of the cortical watershed zones; DSA = digital subtraction angiography (A1, A2, M1, M2, P1, P2 = first and second segments of ACA, MCA and PCA ipsilateral to the subdural electrodes); DSA_{A1–P2} score = total score achieved by the summation of values for A1, A2, M1, M2, P1 and P2 divided by the number of vessel segments assessed; ECl_{ACA} = early infarct volume in the territory of the anterior cerebral artery; ECl_{deep} = early infarct volume below the cortex including perforator infarcts, singular white matter infarcts without cortical involvement and anterior choroidal artery infarcts; ECl_{MCA} = early infarct volume in the territory of the middle cerebral artery; ECl_{PCA} = early infarct volume in the territory of the posterior cerebral artery; ECl_{watershed} = early infarct volume in the territory of the cortical watershed zones; ICH = intracerebral haemorrhage; IVH = intraventricular haemorrhage; peak_{clusSD}-delayed = peak number of clustered spreading depolarizations (SD) of a recording day during the delayed period between the early post-intervention neuroimage and the late neuroimage after completion of neuromonitoring (clustered SD = SD that occurred less than 1 h apart from the previous SD); peak_{isoSD}-delayed = peak number of isoelectric SDs of a recording day during the delayed period (isoelectric SD = SD in electrically inactive tissue); peak_{SD}-delayed = peak number of SDs of any type of a recording day during the delayed period; PTDDD_{delayed} = peak value of a recording day for the total (cumulative) SD-induced depression durations during the delayed period; sum of blood_{convex} + inter + Sylvian + basal = total subarachnoid blood volume (blood_{convex} + blood_{inter} + blood_{Sylvian} + blood_{basal}); sum of blood_{convex} + inter + Sylvian + basal + IVH = blood_{convex} + blood_{inter} + blood_{Sylvian} + blood_{basal} + IVH.

In the bottom part of the table, we added the delayed infarct volumes DCI_{ACA} + DCI_{MCA} + DCI_{PCA} and correlated this composite infarct volume with several summary measures, namely, the total subarachnoid blood volume (blood_{convex} + blood_{inter} + blood_{Sylvian} + blood_{basal}) with and without IVH volume, the average of mbfv_{ACA} + mbfv_{MCA} + and mbfv_{PCA}, the average score based on DSA_{A1–P2}, and the four SD variables to provide an overview. Large subarachnoid haematoma with space-occupying effect and perifocal oedema are not listed separately in this table but are included in blood_{inter} and blood_{Sylvian}. In total, we encountered 22 (16.2%) such cases with large subarachnoid haematomas with a median blood volume of 29 (IQR: 16–46) ml, 19 cases in the Sylvian fissure and 3 cases in the interhemispheric fissure.

^aZero values included.

^bVessel narrowing <11%.

^cVessel narrowing 11–33%.

^dVessel narrowing 34–66%.

^eVessel narrowing >66%.

and anterior choroidal artery infarcts. Ischaemic tissue adjacent to the aneurysm was excluded. The location of delayed infarcts was determined according to arterial territory maps specified by Tatu *et al.*⁷⁵

Haemorrhage volumes

V.H. used the pre-interventional CT performed on median Day 0 (IQR: 0–0, range: 0–3) for volumetric haemorrhage quantification of the hemisphere ipsilateral to the subdural electrodes. Epidural, subdural, contralateral and infratentorial haemorrhages were not considered. Manual segmentation was carried out on non-contrast-enhanced images with a slice thickness between 3 and 6 mm using the paintbrush mode of ITK-Snap, Version 3.8.0 (www.itksnap.org). Ipsilateral haemorrhage was segmented into six predefined regions: subarachnoid blood accumulations on (i) the cerebral convexity (blood_{convex}); (ii) in the interhemispheric fissure (blood_{inter}); (iii) Sylvian fissure (blood_{Sylvian}), or (iv) basal cisterns (blood_{basal}); (v) ICH, or (vi) intraventricular haemorrhage (IVH) (see Fig. 1B and C). According to van der Zande *et al.*,⁷⁶ we differentiated blood_{Sylvian} from ICH using CT angiography. Contrast-enhancing arteries within a haematoma indicated blood_{Sylvian}, whereas a haematoma without visible contrast-enhancing vessels indicated ICH.

Statistical analysis

The statistical analysis was performed by P.M., the trial statistician of DISCHARGE-1. Unless otherwise stated, data are given as median (IQR). Relationships between the variable groups related to blood volume, SD, DSA, TCD-determined peak mbfvs and delayed infarct volumes were analysed bivariately using Spearman correlations. Correlations with uncorrected *P*-values <0.05 were discussed. However, for each group of comparisons it was noted which correlations remained significant after Bonferroni correction. In the next step, principal component analyses were performed for each of the variable groups, and only the first principal component was used in further analyses. In principal component analyses, log transformations were applied for blood volume variables, SD variables, DSA variables and delayed infarct volumes, but not for TCD-determined peak mbfvs. The obtained components were included in path models with *a priori* defined structure, treating blood volume variables as extrinsic variables, SD variables, DSA variables and TCD-determined peak mbfvs as potential mediator variables but also possibly extrinsic variables, and infarct volumes due to DCI as outcome. Analyses were performed using SPSS for Windows release 26. The path models were calculated using Amos release 26.

Data availability

Electronic recording, processing and storage of the data were approved by the data protection officer of the Charité—Universitätsmedizin Berlin (data protection votes from 28 May 2008 to 5 May 2014). The datasets analysed during

the current study are not publicly available because the patient's informed consent only permits the data analysis and publication by the investigators.

Results

The DISCHARGE-1 cohort has been described previously.⁴ The present substudy included 90 (66.2%) females and 46 (33.8%) males. Median age was 56 (IQR: 47–63) years. All given data refer to the hemisphere ipsilateral to the subdural electrodes. Table 1 summarises the radiographic characteristics including haemorrhage and infarct volumes. The image_{early} revealed early infarcts in 80 (58.8%) patients with a total volume of 1156.3 ml. The image_{late} showed delayed infarcts in 69 (50.7%) patients with a total volume of 2599.7 ml. In addition, early and delayed infarcts are listed in Table 1 according to the five categories explained above. Because delayed cortical watershed infarcts and deep infarcts accounted for only a very small proportion of infarcts, they were not considered in further analyses. Table 1 also includes correlations of the composite delayed infarct volume in the ipsilateral ACA, MCA and PCA territories with various summary measures.

Illustrative case

A 48-year-old man was admitted to the emergency room after a seizure and continued loss of consciousness. The initial CT scan demonstrated Grade 4 aSAH (modified Fisher scale) (Fig. 2A) due to rupture of a DSA-proven aneurysm at the left MCA bifurcation. On Day 1, the aneurysm was secured by surgical clip ligation and a subdural electrode strip was placed. On Day 2, MRI showed no early cerebral infarction. Due to the reduced level of consciousness, neurological assessment was limited during neurocritical care. On Day 7, an intense SD cluster suddenly began (TDDD: 324.0 min) (Fig. 3). Figure 2B gives a fluid-attenuated inversion recovery (FLAIR) image on Day 9 that revealed a new hyperintense lesion in the left temporal cortex consistent with delayed cerebral infarction in the left MCA territory. DSA on the same day showed severe angiographic vasospasm (Fig. 2C). Daily TCD examinations of the ipsilateral MCA demonstrated increased mbfvs on 2 days (>120 cm/s), but the peak mbfv of 144 cm/s on Day 8 did not reach the critical threshold of 200 cm/s.⁷⁷ Figure 2D visualises the spatial relation between delayed MCA infarct and location of the subdural electrodes.

Correlation analysis

Our basic hypothesis was that certain blood volumes [(i) blood_{convex}; (ii) blood_{inter}; (iii) blood_{Sylvian}; (iv) blood_{basal}; (v) ICH and (vi) IVH] are associated with delayed infarct volumes. To this aim, we calculated Spearman correlations with delayed infarct volumes in the territories of ACA (DCI_{ACA}), MCA (DCI_{MCA}) and PCA (DCI_{PCA}) (Table 2). We found correlations between blood_{convex} and DCI_{MCA} ($r = 0.32$, $P < 0.001$), blood_{inter} and DCI_{ACA} ($r = 0.19$, $P = 0.030$), blood_{Sylvian} and DCI_{MCA} ($r = 0.25$, $P = 0.003$),

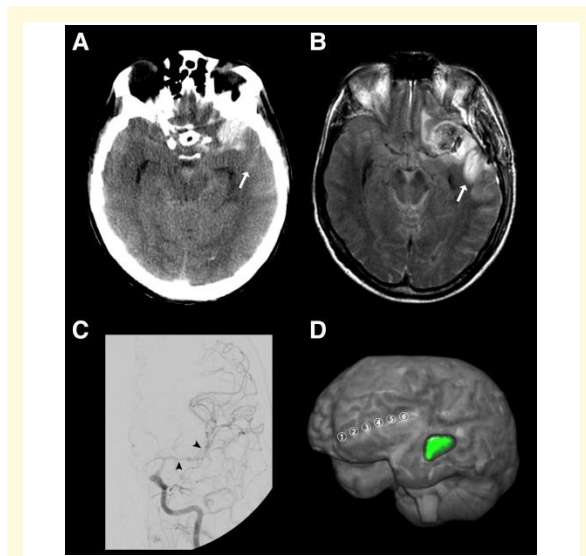


Figure 2 Example case illustrating delayed cerebral infarction adjacent to blood on the cerebral convexity that was associated with a cluster of SDs and angiographic vasospasm.

(A) Representative CT image of the initial scan at the skull base. The initial scan was performed on Day 1 after the initial haemorrhage. Linear hyperdense abnormalities were observed in the sulci of the left cerebral convexity consistent with SAH that extensively covered the cortical surface (10.6 ml). Note that the anterior portion of the left superior temporal sulcus was also filled with blood (arrow). Furthermore, the left MCA aneurysm was surrounded by a hyperdense mass at the left temporal pole consistent with perianeurysmal haematoma that extended into cerebral parenchyma (11.8 ml). Only small to moderate amounts of blood were found in the Sylvian fissure (5.5 ml), the basal cisterns (4.5 ml), the interhemispheric fissure (1.2 ml) and in the ventricles (1.1 ml). (B) Representative FLAIR image of ImageLate on Day 9 at the skull base. A new hyperintense signal was observed in the anterior portion of the superior temporal sulcus (arrow). The corresponding area showed hyperintensity on diffusion-weighted images and hypointensity on the apparent diffusion coefficient (ADC) map. These findings suggested a new delayed infarct in the temporal MCA territory adjacent to the sulcal blood clot seen on the initial CT scan (arrow). (C) The left angiogram on Day 9 revealed severe vasospasm in the intracranial segment of the internal carotid artery, the A1, M1 and M2 segments (see arrowheads for left MCA vasospasm). (D) The 3D visualization depicts the spatial relationship between the delayed MCA infarct (green label) and the electrode strip (electrodes 1–6). The strip was located on the left frontolateral cortex, whereas the delayed infarct evolved in the left temporal cortex. The shortest distance was measured between the infarct boundary and electrode 6. It amounted to 28 mm.

blood_{basal} and DCI_{MCA} ($r = 0.23$, $P = 0.008$), and IVH and DCI_{ACA} ($r = 0.23$, $P = 0.007$) (Fig. 4Bi). Applying a Bonferroni correction with factor 18 (six blood volumes, three delayed infarct variables), the correlation between blood_{convex} and DCI_{MCA} remained significant. Thus, the basic hypothesis was proven for blood_{convex} and DCI_{MCA} (Fig. 4Ai).

Then, we investigated the role of potential mediator variables (SD variables, TCD-determined peak mbfv_s and DSA variables), which should be associated with blood volume variables (Table 3) and delayed infarct volume variables (Table 4). First, we investigated the correlations between blood volumes and SD variables. Because the four SD variables were highly correlated with each other, there was a clear pattern: blood_{convex} (correlations between 0.24 and 0.29) (Fig. 4Aii) and blood_{Sylvian} (correlations between 0.21 and 0.30) were correlated with each SD variable, whereas blood_{inter}, blood_{basal}, ICH and IVH were not. Applying a Bonferroni correction with factor 24 (six blood volumes, four SD variables), four of these eight correlations remained significant. Furthermore, SD variables were correlated with each of the delayed infarct volume variables. Correlations of SD variables were larger with DCI_{MCA} (0.46–0.55) (Fig. 4Aiii) and smaller with DCI_{ACA} (0.18–0.23) and DCI_{PCA} (0.19–0.26). After Bonferroni correction with factor 12 (four SD variables, three delayed infarct volume variables), each of the four correlations between SD variables and DCI_{MCA} remained significant. Thus, using the assumption that SD variables are in the pathway between blood volume variables and delayed infarct volume variables, the role of a mediator was supported by the correlation analyses. A more precise analysis is presented in the ‘Path analysis’ section.

Applying the same procedure to peak mbfv_s, we only found one correlation between blood_{convex} and mbfv_{MCA} ($r = 0.21$, $P = 0.02$), which was not significant after Bonferroni correction with factor 18 (six blood volume variables, three peak mbfv_s for MCA, ACA and PCA). Of nine correlations between peak mbfv_s and delayed infarct variables, four had uncorrected P -values smaller than 0.05 [mbfv_{MCA} with DCI_{MCA}, ($r = 0.20$, $P = 0.02$), mbfv_{ACA} with DCI_{MCA} ($r = 0.24$, $P = 0.01$), mbfv_{ACA} with DCI_{PCA} ($r = 0.32$, $P < 0.001$) and mbfv_{PCA} with DCI_{MCA} ($r = 0.22$, $P = 0.03$)]. The correlation between mbfv_{ACA} and DCI_{PCA} remained significant after Bonferroni correction. We concluded that peak mbfv_s were not a mediator variable although they were associated with delayed infarcts. Based on these results, we did not further examine this variable in the path analysis. Regarding DSA variables, we found eight correlations, one between blood_{convex} and DSA_{M2}, two between blood_{inter} and DSA_{A1} and DSA_{A2}, none between blood_{Sylvian} or ICH and any DSA variable, one between blood_{basal} and DSA_{A2}, and four between IVH and DSA_{M2}, DSA_{A2}, DSA_{P1} and DSA_{P2}. Two of these correlations, blood_{inter} with DSA_{A2} ($r = 0.31$, $P = 0.001$) and IVH with DSA_{A2} ($r = 0.35$, $P = 0.001$) (Fig. 4Bii) remained significant after Bonferroni correction with factor 36 (six blood volumes and six DSA variables). Furthermore, we found eight correlations between DSA variables and delayed infarct volume variables. Each of the DSA variables was correlated with DCI_{ACA}, and additionally, DSA_{M1} and DSA_{A1} with DCI_{MCA}. After Bonferroni correction with factor 18 (six DSA variables, three delayed infarct

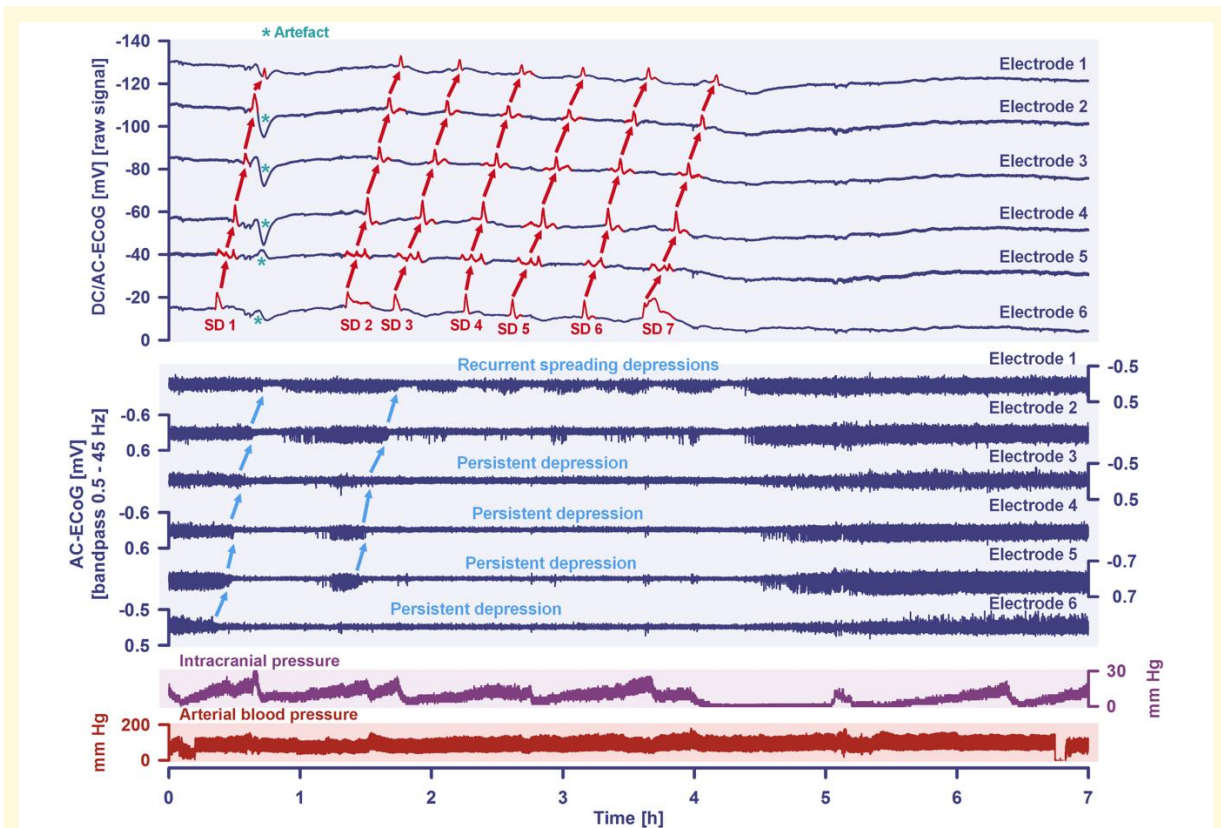


Figure 3 A cluster of seven SDs is shown that occurred in the same patient as in Fig. 2 during a period of 4 h on Day 7 after the initial haemorrhage. Traces 1–6 from top to bottom give the DC/AC-ECoG recordings (band-pass: 0–45 Hz). SDs are observed as a negative DC shift (marked in red in the traces). The SDs propagated across the cortex from electrode 6 to electrode 1. The direction of the propagation (shown by the red arrows) suggests that the SDs originated in an area closer to electrode 6 than to electrode 1. An artefact that likely relates to a systemic change in partial pressure of oxygen is marked with an asterisk after the first SD in traces 2–6. The following six traces (7–12) show the depressive effect of the SDs on the spontaneous brain activity as assessed in the high frequency band (AC-ECoG, band-pass: 0.5–45 Hz). Note that the activity depression propagates together with the SDs in the tissue (blue arrows). The spontaneous activity recovers after each SD only in electrode 1 (trace 7) and partially in electrode 2 (trace 8). In contrast, a persistent depression of activity is observed after the second SD in electrodes 3–5 (traces 9–11) and after the first SD in electrode 6 (trace 12). Thus, SDs 2–7 propagate in electrically silent tissue and are classified accordingly as isoelectric SDs.⁷² Of note, the longest SD-induced activity depression is found in trace 12 closer to the origin of SDs. Trace 13 shows the intracranial pressure measured via extraventricular drainage catheter. Trace 14 shows the systemic arterial pressure (measured via radial artery catheter).

variables), the correlations of DSA_{A2} with DCI_{ACA} ($r = 0.33$, $P = 0.001$) (Fig. 4Biii), and of DSA_{P1} with DCI_{ACA} ($r = 0.33$, $P = 0.002$) remained significant. Therefore, we considered angiographic vasospasm as a potential mediator in the path analysis.

Principal component and path analysis

For each group of variables, the first principal component was used in the path analysis. We refrained from calculating a structural equation model, as single variables were far from normally distributed, although the principal components of blood volume ($blood_{component}$), SD variables ($SD_{component}$), peak mbfvs ($mbfv_{component}$) and angiographic vasospasm

($DSA_{component}$) were close to normal distribution. In the first path model, we only included SD variables, as there were many missing values for peak mbfvs and DSA variables and our primary interest was to investigate the potential role of SDs. Standardised path coefficients (pc) were 0.22 for the path from $blood_{component}$ to $SD_{component}$ ($P = 0.010$, $z = 2.56$); and 0.44 for the path from $SD_{component}$ to the first principal component of delayed infarct volume ($DCI_{component}$) ($P < 0.001$, $z = 5.54$); but only 0.07 for the direct path from $blood_{component}$ to $DCI_{component}$ ($P = 0.36$, $z = 0.91$) (Fig. 5A). Thus, the role of SDs as a mediator between blood volume and delayed infarct volume was confirmed.

For DSA variables, the path from $DSA_{component}$ to $DCI_{component}$ had a standardised pc of 0.37 ($P < 0.001$, $z =$

Table 2 Spearman correlations between region-specific blood volumes and delayed cortical infarct volumes

Statistical analysis	Variable	Spearman coefficient	P-value	Number of patients
Association analysis with DCI _{ACA}	blood _{convex}	-0.03	0.691	136
	blood _{inter}	0.19	0.030	136
	blood _{Sylvian}	0.01	0.899	136
	blood _{basal}	0.07	0.409	136
	ICH	0.07	0.418	136
	IVH	0.23	0.007	136
Association analysis with DCI _{MCA}	blood _{convex}	0.32	<0.001	136
	blood _{inter}	0.09	0.297	136
	blood _{Sylvian}	0.25	0.003	136
	blood _{basal}	0.23	0.008	136
	ICH	0.07	0.420	136
	IVH	0.12	0.181	136
Association analysis with DCI _{PCA}	blood _{convex}	0.10	0.269	136
	blood _{inter}	-0.05	0.572	136
	blood _{Sylvian}	0.03	0.704	136
	blood _{basal}	0.01	0.890	136
	ICH	0.10	0.268	136
	IVH	0.15	0.085	136

Statistically significant values are marked in bold.

All given data only refer to the hemisphere ipsilateral to the subdural electrodes. blood_{basal} = subarachnoid blood volume in the basal cisterns; blood_{convex} = subarachnoid blood volume on the cerebral convexity; blood_{inter} = subarachnoid blood volume in the interhemispheric fissure; blood_{Sylvian} = subarachnoid blood volume in the Sylvian fissure; DCI_{ACA} = delayed infarct volume in the territory of the anterior cerebral artery; DCI_{MCA} = delayed infarct volume in the territory of the middle cerebral artery; DCI_{PCA} = delayed infarct volume in the territory of the posterior cerebral artery; ICH = intracerebral haemorrhage; IVH = intraventricular haemorrhage.

3.67). However, the pc was only 0.12 ($P = 0.28$, $z = 1.08$) for the path from blood_{component} to DSA_{component} which questions the role of angiographic vasospasm as a mediator variable between blood volume and delayed infarct volume, although there was a clear association between angiographic vasospasm and delayed infarct volume. For mbfv_{components}, pc were all <0.20 . Therefore, this component was not included in further analyses.

Based on these analyses, we constructed a path model with the extrinsic variables blood volume and angiographic vasospasm, one mediator variable (SD) and the outcome variable delayed infarct volume. In this model, pc did not change considerably compared to the separate analyses for SD and angiographic vasospasm: There was a path from blood_{component} to SD_{component} (pc = 0.19, $P = 0.03$, $z = 2.17$), and from SD_{component} to DCI_{component} (pc = 0.27, $P = 0.002$, $z = 3.06$), and a direct path from DSA_{component} to DCI_{component} (pc = 0.30, $P < 0.001$, $z = 3.65$). The model showed an excellent fit (Chi-Square = 1.8, degrees of freedom = 3, $P = 0.61$) (Fig. 5B).

In the principal component analysis, IVH was not represented in the first component. Thus, based on the correlation analyses, we constructed a second path model with the principal component of blood volume without IVH as first and

IVH as second extrinsic variable. There were two paths, one from blood_{component} to DCI_{component} with SD_{component} as mediator variable (pc from blood_{component} to SD_{component} = 0.23, $P = 0.03$, $z = 2.17$; pc from SD_{component} to DCI_{component} = 0.29, $P = 0.002$, $z = 3.06$), and one from IVH to DCI_{component} with DSA_{component} as mediator variable (pc from IVH to DSA_{component} = 0.24, $P = 0.03$, $z = 2.17$; pc from DSA_{component} to DCI_{component} = 0.35, $P < 0.001$, $z = 3.65$). No additional paths in this model were significant. This model also showed an excellent fit (Chi-Square = 5.3, degrees of freedom = 6, $P = 0.51$) (Fig. 5C).

Further associations

Supplementary Table 1 shows correlations between SD variables, DSA variables and peak mbfvs. SD and DSA variables did not correlate (Fig. 4Ci). Of 12 correlations between SD variables and peak mbfvs, 4 had uncorrected P -values smaller than 0.05. None of these remained significant after Bonferroni correction. Of 18 correlations between peak mbfvs and DSA variables, 4 had uncorrected P -values smaller than 0.05. After Bonferroni correction with factor 18 (three mbfvs, six DSA variables), the correlation between mbfv_{MCA} with DSA_{M1} remained significant (Fig. 4Cii).

Discussion

It is assumed that the amount of subarachnoid blood on the initial CT scan predicts DCI.¹ Supplementary Table 2 lists the studies we found in which blood was quantified and all studies supported this.⁷⁹⁻⁸⁴ Our study basically reaches the same conclusion. However, we also quantified blood in the sulci of the cerebral convexity, and this component had the strongest statistical association with delayed infarcts in the MCA territory, which in turn accounted for 70.8% of the total cumulative infarct volume in the 136 patients. In fact, only the correlation between blood_{convex} and DCI_{MCA} remained significant with strict Bonferroni correction. However, with 18 tests, only 1 uncorrected significant result is expected by chance, and we observed such significances in 5 tests (Table 2). Four of these were related to the same fundamental hypothesis—local blood deposition on the cortex contributes to delayed infarct pathogenesis. Therefore, we estimate Bonferroni correction to be very conservative here and believe that the fundamental hypothesis above is also supported by the additional tests, which were significant without Bonferroni correction. For example, blood_{inter} without Bonferroni correction correlated significantly with delayed infarcts in the ACA territory adjacent to the interhemispheric fissure, and blood_{Sylvian} showed the second strongest correlation with delayed infarcts in the MCA territory surrounding the Sylvian fissure.

Human autopsy studies shaped the hypothesis that local blood deposition on the cortex is largely responsible for infarcts after aSAH,⁵⁵ which is further supported by radiological findings^{61,85-87} and a primate study.⁶³ This hypothesis implies that direct exposure to factors released from the clot is critically involved in cortical infarct development below the clot. Experimentally, an important effect of such

Table 3 Spearman correlations between region-specific blood volumes and potential mediators of delayed infarction

Statistical analysis	Variable	Spearman coefficient	P-value	Number of patients
Association analysis with blood _{convex}	PTDDD _{delayed}	0.29	0.001	136
	peak _{SD-delayed}	0.25	0.003	136
	peak _{isoSD-delayed}	0.25	0.003	136
	peak _{clusSD-delayed}	0.24	0.005	136
	mbf _{ACA}	0.11	0.265	112
	mbf _{MCA}	0.21	0.020	128
	mbf _{PCA}	0.08	0.442	98
	DSA _{A1}	-0.01	0.915	103
	DSA _{A2}	-0.14	0.165	104
	DSA _{M1}	0.10	0.302	105
	DSA _{M2}	0.24	0.014	105
	DSA _{P1}	0.05	0.633	91
	DSA _{P2}	0.02	0.842	90
Association analysis with blood _{inter}	PTDDD _{delayed}	0.08	0.342	136
	peak _{SD-delayed}	0.04	0.647	136
	peak _{isoSD-delayed}	0.05	0.542	136
	peak _{clusSD-delayed}	0.03	0.716	136
	mbf _{ACA}	-0.08	0.420	112
	mbf _{MCA}	0.00	0.993	128
	mbf _{PCA}	0.13	0.215	98
	DSA _{A1}	0.21	0.032	103
	DSA _{A2}	0.31	0.001	104
	DSA _{M1}	0.09	0.345	105
	DSA _{M2}	-0.07	0.454	105
	DSA _{P1}	-0.01	0.957	91
	DSA _{P2}	0.05	0.677	90
Association analysis with blood _{Sylvian}	PTDDD _{delayed}	0.28	0.001	136
	peak _{SD-delayed}	0.25	0.004	136
	peak _{isoSD-delayed}	0.30	<0.001	136
	peak _{clusSD-delayed}	0.21	0.016	136
	mbf _{ACA}	-0.02	0.843	112
	mbf _{MCA}	0.11	0.215	128
	mbf _{PCA}	0.01	0.930	98
	DSA _{A1}	-0.06	0.560	103
	DSA _{A2}	-0.11	0.281	104
	DSA _{M1}	-0.04	0.654	105
	DSA _{M2}	0.15	0.126	105
	DSA _{P1}	0.05	0.663	91
	DSA _{P2}	0.07	0.514	90
Association analysis with blood _{basal}	PTDDD _{delayed}	0.14	0.100	136
	peak _{SD-delayed}	0.09	0.292	136
	peak _{isoSD-delayed}	0.15	0.088	136
	peak _{clusSD-delayed}	0.08	0.331	136
	mbf _{ACA}	-0.07	0.491	112
	mbf _{MCA}	0.06	0.525	128
	mbf _{PCA}	0.16	0.113	98
	DSA _{A1}	0.16	0.097	103
	DSA _{A2}	0.20	0.043	104
	DSA _{M1}	0.03	0.761	105
	DSA _{M2}	-0.02	0.876	105
	DSA _{P1}	0.08	0.453	91
	DSA _{P2}	0.16	0.125	90
Association analysis with ICH	PTDDD _{delayed}	0.10	0.274	136
	peak _{SD-delayed}	0.07	0.413	136
	peak _{isoSD-delayed}	0.04	0.622	136
	peak _{clusSD-delayed}	0.06	0.500	136
	mbf _{ACA}	0.08	0.413	112
	mbf _{MCA}	-0.03	0.703	128
	mbf _{PCA}	0.03	0.806	98
	DSA _{A1}	0.08	0.419	103
	DSA _{A2}	0.06	0.548	104
	DSA _{M1}	0.14	0.157	105
	DSA _{M2}	0.04	0.697	105

(continued)

Table 3 (continued)

Statistical analysis	Variable	Spearman coefficient	P-value	Number of patients
Association analysis with IVH	DSA _{P1}	0.08	0.450	91
	DSA _{P2}	0.04	0.691	90
	PTDDD _{delayed}	0.05	0.551	136
	peak _{SD-delayed}	0.00	0.977	136
	peak _{isoSD-delayed}	-0.03	0.734	136
	peak _{clusSD-delayed}	0.03	0.718	136
	mbfv _{ACA}	0.10	0.290	112
	mbfv _{MCA}	0.08	0.399	128
	mbfv _{PCA}	0.16	0.127	98
	DSA _{A1}	0.19	0.058	103
	DSA _{A2}	0.35	<0.001	104
	DSA _{M1}	0.17	0.088	105
	DSA _{M2}	0.20	0.041	105
	DSA _{P1}	0.31	0.003	91
	DSA _{P2}	0.26	0.015	90

Statistically significant values are marked in bold.

All given data only refer to the hemisphere ipsilateral to the subdural electrodes. blood_{basal} = subarachnoid blood volume in the basal cisterns; blood_{convex} = subarachnoid blood volume on the cerebral convexity; blood_{inter} = subarachnoid blood volume in the interhemispheric fissure; blood_{Sylvian} = subarachnoid blood volume in the Sylvian fissure; DSA = digital subtraction angiography [A1, A2, M1, M2, P1, P2 = first and second segments of anterior cerebral artery (ACA), middle cerebral artery (MCA) and posterior cerebral artery (PCA) ipsilateral to the subdural electrodes]; ICH = intracerebral haemorrhage; IVH = intraventricular haemorrhage; mbfv_{ACA} = transcranial Doppler-sonography (TCD)-determined peak mean blood flow velocity of ACA; mbfv_{MCA} = TCD-determined peak mean blood flow velocity of MCA; mbfv_{PCA} = TCD-determined peak mean blood flow velocity of PCA; peak_{clusSD-delayed} = peak number of clustered spreading depolarizations (SD) of a recording day during the delayed period between the early post-intervention neuroimage and the late neuroimage after completion of neuromonitoring (clustered SD = SD that occurred less than 1 h apart from the previous SD); peak_{isoSD-delayed} = peak number of isoelectric SDs of a recording day during the delayed period (isoelectric SD = SD in electrically inactive tissue); peak_{SD-delayed} = peak number of SDs of any type of a recording day during the delayed period; PTDDD_{delayed} = peak value of a recording day for the total (cumulative) SD-induced depression durations during the delayed period.

factors is to induce SDs, which in turn initiate and maintain neuronal cytotoxic oedema associated with the risk of developing into infarction. Consistently, focal accumulation of subarachnoid blood was a sufficient insult to trigger SDs and early infarcts in a swine model.⁴⁷ SD induction was also previously demonstrated in a rat model mimicking post-aSAH conditions.²¹ In this model, artificial cerebrospinal fluid (aCSF), with an increased K⁺ concentration ([K⁺]_{aCSF}) and either a nitric oxide synthase (NOS) inhibitor or the nitric oxide (NO) scavenger haemoglobin, was applied topically on the brain.²¹ The same protocol also induced SDs in brain slices devoid of intact blood circulation.³⁹ For the complex role of K⁺, the reader is referred to previous work.^{5,88} The prominent role of decreased NO availability agrees well with the increasingly recognised hypothesis, originally from Furchgott *et al.*, that clot-derived factors cause NO deficiency after aSAH.^{57,58,89,90} NO deficiency leads directly to vasoconstriction and, by absence of its permissive effect for other vasodilators, indirectly as well.^{5,58} NO deficiency also lowers the SD threshold. This was found not only *in vivo*²⁴ but also in brain slices³⁹ devoid of intact blood circulation. Previous work suggested that loss of cyclic guanosine monophosphate (cGMP)-independent modulatory effects of NO on neuronal P/Q-type voltage-gated Ca²⁺ channels and N-methyl-D-aspartate receptor-controlled channels are responsible for this.⁹¹ However, even in absence of NO-lowering agents, increased microvascular tone can cause SDs due to an imbalance between energy supply and demand of neurons. This was demonstrated in an *in vivo* model with ascending epidurally applied concentrations of the vasoconstrictor polypeptide endothelin-1, which failed in brain slices.⁹² There are both arguments in favour

of and against vasoconstriction triggering SDs after aSAH.⁹³ For example, this hypothesis is supported by the fact that SD-induced spreading ischaemia leading to cerebral infarction started at a median p_{ti}O₂ of 12.5 (IQR: 9.2, 15.2) mmHg,¹⁶ which is already below the normal range.⁹⁴ During spreading ischaemia, p_{ti}O₂ then fell further to 3.3 (2.4, 7.4) mmHg.¹⁶ Similarly, rCBF showed a downward trend even before the onset of SD-induced spreading ischaemia. Immediately before the onset of the spreading ischaemia leading to infarction, rCBF was 57 (53, 65) % compared to baseline and then dropped to 26 (16, 42) % during the spreading ischaemia.¹⁶ On the other hand, it argues against the hypothesis of vasoconstriction being responsible for SDs after aSAH that DSA-derived peripheral cerebral circulation time as a measure of microcirculatory resistance did not correlate with SD variables or DCI in patients.⁹⁵ In addition, SD clusters after aSAH correlate strongly with clinical neurologic deficits, but there are cases of aSAH patients in whom SD clusters were not followed by delayed infarcts but only by reversible delayed vasogenic cortex oedema, reminiscent of MRI findings in familial hemiplegic migraine.⁴ In the present study, we cannot clarify the exact pathomechanisms by which SDs arise, but we found evidence that subarachnoid clots overlying the cortex are associated with SD variables, that SD variables are significantly associated with delayed infarcts, and that the SD component is a statistical mediator between subarachnoid blood and delayed infarcts. The fact that extravascular blood products and especially haemoglobin have complex degradation pathways⁹⁶ that may vary from patient to patient and could have an important influence on the development of DCI and even beyond on patient outcome could not be considered in the present

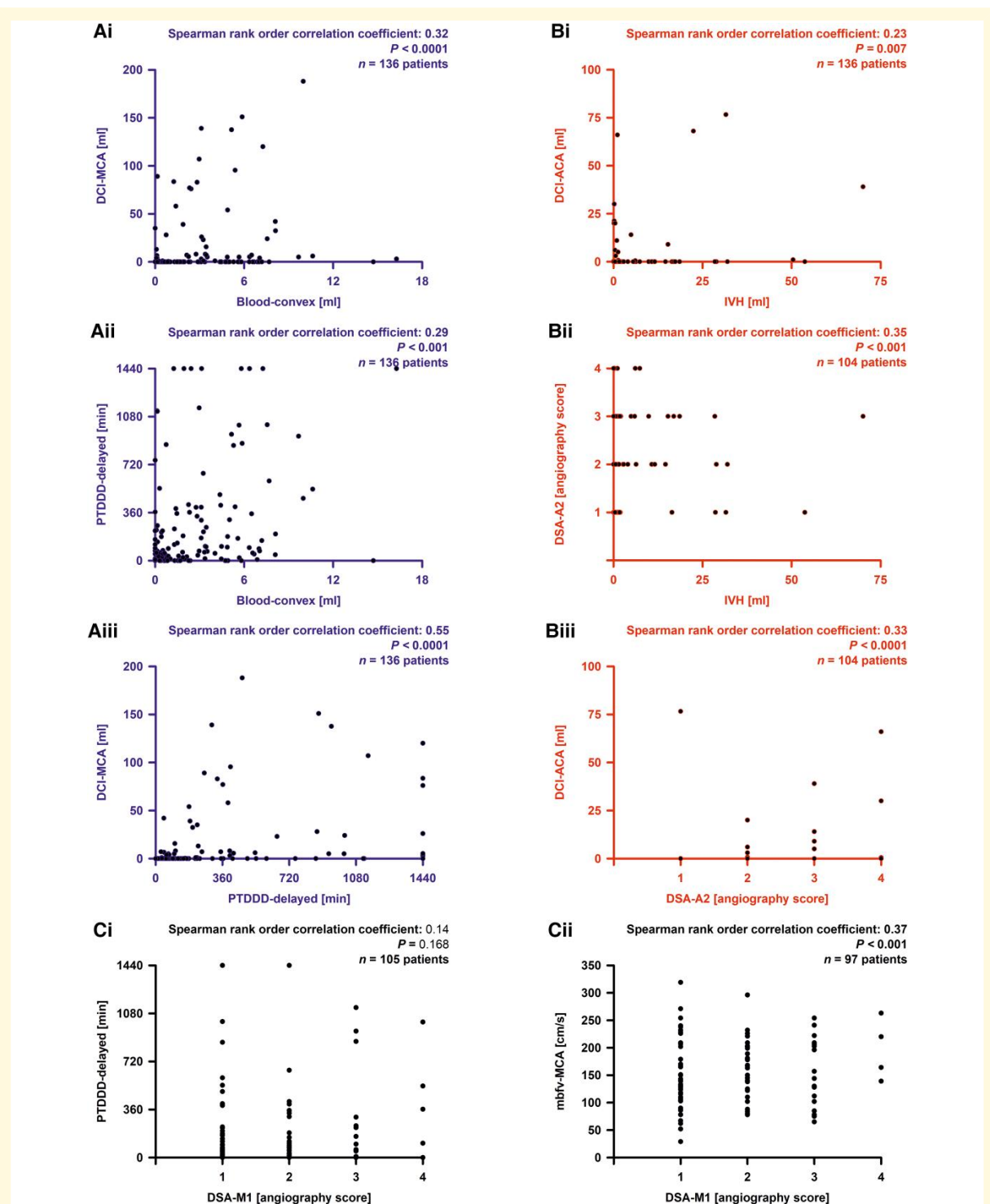


Figure 4 Correlation analyses. In the principal component and path analyses, we found two paths, one from extravascular blood volume component (blood_{component}) to delayed cerebral ischaemia component (DCI_{component}) with spreading depolarization component (SD_{component}) as mediator variable, and one from IVH to DCI_{component} with DSA component as mediator variable. **(A)** Three strongest correlations between individual variables from the three variable groups involved in the path from blood_{component} to SD_{component} to DCI_{component}. **(B)** Three strongest correlations between individual variables from the three variable groups involved in the path from IVH to DSA_{component} to DCI_{component}. **(C)** The electrode strip was typically located on the cortex of the territory of the MCA. However, there was no correlation between angiographic

Table 4 Spearman correlations between potential mediators and delayed cortical infarct volumes

Statistical analysis	Variable	Spearman coefficient	P-value	Number of patients
Association analysis with DCI _{ACA}	PTDDD _{delayed}	0.19	0.024	136
	peak _{SD-delayed}	0.18	0.042	136
	peak _{isoSD-delayed}	0.23	0.006	136
	peak _{clusSD-delayed}	0.18	0.033	136
	mbfv _{ACA}	0.15	0.126	112
	mbfv _{MCA}	0.16	0.076	128
	mbfv _{PCA}	0.01	0.936	98
	DSA _{A1}	0.23	0.017	103
	DSA _{A2}	0.33	0.001	104
	DSA _{M1}	0.22	0.025	105
	DSA _{M2}	0.21	0.031	105
	DSA _{P1}	0.33	0.002	91
	DSA _{P2}	0.31	0.003	90
	Association analysis with DCI _{MCA}	PTDDD _{delayed}	0.55	<0.001
peak _{SD-delayed}		0.47	<0.001	136
peak _{isoSD-delayed}		0.50	<0.001	136
peak _{clusSD-delayed}		0.46	<0.001	136
mbfv _{ACA}		0.24	0.010	112
mbfv _{MCA}		0.20	0.021	128
mbfv _{PCA}		0.22	0.031	98
DSA _{A1}		0.21	0.030	103
DSA _{A2}		0.10	0.318	104
DSA _{M1}		0.25	0.012	105
DSA _{M2}		0.16	0.099	105
DSA _{P1}		0.08	0.456	91
DSA _{P2}		0.12	0.257	90
Association analysis with DCI _{PCA}		PTDDD _{delayed}	0.22	0.012
	peak _{SD-delayed}	0.26	0.003	136
	peak _{isoSD-delayed}	0.24	0.006	136
	peak _{clusSD-delayed}	0.19	0.031	136
	mbfv _{ACA}	0.32	<0.001	112
	mbfv _{MCA}	0.12	0.172	128
	mbfv _{PCA}	0.19	0.056	98
	DSA _{A1}	0.11	0.265	103
	DSA _{A2}	0.15	0.122	104
	DSA _{M1}	0.06	0.563	105
	DSA _{M2}	-0.02	0.874	105
	DSA _{P1}	-0.02	0.868	91
	DSA _{P2}	0.04	0.700	90

Statistically significant values are marked in bold.

All given data only refer to the hemisphere ipsilateral to the subdural electrodes. DCI_{ACA} = delayed infarct volume in the territory of the anterior cerebral artery; DCI_{MCA} = delayed infarct volume in the territory of the middle cerebral artery; DCI_{PCA} = delayed infarct volume in the territory of the posterior cerebral artery; DSA = digital subtraction angiography (A1, A2, M1, M2, P1, P2 = first and second segments of ACA, MCA and PCA ipsilateral to the subdural electrodes); ICH = intracerebral haemorrhage; IVH = intraventricular haemorrhage; mbfv_{ACA} = transcranial Doppler-sonography (TCD)-determined peak mean blood flow velocity of ACA; mbfv_{MCA} = TCD-determined peak mean blood flow velocity of MCA; mbfv_{PCA} = TCD-determined peak mean blood flow velocity of PCA; peak_{clusSD-delayed} = peak number of clustered spreading depolarizations (SD) of a recording day during the delayed period between the early post-intervention neuroimage and the late neuroimage after completion of neuromonitoring (clustered SD = SD that occurred less than 1 h apart from the previous SD); peak_{isoSD-delayed} = peak number of isoelectric SDs of a recording day during the delayed period (isoelectric SD = SD in electrically inactive tissue); peak_{SD-delayed} = peak number of SDs of any type of a recording day during the delayed period; PTDDD_{delayed} = peak value of a recording day for the total (cumulative) SD-induced depression durations during the delayed period.

study for methodological reasons. Iron deposits, which are likely toxic and an end product of these degradation pathways, can still be detected in the cortex months after the initial haemorrhage, which may further worsen long-term patient outcomes.^{61,97}

Analysis of angiographic vasospasm revealed that both the correlation of blood_{inter} and IVH with DSA_{A2} remained significant with strict Bonferroni correction. Furthermore, only two uncorrected significant results are expected by chance in 36 tests, but we observed such significances in a

Figure 4 Continued

vasospasm in the M1 segment (or M2 segment, see [Supplementary Table 1](#)) of the MCA (DSA_{M1}) with the SD variables [shown here is the PTDDD_{delayed} (peak value of a recording day for the total (cumulative) SD-induced depression durations during the delayed period)]. (Cii) In contrast, the TCD-determined peak mean blood flow velocity of the MCA (mbfv_{MCA}) correlated with DSA_{M1}. blood_{convex} = subarachnoid blood volume on the cerebral convexity; DCI_{ACA} = delayed infarct volume in the territory of the anterior cerebral artery (ACA); DCI_{MCA} = delayed infarct volume in the territory of the MCA; DSA_{A2} = DSA score of the A2 segment of the ACA.

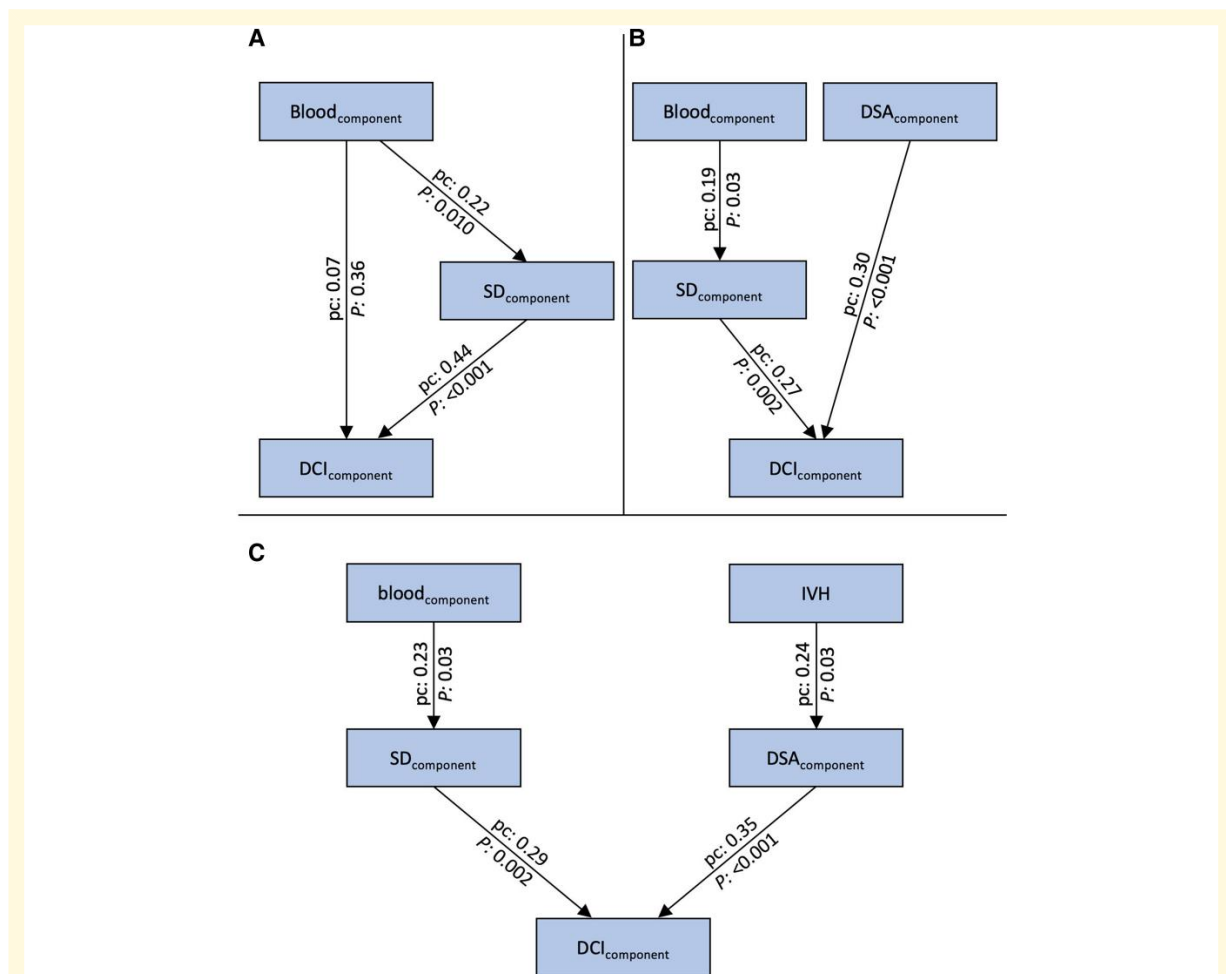


Figure 5 Path models. (A) The first principal component of the SD variables ($SD_{component}$) mediates the effect of the blood volume variables ($blood_{component}$) on delayed infarct volumes ($DCI_{component}$). (B) Path model treating $blood_{component}$ and the first principal component of the DSA variables ($DSA_{component}$) as extrinsic variables and $SD_{component}$ as mediator variable. (C) Path model including IVH into the analysis. There were two paths, one from $blood_{component}$ to $DCI_{component}$ with $SD_{component}$ as mediator variable, and one from IVH to $DCI_{component}$ with $DSA_{component}$ as mediator variable. The numbers at the arrows represent the pc and the P-values (the corresponding z-values are found in the text). P-values of path models use the standard normal distribution for quotients of unstandardised pc and their standard errors and Chi-square tests for model fit with degrees of freedom equal to 'number of parameters saturated model minus number of parameters actual model'.⁷⁸

total of 8 correlations between blood and DSA variables (Table 3). In the correlation analyses between DSA variables and delayed infarcts, two correlations remained significant with Bonferroni correction. Without Bonferroni correction, we observed significances in eight correlations, while only one uncorrected significant result would be expected by chance. Overall, this supports an association between blood volume and DSA variables and another association between DSA variables and delayed infarcts. In the path analyses, the DSA component was a statistical mediator in a path from IVH to delayed infarcts. Possibly, blood products from the ventricles slowly move to the venous system via the glymphatic system, i.e. via para-arterial spaces. In this way, they could reach the arterial tunica

media and induce a local and, via conduction mechanisms between myocytes, also more widespread vasospasm. A prominent role of IVH for angiographic vasospasm has been discussed previously, for example, in the context of angiographic vasospasm after rupture of arteriovenous malformations.^{98,99}

SD and DSA variables did not correlate. Of 12 correlations between SD variables and peak mbfvs, 4 had uncorrected P-values <0.05, while <1 would have been expected by chance. However, none of these correlations remained significant after Bonferroni correction. Reduced perfusion from proximal vasospasm should favour SDs according to animal studies,^{5,92} but in agreement with previous clinical observations, we found no statistically significant evidence for this.^{4,95}

Cerebral infarction is tissue death (necrosis) in which, in addition to SD/neuronal cytotoxic oedema, a lack of rCBF to the tissue, commonly referred to as ischaemia, occurred before the development of necrosis. As explained in the 'Introduction' section, cerebral ischaemia may occur primarily and trigger secondary SD/neuronal cytotoxic oedema with a delay of 1–5 min, such as after MCA occlusion,¹⁶ or SD/neuronal cytotoxic oedema may occur primarily, e.g. as a result of primary neuronal or astrocytic disruption or local inflammation, and trigger spreading ischaemia within seconds via the mechanism of the inverse haemodynamic response.^{5,21} The standard experimental protocol for causing spreading ischaemia is brain topical application of aCSF containing elevated $[K^+]_{aCSF}$ combined with either an NOS inhibitor or the NO scavenger haemoglobin.²¹ The original hypothesis in 1998 that spreading ischaemia might be a pathophysiological correlate of delayed infarcts after aSAH was based on the consideration that the release of blood products from the clot creates a microenvironment similar to that which experimentally leads to spreading ischaemia.²¹ Indeed, the phenomenology of spreading ischaemia later recorded in aSAH patients using subdural optoelectrode strips and oxygen sensors is not different from experimentally recorded spreading ischaemia in the animal model.^{4,16,22} In 2018, using neuromonitoring in combination with longitudinal neuroimaging, the entire sequence of infarct development after aSAH with SD-induced persistent activity depression, SD-induced spreading ischaemia and transition from clustered SDs to NUP was demonstrated in a small patient population where the recording devices were located directly in the area of newly developing infarcts.¹⁶ The concept that local factors at the cortex surface suffice to initiate the mechanism of spreading ischaemia²¹ is also consistent with observations in DISCHARGE-1 that 14.5% of patients with delayed infarcts had no angiographic vasospasm and 50% had only relatively mild angiographic vasospasm.⁴ The often extreme hyperaemia typically observed in aSAH patients immediately following severe spreading ischaemia also argues against sustained upstream restriction of rCBF as the principal cause of spreading ischaemia, as sustained upstream restriction of rCBF would not allow hyperaemia of such high amplitude to occur (compare figure 7 in Dreier *et al.*²² and figure 6A in Luckl *et al.*¹⁶). Nevertheless, experimentally, upstream reduction in rCBF further shifts the normal haemodynamic response to SD towards the inverse haemodynamic response.^{70,100} That is, proximal vasospasm should exacerbate spreading ischaemia, although this may not necessarily translate into a statistically significant change in SD count or depression periods, which, after all, are measured in 71% of patients with electrodes outside the ischaemic zone proper, i.e. outside the zone where spreading ischaemia occurs.⁴

Conclusion

We found that SDs are a statistical mediator between subarachnoid blood and delayed infarcts. Our results suggest

that especially the blood in sulci and fissures, which was usually not considered in previous analyses, plays a major role in the pathogenesis of delayed infarcts. Thus, delayed infarcts may depend on downstream rather than upstream mechanisms and on not only vascular but also important parenchymal factors. This may explain why robust antagonization of proximal vasospasm alone did not suffice to effectively prevent delayed infarcts.^{101–103} However, our results also support that angiographic vasospasm, SD and spreading ischaemia are not mutually exclusive pathomechanisms but complement each other, and we would therefore advocate that therapeutic combination approaches also be pursued further. A limitation of our study is the restricted spatial sampling with only six subdural electrodes. The majority of the electrodes were typically located over MCA territory. Accordingly, the correlation between SD variables and DCI_{MCA} was higher than the correlations between SD variables and DCI_{ACA} or DCI_{PCA} . On the other hand, the fact that correlations between SD variables and DCI_{ACA} or DCI_{PCA} were also statistically significant illustrates once again that subdural neuromonitoring affords even remote detection of injury because SDs propagate widely from metabolically stressed zones.⁷² This is a particular advantage of ECoG over other neuromonitoring modalities, such as microdialysis and partial pressure of oxygen measurements, that measure only local conditions and may not detect clinically important changes developing elsewhere in the hemisphere. Remote diagnosis of new ischaemic zones is of particular relevance to patients with aSAH because the exact location of future developing pathology is usually unknown when the neurosurgeon implants neuromonitoring devices.

Supplementary material

Supplementary material is available at *Brain Communications* online.

Acknowledgements

We thank all the trial participants for their participation in the study and commitment to advancing knowledge regarding aSAH and focal brain damage. We would like to thank the study nurses and the nursing staff of the participating intensive care units, without whose help this study would not have been possible. We appreciate the data and safety monitoring board.

Funding

This work was supported by grants from the Deutsche Forschungsgemeinschaft (DFG) (German Research Council) (DFG DR 323/5-1 to O.W.S., H.V., P.V., J.W., P.M. and J.P.D.; DFG DR 323/10-1 to J.P.D.) and BMBF Bundesministerium fuer Bildung und Forschung (Era-Net Neuron EBio2, with funds from BMBF 01EW2004) to J.P.D. N.H. is Berlin Institute of Health Clinical Fellow, funded by Stiftung Charité.

Competing interests

The authors report no competing interests.

References

- Macdonald RL, Schweizer TA. Spontaneous subarachnoid haemorrhage. *Lancet*. 2017;389(10069):655-666.
- Lawton MT, Vates GE. Subarachnoid hemorrhage. *N Engl J Med*. 2017;377(3):257-266.
- Johnston SC, Selvin S, Gress DR. The burden, trends, and demographics of mortality from subarachnoid hemorrhage. *Neurology*. 1998;50(5):1413-1418.
- Dreier JP, Winkler MKL, Major S, et al. Spreading depolarizations in ischaemia after subarachnoid haemorrhage, a diagnostic phase III study. *Brain*. 2022;145(4):1264-1284.
- Dreier JP. The role of spreading depression, spreading depolarization and spreading ischemia in neurological disease. *Nat Med*. 2011;17(4):439-447.
- Westermaier T, Pham M, Stetter C, et al. Value of transcranial Doppler, perfusion-CT and neurological evaluation to forecast secondary ischemia after aneurysmal SAH. *Neurocrit Care*. 2014;20(3):406-412.
- Dreier JP, Isele T, Reiffurth C, et al. Is spreading depolarization characterized by an abrupt, massive release of Gibbs free energy from the human brain cortex? *Neuroscientist*. 2013;19(1):25-42.
- Dreier JP, Reiffurth C. The stroke-migraine depolarization continuum. Review. *Neuron*. 2015;86(4):902-922.
- Kirov SA, Fomitcheva IV, Sword J. Rapid neuronal ultrastructure disruption and recovery during spreading depolarization-induced cytotoxic edema. *Cereb Cortex*. 2020;30(10):5517-5531.
- Dreier JP, Lemale CL, Kola V, Friedman A, Schoknecht K. Spreading depolarization is not an epiphenomenon but the principal mechanism of the cytotoxic edema in various gray matter structures of the brain during stroke. *Neuropharmacology*. 2018;134(Pt B):189-207.
- Lemale CL, Luckl J, Horst V, et al. Migraine aura, transient ischemic attacks, stroke, and dying of the brain share the same key pathophysiological process in neurons driven by Gibbs-Donnan forces, namely spreading depolarization. *Front Cell Neurosci*. 2022;16:837650.
- Gerkau NJ, Rakers C, Petzold GC, Rose CR. Differential effects of energy deprivation on intracellular sodium homeostasis in neurons and astrocytes. *J Neurosci Res*. 2017;95(11):2275-2285.
- Windmuller O, Lindauer U, Foddiss M, et al. Ion changes in spreading ischaemia induce rat middle cerebral artery constriction in the absence of NO. *Brain*. 2005;128(Pt 9):2042-2051.
- Hansen AJ, Zeuthen T. Extracellular ion concentrations during spreading depression and ischemia in the rat brain cortex. *Acta Physiol Scand*. 1981;113(4):437-445.
- Kraig RP, Nicholson C. Extracellular ionic variations during spreading depression. *Neuroscience*. 1978;3(11):1045-1059.
- Luckl J, Lemale CL, Kola V, et al. The negative ultraslow potential, electrophysiological correlate of infarction in the human cortex. *Brain*. 2018;141(6):1734-1752.
- Vinokurova D, Zakharov A, Chernova K, et al. Depth-profile of impairments in endothelin-1-induced focal cortical ischemia. *J Cereb Blood Flow Metab*. 2022;42(10):1944-1960.
- Jarvis CR, Anderson TR, Andrew RD. Anoxic depolarization mediates acute damage independent of glutamate in neocortical brain slices. *Cereb Cortex*. 2001;11(3):249-259.
- Lauritzen M. Pathophysiology of the migraine aura. The spreading depression theory. *Brain*. 1994;117(Pt 1):199-210.
- Van Harreveld A, Ochs S. Electrical and vascular concomitants of spreading depression. *Am J Physiol*. 1957;189(1):159-166.
- Dreier JP, Korner K, Ebert N, et al. Nitric oxide scavenging by hemoglobin or nitric oxide synthase inhibition by N-nitro-L-arginine induces cortical spreading ischemia when K₊ is increased in the subarachnoid space. *J Cereb Blood Flow Metab*. 1998;18(9):978-990.
- Dreier JP, Major S, Manning A, et al. Cortical spreading ischaemia is a novel process involved in ischaemic damage in patients with aneurysmal subarachnoid haemorrhage. *Brain*. 2009;132(Pt 7):1866-1881.
- Nedergaard M, Hansen AJ. Spreading depression is not associated with neuronal injury in the normal brain. *Brain Res*. 1988;449(1-2):395-398.
- Dreier JP, Ebert N, Priller J, et al. Products of hemolysis in the subarachnoid space inducing spreading ischemia in the cortex and focal necrosis in rats: A model for delayed ischemic neurological deficits after subarachnoid hemorrhage? *J Neurosurg*. 2000;93(4):658-666.
- Shin HK, Dunn AK, Jones PB, Boas DA, Moskowitz MA, Ayata C. Vasoconstrictive neurovascular coupling during focal ischemic depolarizations. *J Cereb Blood Flow Metab*. 2006;26(8):1018-1030.
- Strong AJ, Anderson PJ, Watts HR, et al. Peri-infarct depolarizations lead to loss of perfusion in ischaemic gyrencephalic cerebral cortex. *Brain*. 2007;130(Pt 4):995-1008.
- Bere Z, Obrenovitch TP, Kozak G, Bari F, Farkas E. Imaging reveals the focal area of spreading depolarizations and a variety of hemodynamic responses in a rat microembolic stroke model. Research Support, Non-U.S. Gov't. *J Cereb Blood Flow Metab*. 2014;34(10):1695-1705.
- Zhao HT, Tuohy MC, Chow D, et al. Neurovascular dynamics of repeated cortical spreading depolarizations after acute brain injury. *Cell Rep*. 2021;37(1):109794.
- Takeda Y, Zhao L, Jacewicz M, Pulsinelli WA, Nowak TS Jr. Metabolic and perfusion responses to recurrent peri-infarct depolarization during focal ischemia in the spontaneously hypertensive rat: Dominant contribution of sporadic CBF decrements to infarct expansion. *J Cereb Blood Flow Metab*. 2011;31(9):1863-1873.
- Dreier JP, Kleeberg J, Alam M, et al. Endothelin-1-induced spreading depression in rats is associated with a microarea of selective neuronal necrosis. *Exp Biol Med (Maywood)*. 2007;232(2):204-213.
- Unekawa M, Tomita Y, Masamoto K, Kanno I, Nakahara J, Izawa Y. Close association between spreading depolarization and development of infarction under experimental ischemia in anesthetized male mice. *Brain Res*. 2022;1792:148023.
- Higuchi T, Takeda Y, Hashimoto M, Nagano O, Hirakawa M. Dynamic changes in cortical NADH fluorescence and direct current potential in rat focal ischemia: Relationship between propagation of recurrent depolarization and growth of the ischemic core. *J Cereb Blood Flow Metab*. 2002;22(1):71-79.
- Nozari A, Dilekoz E, Sukhotinsky I, et al. Microemboli may link spreading depression, migraine aura, and patent foramen ovale. *Ann Neurol*. 2010;67(2):221-229.
- Maslarova A, Alam M, Reiffurth C, Lapilover E, Gorji A, Dreier JP. Chronically epileptic human and rat neocortex display a similar resistance against spreading depolarization in vitro. *Stroke*. 2011;42(10):2917-2922.
- Gorji A, Scheller D, Straub H, et al. Spreading depression in human neocortical slices. *Brain Res*. 2001;906(1-2):74-83.
- Dreier JP, Major S, Pannek HW, et al. Spreading convulsions, spreading depolarization and epileptogenesis in human cerebral cortex. *Brain*. 2012;135(Pt 1):259-275.
- Avoli M, Drapeau C, Louvel J, Pumain R, Olivier A, Villemure JG. Epileptiform activity induced by low extracellular magnesium in the human cortex maintained in vitro. *Ann Neurol*. 1991;30(4):589-596.
- Petzold GC, Windmuller O, Haack S, et al. Increased extracellular K₊ concentration reduces the efficacy of N-methyl-D-aspartate

- receptor antagonists to block spreading depression-like depolarizations and spreading ischemia. *Stroke*. 2005;36(6):1270-1277.
39. Petzold GC, Haack S, von Bohlen Und Halbach O, *et al*. Nitric oxide modulates spreading depolarization threshold in the human and rodent cortex. *Stroke*. 2008;39(4):1292-1299.
 40. Köhling R, Koch UR, Hagemann G, Redecker C, Straub H, Speckmann EJ. Differential sensitivity to induction of spreading depression by partial disinhibition in chronically epileptic human and rat as compared to native rat neocortical tissue. *Brain Res*. 2003;975(1-2):129-134.
 41. Dreier JP, Woitzik J, Fabricius M, *et al*. Delayed ischaemic neurological deficits after subarachnoid haemorrhage are associated with clusters of spreading depolarizations. *Brain*. 2006;129(Pt 12):3224-3237.
 42. Sugimoto K, Nomura S, Shirao S, *et al*. Cilostazol decreases duration of spreading depolarization and spreading ischemia after aneurysmal subarachnoid hemorrhage. *Ann Neurol*. 2018;84(6):873-885.
 43. Major S, Huo S, Lemale CL, *et al*. Direct electrophysiological evidence that spreading depolarization-induced spreading depression is the pathophysiological correlate of the migraine aura and a review of the spreading depolarization continuum of acute neuronal mass injury. *Geroscience*. 2020;42(1):57-80.
 44. Fabricius M, Fuhr S, Willumsen L, *et al*. Association of seizures with cortical spreading depression and peri-infarct depolarisations in the acutely injured human brain. *Clin Neurophysiol*. 2008; 119(9):1973-1984.
 45. Revankar GS, Winkler MKL, Major S, *et al*. Spreading depolarizations and seizures in clinical subdural electrocorticographic recordings. In: Varelas PN, Claassen J, eds. *Seizures in critical care A guide to diagnosis and therapeutics*. Springer; 2017:77-90.
 46. Oliveira-Ferreira AI, Milakara D, Alam M, *et al*. Experimental and preliminary clinical evidence of an ischemic zone with prolonged negative DC shifts surrounded by a normally perfused tissue belt with persistent electrocorticographic depression. *J Cereb Blood Flow Metab*. 2010;30(8):1504-1519.
 47. Hartings JA, York J, Carroll CP, *et al*. Subarachnoid blood acutely induces spreading depolarizations and early cortical infarction. *Brain*. 2017;140(10):2673-2690.
 48. Eriksen N, Rostrup E, Fabricius M, *et al*. Early focal brain injury after subarachnoid hemorrhage correlates with spreading depolarizations. *Neurology*. 2019;92(4):e326-e341.
 49. Drenckhahn C, Winkler MK, Major S, *et al*. Correlates of spreading depolarization in human scalp electroencephalography. *Brain*. 2012;135(Pt 3):853-868.
 50. Carlson AP, Shuttleworth CW, Major S, Lemale CL, Dreier JP, Hartings JA. Terminal spreading depolarizations causing electrocortical silencing prior to clinical brain death: Case report. *J Neurosurg*. 2019;131(6):1773-1779.
 51. Dreier JP, Major S, Lemale CL, *et al*. Correlates of spreading depolarization, spreading depression, and negative ultraslow potential in epidural versus subdural electrocorticography. *Front Neurosci*. 2019;13:373.
 52. Dreier JP, Major S, Foreman B, *et al*. Terminal spreading depolarization and electrical silence in death of human cerebral cortex. *Ann Neurol*. 2018;83(2):295-310.
 53. Fiehler J, Knudsen K, Kucinski T, *et al*. Predictors of apparent diffusion coefficient normalization in stroke patients. *Stroke*. 2004; 35(2):514-519.
 54. Cain SM, Bohnet B, LeDue J, *et al*. In vivo imaging reveals that pregabalin inhibits cortical spreading depression and propagation to subcortical brain structures. *Proc Natl Acad Sci U S A*. 2017; 114(9):2401-2406.
 55. Stoltenburg-Didinger G, Schwarz K. Brain lesions secondary to subarachnoid hemorrhage due to ruptured aneurysms. In: Cervós-Navarro J, Ferszt R, eds. *Stroke and microcirculation*. Raven Press; 1987:471-480.
 56. Ohkuma H, Manabe H, Tanaka M, Suzuki S. Impact of cerebral microcirculatory changes on cerebral blood flow during cerebral vasospasm after aneurysmal subarachnoid hemorrhage. *Stroke*. 2000;31(7):1621-1627.
 57. Furchgott RF, Martin W, Cherry PD. Blockade of endothelium-dependent vasodilation by hemoglobin: A possible factor in vasospasm associated with hemorrhage. *Adv Prostaglandin Thromboxane Leukot Res*. 1985;15:499-502.
 58. Pluta RM, Hansen-Schwartz J, Dreier J, *et al*. Cerebral vasospasm following subarachnoid hemorrhage: Time for a new world of thought. *Neurol Res*. 2009;31(2):151-158.
 59. Neil-Dwyer G, Lang DA, Doshi B, Gerber CJ, Smith PW. Delayed cerebral ischaemia: The pathological substrate. *Acta Neurochir (Wien)*. 1994;131(1-2):137-145.
 60. Robertson EG. Cerebral lesions due to intracranial aneurysms. *Brain*. 1949;72(Pt 2):150-185.
 61. Dreier JP, Sakowitz OW, Harder A, *et al*. Focal laminar cortical MR signal abnormalities after subarachnoid hemorrhage. *Ann Neurol*. 2002;52(6):825-829.
 62. Birse SH, Tom MI. Incidence of cerebral infarction associated with ruptured intracranial aneurysms. A study of 8 unoperated cases of anterior cerebral aneurysm. *Neurology*. 1960;10:101-106.
 63. Scharlo B, Dreier JP, Glasker S, *et al*. Report of selective cortical infarcts in the primate clot model of vasospasm after subarachnoid hemorrhage. *Neurosurgery*. 2010;67(3):721-8; discussion 728-9.
 64. Dreier JP, Petzold G, Tille K, *et al*. Ischaemia triggered by spreading neuronal activation is inhibited by vasodilators in rats. *J Physiol*. 2001;531(Pt 2):515-526.
 65. Dreier JP, Windmuller O, Petzold G, Lindauer U, Einhaupl KM, Dirnagl U. Ischemia triggered by red blood cell products in the subarachnoid space is inhibited by nimodipine administration or moderate volume expansion/hemodilution in rats. *Neurosurgery*. 2002;51(6):1457-1465; discussion 1465-1467.
 66. Dijkhuizen RM, Beekwilder JP, van der Worp HB, Berkelbach van der Sprenkel JW, Tulleken KA, Nicolay K. Correlation between tissue depolarizations and damage in focal ischemic rat brain. *Brain Res*. 1999;840(1-2):194-205.
 67. Koroleva VI, Bures J. The use of spreading depression waves for acute and long-term monitoring of the penumbra zone of focal ischemic damage in rats. *Proc Natl Acad Sci U S A*. 1996;93(8): 3710-3714.
 68. Nedergaard M, Hansen AJ. Characterization of cortical depolarizations evoked in focal cerebral ischemia. *J Cereb Blood Flow Metab*. 1993;13(4):568-574.
 69. Strong AJ, Smith SE, Whittington DJ, *et al*. Factors influencing the frequency of fluorescence transients as markers of peri-infarct depolarizations in focal cerebral ischemia. *Stroke*. 2000;31(1): 214-222.
 70. Feuerstein D, Takagaki M, Gramer M, *et al*. Detecting tissue deterioration after brain injury: Regional blood flow level versus capacity to raise blood flow. Research Support, Non-U.S. Gov't. *J Cereb Blood Flow Metab*. 2014;34(7):1117-1127.
 71. Woitzik J, Hecht N, Pinczolits A, *et al*. Propagation of cortical spreading depolarization in the human cortex after malignant stroke. Research Support, Non-U.S. Gov't. *Neurology*. 2013;80(12):1095-1102.
 72. Dreier JP, Fabricius M, Ayata C, *et al*. Recording, analysis, and interpretation of spreading depolarizations in neurointensive care: Review and recommendations of the COSBID research group. *J Cereb Blood Flow Metab*. 2017;37(5):1595-1625.
 73. Hartings JA, Andaluz N, Bullock MR, *et al*. Prognostic value of spreading depolarizations in patients with severe traumatic brain injury. *JAMA Neurol*. 2020;77(4):489-499.
 74. Weidauer S, Lanfermann H, Raabe A, Zanella F, Seifert V, Beck J. Impairment of cerebral perfusion and infarct patterns attributable to vasospasm after aneurysmal subarachnoid hemorrhage: A prospective MRI and DSA study. *Stroke*. 2007;38(6):1831-1836.
 75. Tatu L, Moulin T, Bogousslavsky J, Duvernoy H. Arterial territories of the human brain: Cerebral hemispheres. *Neurology*. 1998; 50(6):1699-1708.

76. van der Zande JJ, Hendrikse J, Rinkel GJ. CT Angiography for differentiation between intracerebral and intra-sylvian hematoma in patients with ruptured middle cerebral artery aneurysms. *Am J Neuroradiol.* 2011;32(2):271-275.
77. Vora YY, Suarez-Almazor M, Steinke DE, Martin ML, Findlay JM. Role of transcranial Doppler monitoring in the diagnosis of cerebral vasospasm after subarachnoid hemorrhage. *Neurosurgery.* 1999;44(6):1237-1247; discussion 1247-1248.
78. Bollen KA. *Structural equations with latent variables.* John Wiley and Sons, Inc.; 1989.
79. Ko SB, Choi HA, Carpenter AM, et al. Quantitative analysis of hemorrhage volume for predicting delayed cerebral ischemia after subarachnoid hemorrhage. *Stroke.* 2011;42(3):669-674.
80. Reilly C, Amidei C, Tolentino J, Jahromi BS, Macdonald RL. Clot volume and clearance rate as independent predictors of vasospasm after aneurysmal subarachnoid hemorrhage. *J Neurosurg.* 2004;101(2):255-261.
81. van der Steen WE, Zijlstra IA, Verbaan D, et al. Association of quantified location-specific blood volumes with delayed cerebral ischemia after aneurysmal subarachnoid hemorrhage. *Am J Neuroradiol.* 2018;39(6):1059-1064.
82. van der Steen WE, Leemans EL, van den Berg R, et al. Radiological scales predicting delayed cerebral ischemia in subarachnoid hemorrhage: Systematic review and meta-analysis. *Neuroradiology.* 2019;61(3):247-256.
83. Friedman JA, Goerss SJ, Meyer FB, et al. Volumetric quantification of Fisher grade 3 aneurysmal subarachnoid hemorrhage: A novel method to predict symptomatic vasospasm on admission computerized tomography scans. *J Neurosurg.* 2002;97(2):401-407.
84. Zijlstra IA, Gathier CS, Boers AM, et al. Association of automatically quantified total blood volume after aneurysmal subarachnoid hemorrhage with delayed cerebral ischemia. *Am J Neuroradiol.* 2016;37(9):1588-1593.
85. Weidauer S, Vatter H, Beck J, et al. Focal laminar cortical infarcts following aneurysmal subarachnoid haemorrhage. *Neuroradiology.* 2008;50(1):1-8.
86. Schinke C, Horst V, Schlemm L, et al. A case report of delayed cortical infarction adjacent to sulcal clots after traumatic subarachnoid hemorrhage in the absence of proximal vasospasm. *BMC Neurol.* 2018;18(1):210.
87. Robinson D, Kreitzer N, Ngwenya LB, et al. Diffusion-Weighted imaging reveals distinct patterns of cytotoxic edema in patients with subdural hematomas. *J Neurotrauma.* 2021;38(19):2677-2685.
88. Major S, Petzold GC, Reiffurth C, et al. A role of the sodium pump in spreading ischemia in rats. *J Cereb Blood Flow Metab.* 2017;37(5):1687-1705.
89. Sakowitz OW, Wolfrum S, Sarrafzadeh AS, et al. Relation of cerebral energy metabolism and extracellular nitrite and nitrate concentrations in patients after aneurysmal subarachnoid hemorrhage. *J Cereb Blood Flow Metab.* 2001;21(9):1067-1076.
90. Fung C, Z'Graggen WJ, Jakob SM, et al. Inhaled nitric oxide treatment for aneurysmal SAH patients with delayed cerebral ischemia. *Front Neurol.* 2022;13:817072.
91. Petzold GC, Scheibe F, Braun JS, et al. Nitric oxide modulates calcium entry through P/Q-type calcium channels and N-methyl-D-aspartate receptors in rat cortical neurons. *Brain Res.* 2005;1063(1):9-14.
92. Dreier JP, Kleeberg J, Petzold G, et al. Endothelin-1 potently induces Leao's cortical spreading depression in vivo in the rat: A model for an endothelial trigger of migrainous aura? *Brain.* 2002;125(Pt 1):102-112.
93. Petzold GC, Einhaupl KM, Dirnagl U, Dreier JP. Ischemia triggered by spreading neuronal activation is induced by endothelin-1 and hemoglobin in the subarachnoid space. *Ann Neurol.* 2003;54(5):591-598.
94. Winkler MK, Dengler N, Hecht N, et al. Oxygen availability and spreading depolarizations provide complementary prognostic information in neuromonitoring of aneurysmal subarachnoid hemorrhage patients. *J Cereb Blood Flow Metab.* 2017;37(5):1841-1856.
95. Kawano A, Sugimoto K, Nomura S, et al. Association between spreading depolarization and delayed cerebral ischemia after subarachnoid hemorrhage: Post hoc analysis of a randomized trial of the effect of cilostazol on delayed cerebral ischemia. *Neurocrit Care.* 2021.
96. Joerk A, Ritter M, Langguth N, et al. Propenthyolens as heme degradation intermediates constrict mouse cerebral arterioles and are present in the cerebrospinal fluid of patients with subarachnoid hemorrhage. *Circ Res.* 2019;124(12):e101-e114.
97. Galea I, Durnford A, Glazier J, et al. Iron deposition in the brain after aneurysmal subarachnoid hemorrhage. *Stroke.* 2022;53(5):1633-1642.
98. Gross BA, Du R. Vasospasm after arteriovenous malformation rupture. *World Neurosurg.* 2012;78(3-4):300-305.
99. Amuluru K, Al-Mufti F, Romero CE, Gandhi CD. Isolated intraventricular hemorrhage associated with cerebral vasospasm and delayed cerebral ischemia following arteriovenous malformation rupture. *Interv Neurol.* 2018;7(6):479-489.
100. Sukhotinsky I, Dilekoz E, Moskowitz MA, Ayata C. Hypoxia and hypotension transform the blood flow response to cortical spreading depression from hyperemia into hypoperfusion in the rat. *J Cereb Blood Flow Metab.* 2008;28(7):1369-1376.
101. Woitzik J, Dreier JP, Hecht N, et al. Delayed cerebral ischemia and spreading depolarization in absence of angiographic vasospasm after subarachnoid hemorrhage. *J Cereb Blood Flow Metab.* 2012;32(2):203-212.
102. Vergouwen MD, Algra A, Rinkel GJ. Endothelin receptor antagonists for aneurysmal subarachnoid hemorrhage: A systematic review and meta-analysis update. *Stroke.* 2012;43(10):2671-2676.
103. Carrera E, Schmidt JM, Oddo M, et al. Transcranial Doppler for predicting delayed cerebral ischemia after subarachnoid hemorrhage. *Neurosurgery.* 2009;65(2):316-323; discussion 323-324.

Curriculum Vitae

Mein Lebenslauf wird aus datenschutzrechtlichen Gründen in der elektronischen Version meiner Arbeit nicht veröffentlicht.

Publication list

1. Dreier JP, Fabricius M, Ayata C, Sakowitz OW, William Shuttleworth C, Dohmen C, Graf R, Vajkoczy P, Helbok R, Suzuki M, Schiefecker AJ, Major S, Winkler MK, Kang EJ, Milakara D, Oliveira-Ferreira AI, Reiffurth C, Revankar GS, Sugimoto K, Dengler NF, Hecht N, Foreman B, Feyen B, Kondziella D, Friberg CK, Piilgaard H, Rosenthal ES, Westover MB, Maslarova A, Santos E, Hertle D, Sanchez-Porrás R, Jewell SL, Balanca B, Platz J, Hinzman JM, Luckl J, Schoknecht K, Scholl M, Drenckhahn C, Feuerstein D, Eriksen N, **Horst V**, Bretz JS, Jahnke P, Scheel M, Bohner G, Rostrup E, Pakkenberg B, Heinemann U, Claassen J, Carlson AP, Kowoll CM, Lublinsky S, Chassidim Y, Shelef I, Friedman A, Brinker G, Reiner M, Kirov SA, Andrew RD, Farkas E, Guresir E, Vatter H, Chung LS, Brennan KC, Lieutaud T, Marinesco S, Maas AI, Sahuquillo J, Dahlem MA, Richter F, Herreras O, Boutelle MG, Okonkwo DO, Bullock MR, Witte OW, Martus P, van den Maagdenberg AM, Ferrari MD, Dijkhuizen RM, Shutter LA, Andaluz N, Schulte AP, MacVicar B, Watanabe T, Woitzik J, Lauritzen M, Strong AJ, Hartings JA. Recording, analysis, and interpretation of spreading depolarizations in neurointensive care: Review and recommendations of the COSBID research group. *J Cereb Blood Flow Metab.* 2017;37(5):1595-625. IF: 6.960
2. Hartings JA, York J, Carroll CP, Hinzman JM, Mahoney E, Krueger B, Winkler MKL, Major S, **Horst V**, Jahnke P, Woitzik J, Kola V, Du Y, Hagen M, Jiang J, Dreier JP. Subarachnoid blood acutely induces spreading depolarizations and early cortical infarction. *Brain.* 2017;140(10):2673-90. IF: 15.255
3. Luckl J, Lemale CL, Kola V, **Horst V**, Khojasteh U, Oliveira-Ferreira AI, Major S, Winkler MKL, Kang EJ, Schoknecht K, Martus P, Hartings JA, Woitzik J, Dreier JP. The negative ultraslow potential, electrophysiological correlate of infarction in the human cortex. *Brain.* 2018;141(6):1734-52. IF: 15.255
4. Schinke C, **Horst V**, Schlemm L, Wawra M, Scheel M, Hartings JA, Dreier JP. A case report of delayed cortical infarction adjacent to sulcal clots after traumatic subarachnoid hemorrhage in the absence of proximal vasospasm. *BMC Neurol.* 2018;18(1):210. IF: 2.903

-
5. Lublinsky S, Major S, Kola V, **Horst V**, Santos E, Platz J, Sakowitz O, Scheel M, Dohmen C, Graf R, Vatter H, Wolf S, Vajkoczy P, Shelef I, Woitzik J, Martus P, Dreier JP, Friedman A. Early blood-brain barrier dysfunction predicts neurological outcome following aneurysmal subarachnoid hemorrhage. *EBioMedicine*. 2019;43:460-72. IF: 11.205

 6. Dreier JP, Winkler MKL, Major S, **Horst V**, Lublinsky S, Kola V, Lemale CL, Kang EJ, Maslarova A, Salur I, Luckl J, Platz J, Jorks D, Oliveira-Ferreira AI, Schoknecht K, Reiffurth C, Milakara D, Wiesenthal D, Hecht N, Dengler NF, Liotta A, Wolf S, Kowoll CM, Schulte AP, Santos E, Guresir E, Unterberg AW, Sarrafzadeh A, Sakowitz OW, Vatter H, Reiner M, Brinker G, Dohmen C, Shelef I, Bohner G, Scheel M, Vajkoczy P, Hartings JA, Friedman A, Martus P, Woitzik J. Spreading depolarizations in ischaemia after subarachnoid haemorrhage, a diagnostic phase III study. *Brain*. 2022;145(4):1264-84. IF: 15.255

 7. Lemale CL, Luckl J, **Horst V**, Reiffurth C, Major S, Hecht N, Woitzik J, Dreier JP. Migraine Aura, Transient Ischemic Attacks, Stroke, and Dying of the Brain Share the Same Key Pathophysiological Process in Neurons Driven by Gibbs-Donnan Forces, Namely Spreading Depolarization. *Front Cell Neurosci*. 2022;16:837650. IF: 6.147

 8. Vinokurova D, Zakharov A, Chernova K, Burkhanova-Zakirova G, **Horst V**, Lemale CL, Dreier JP, Khazipov R. Depth-profile of impairments in endothelin-1-induced focal cortical ischemia. *J Cerebr Blood F Met*. 2022;42(10):1944-60. IF: 6.960

 9. **Horst V**, Kola V, Lemale CL, Major S, Winkler MKL, Hecht N, Santos E, Platz J, Sakowitz OW, Vatter H, Dohmen C, Scheel M, Vajkoczy P, Hartings JA, Woitzik J, Martus P, Dreier JP. Spreading depolarization and angiographic spasm are separate mediators of delayed infarcts. *Brain Commun*. 2023;5(2).

Acknowledgments

First of all, I would like to express my profound gratitude to my advisor Prof. Dr. med. Jens P. Dreier for the opportunity to work on this exciting project, for sharing his great knowledge and for the patience and continued support in different phases of my thesis. I would also like to thank PD Dr. med. Michael Scheel and PD Dr. med. Paul Jahnke for their neuroradiological advice and support and Prof. Peter Martus for the statistical supervision.

I am grateful for my team colleagues Coline Lemale, Maren Winkler, Vasilis Kola and Clemens Reiffurth, who contributed to this work. In particular, I would like to thank Sebastian Major for his technical assistance. During my work, I have met so many people who have helped me in many ways: Carolyn, Björn, Nadine, Johannes, Philip, Marius, Max, Paul, Leonie, Lando, Jacques, Moa.

Finally, I would like to thank Julia, my friends and my family with whom I could share ups and downs along the way. Dedicated to Philip K.